

Magnetic Microwires for Sensor Applications

A. Zhukov^{1,2,3}*, M. Ipatov^{1,2}, P. Corte-León^{1,2}, J. M. Blanco², and V. Zhukova^{1,2}

¹*Dpto. de Fís. Mater., UPV/EHU San Sebastián 20009, Spain*

²*Dpto. de Fís. Aplicada., UPV/EHU San Sebastián 20009, Spain*

³*Ikerbasque, Basque Foundation for Science, Bilbao, Spain.*

A screenshot of the IARIA website. The header features a blue navigation bar with a logo on the left and several green buttons labeled: HOME, Call for Papers, Committees, Participation, Venue, Program, Post Conference, and Contact. Below the navigation bar is a large banner image of a public square with a fountain. Overlaid on the banner is a white text box containing the following information:

The Eleventh International Conference on Sensor Device Technologies and Applications
SENSORDEVICES 2020
November 21, 2020 to November 25, 2020 - Valencia, Spain

Outline

1. INTRODUCTION

1.1. STATE OF THE ART ON MAGNETIC WIRES, MAGNETIC PROPERTIES AND APPLICATIONS

1. 2.MOTIVATION.

2. MEASUREMENTS METHODS

3. MAGNETIC PROPERTIES OF AS-PREPARED MICROWIRES

3.1. TUNNING OF DOMAIN WALL DYNAMICS

3.2. TUNNING OF HYSTERESIS LOOPS AND GMI

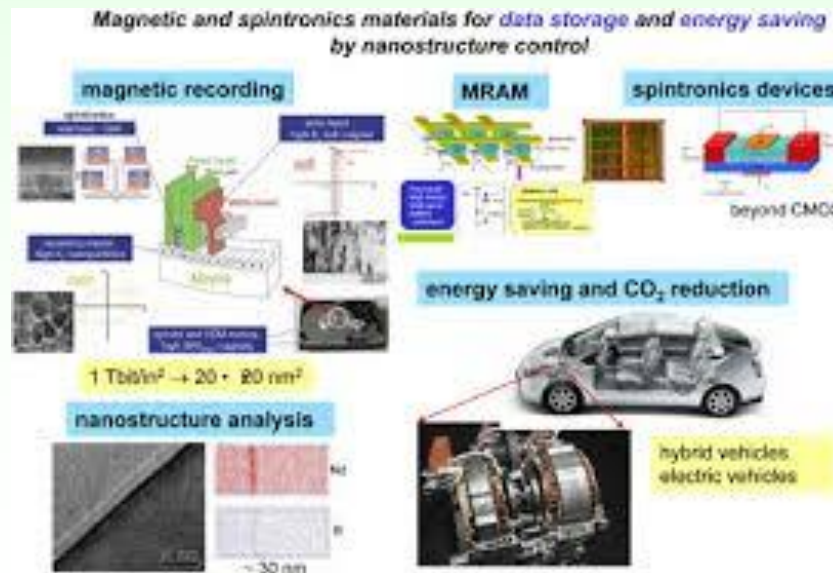
4. CONCLUSIONS



Magnetic materials...

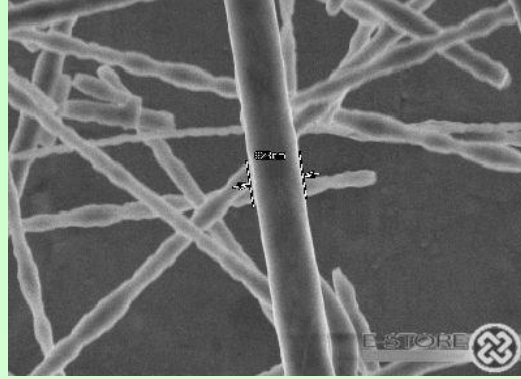


and applications

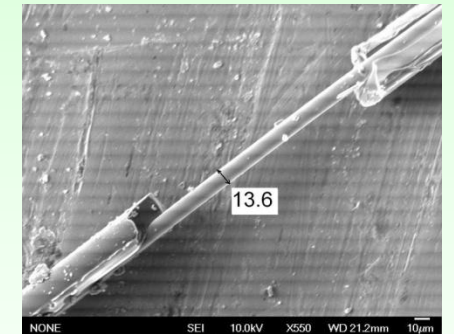
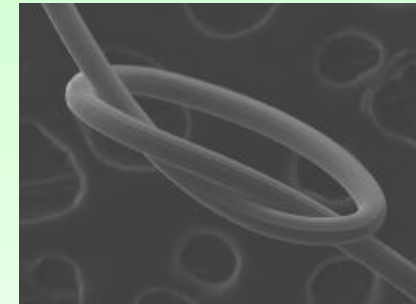
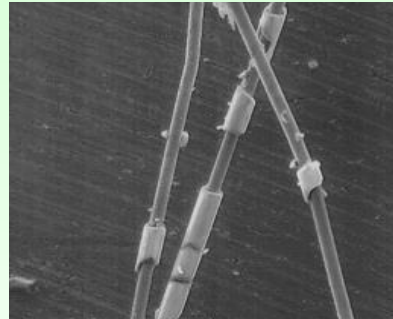
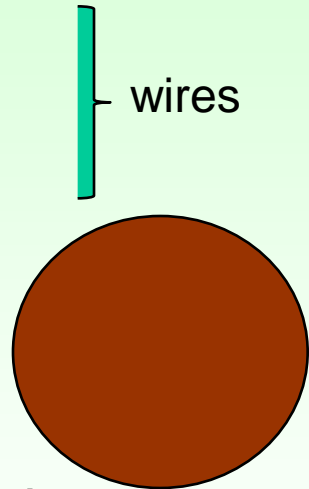


Magnetic wires:

- Iron whiskers
- Wiegman magnetic wires (CoVFe, 1970-th)



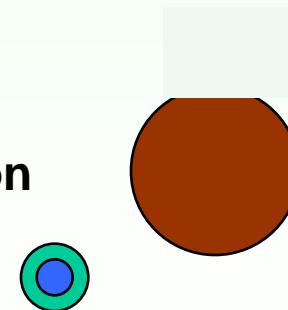
Amorphous: milli
(since 80-th) micro
nano



In-rotating water wires
(can be drawn to 20-30 μm) – rough surface

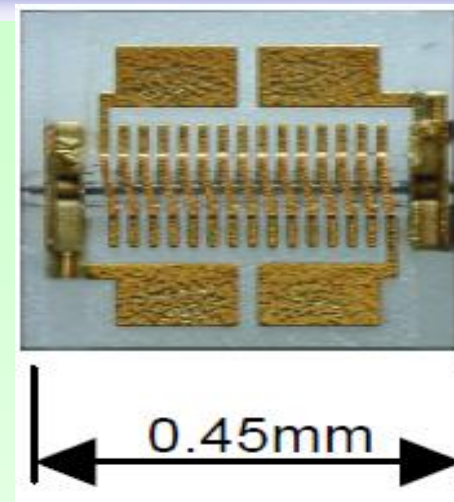
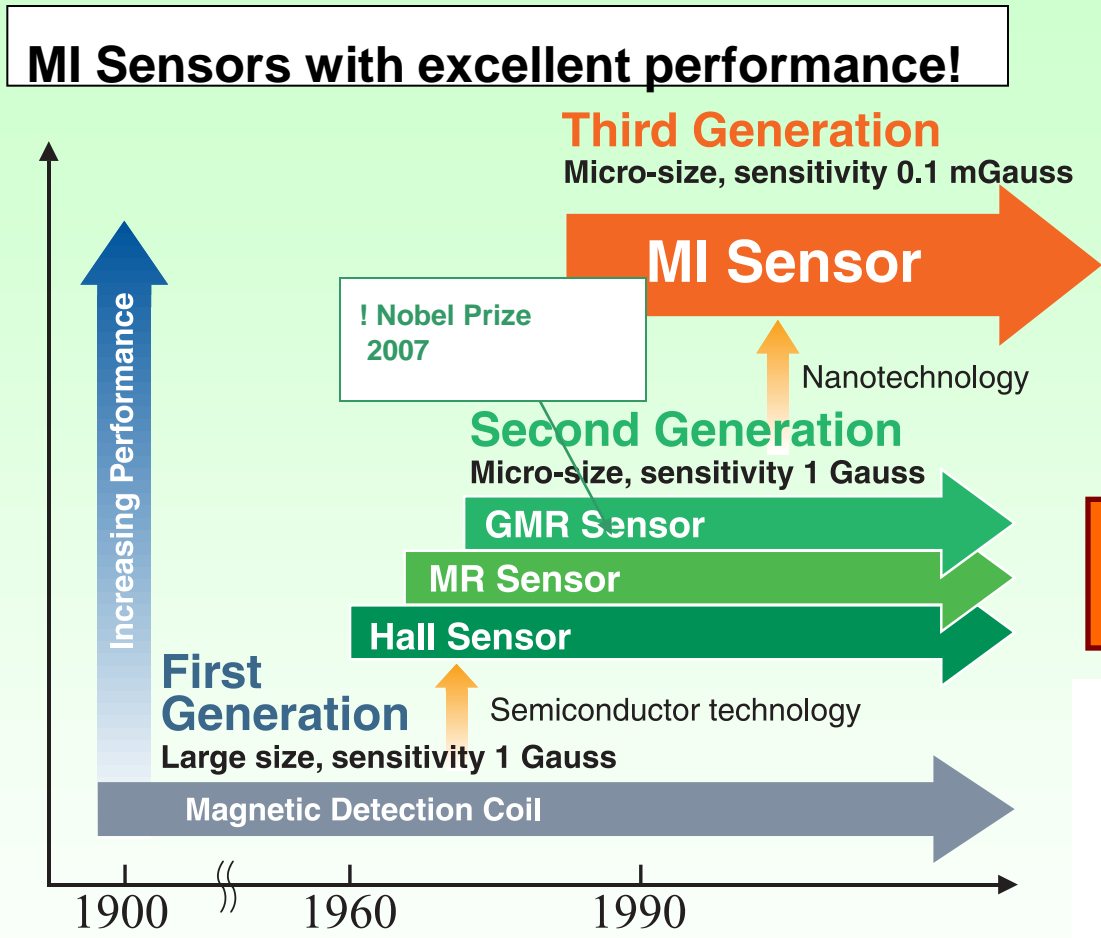
Melt extracted (40-50 μm)- not perfectly cylindrical cross section

Glass coated (0.1-50 μm)- glass coating (stresses)

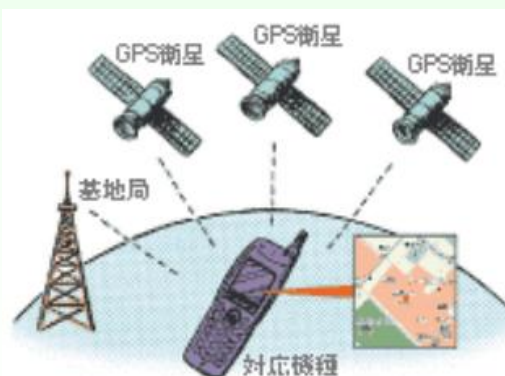
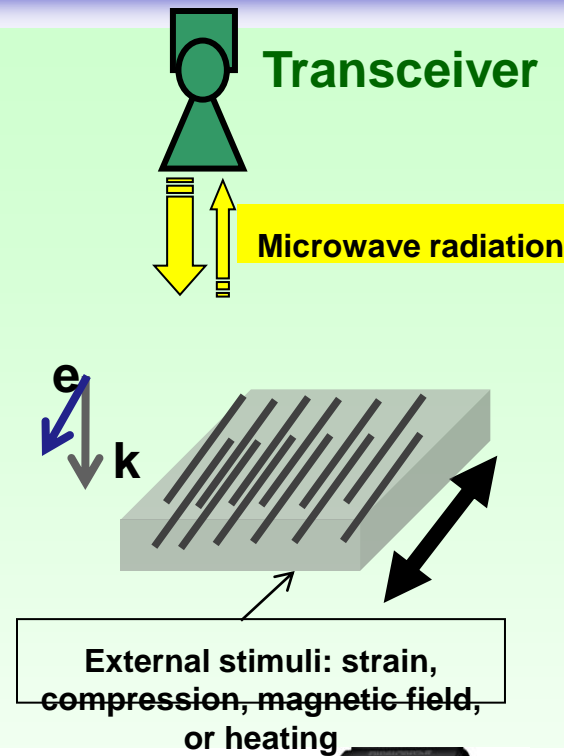


Third Generation of Magnetic Sensors

Smart composites



Based on Amorphous Wire since 2010



Amorphous Wire 3-axis Electronic Compass chip: A MI 308

Resolution	0.16 μ T (160 nT)
Dynamic range	± 1.2 mT (± 12 Oe)
Power voltage V_{dd}	1.7 V
Power current I_{dd}	150 μ A
Power consumption	255 μ W
Operating temperature	-45 ~ 80 $^{\circ}$ C
Chip dimension	2.04 \times 2.04 \times 1.0 mm
Reversibility for big disturbance magnetic field shock	∞



- Advantageous of MI sensor :**
- 1) Micro size and small power consumption (sub-mW)
 - 2) High sensitivity with resolution of 0.01 % for dynamic range (Pico-Tesla resolution)
 - 3) Quick response with GHz
 - 4) High reversibility for big magnetic field disturbance shock
 - 5) High temperature stability

Advanced 3-axis MI sensor chip installed in watch

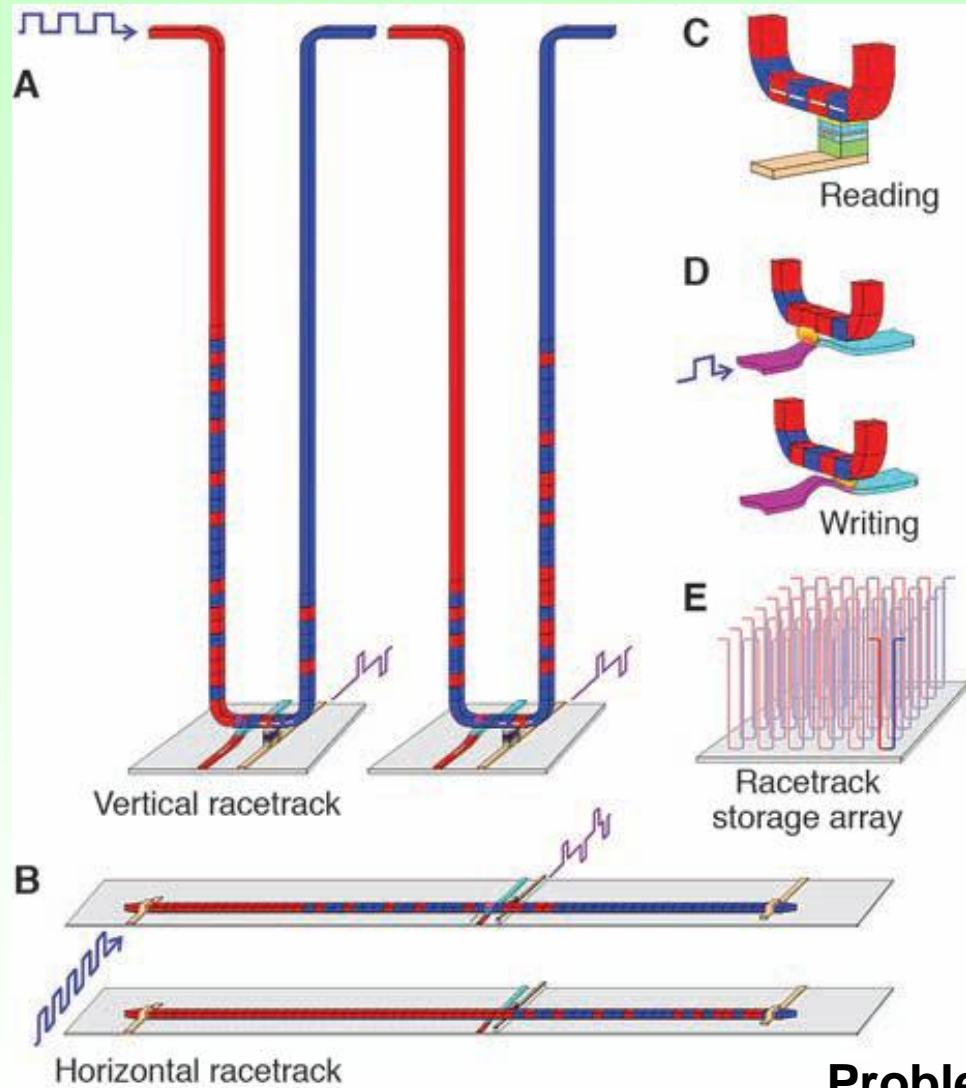
Magnetic Sensor History

Industrial application in Smart phone using MI sensor

Last tendencies: Size reduction, frequency increasing

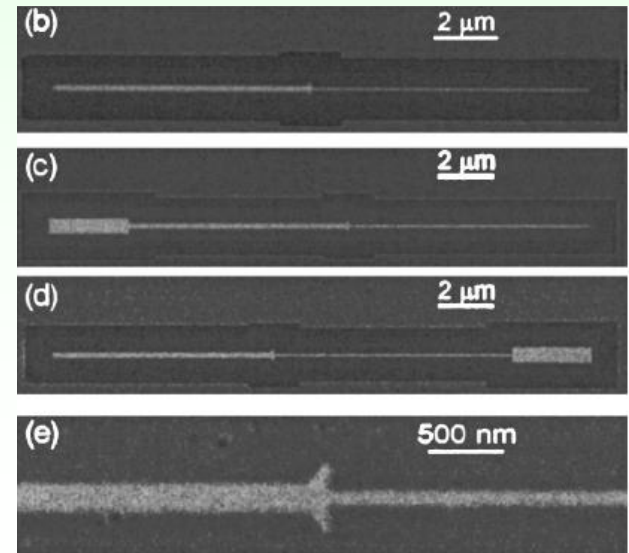
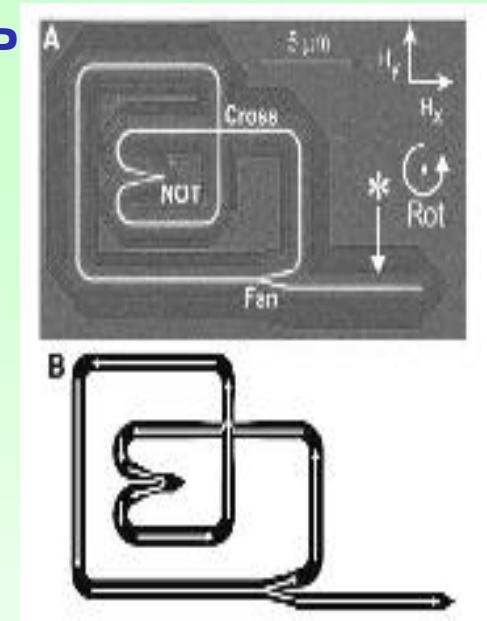
Soft magnets are needed

Promising applications: 2. Magnetic memory and logic based on DWP



Requisite: **controllable DWP**

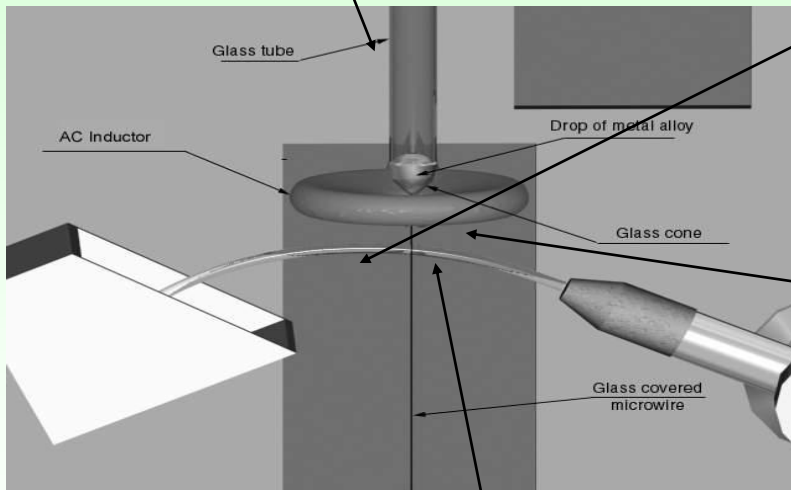
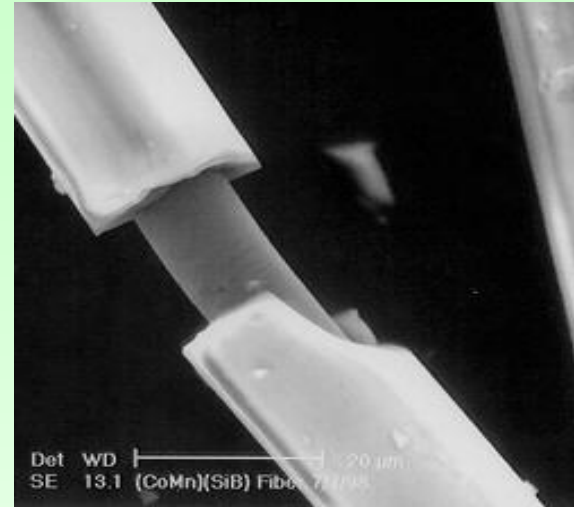
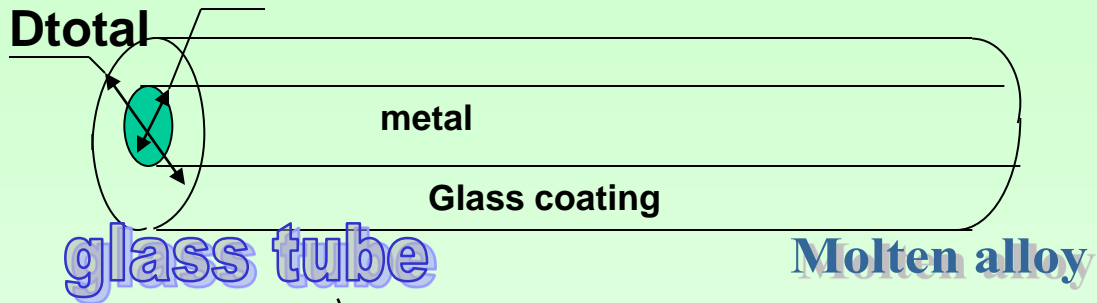
1 of 10 most emerging technologies in 2009
Technology review 2009, published by MIT



- Problems:**
1. Fast DWP (speed)
 2. Controlled DW pinning

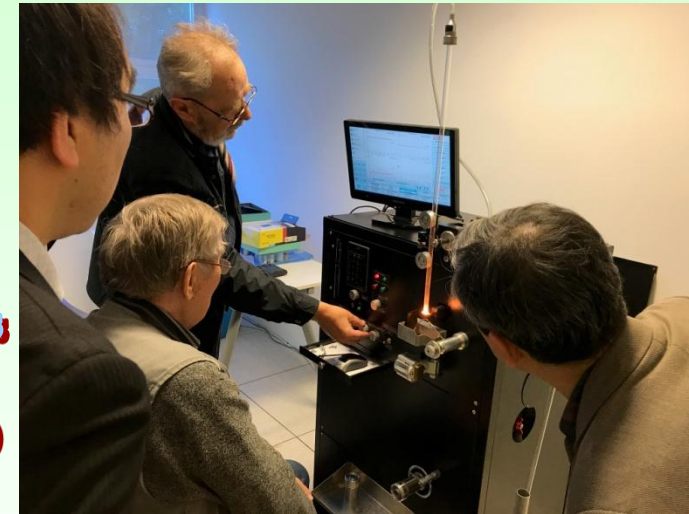
Glass coated microwires

- Co, Ni, Fe and Cu rich compositions
dmetal



HF Inductor

Typical dimensions:
 Total diameter 3-40 microns
 Metallic nucleus diameter 1-30 microns
 Glass coating thickness 1-10 microns
 Length - few km (up to 10 in 1 bobbin)



- Advantages:
1. Unexpensive and simple fabrication method ($1g \approx 1km$)
 2. Excellent soft magnetic properties and high **GMI effect**
 3. **Fast DW propagation**
 4. Also recently Heusler-type and granular microwires
 5. Biocompatibility (glass-coating)

Receiving bobbins

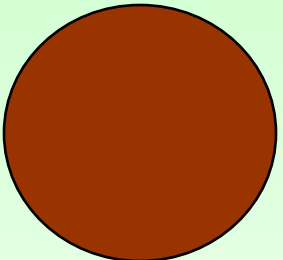
Water jet

Raw materials saving, better corrosion resistance, robust properties, medical applications...

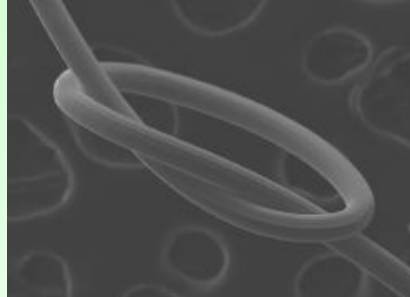
Comparison of microwires with other soft magnetic materials



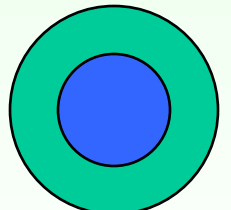
Ribbons, Cross section above $4 \times 10^4 \mu\text{m}^2$, fast and cheap fabrication, extremely soft magnetic properties, too big for microsensors applications



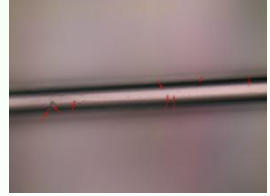
Wires, cross section above $2 \times 10^3 \mu\text{m}^2$, fast and cheap fabrication, good magnetic properties, effect of sample Length - too big for microsensors applications



Thin films, cross section $0.1 - 10^2 \mu\text{m}^2$, slow fabrication, Higher cost, worse magnetic softness, good compatibility in integrated circuits, effect of substrate



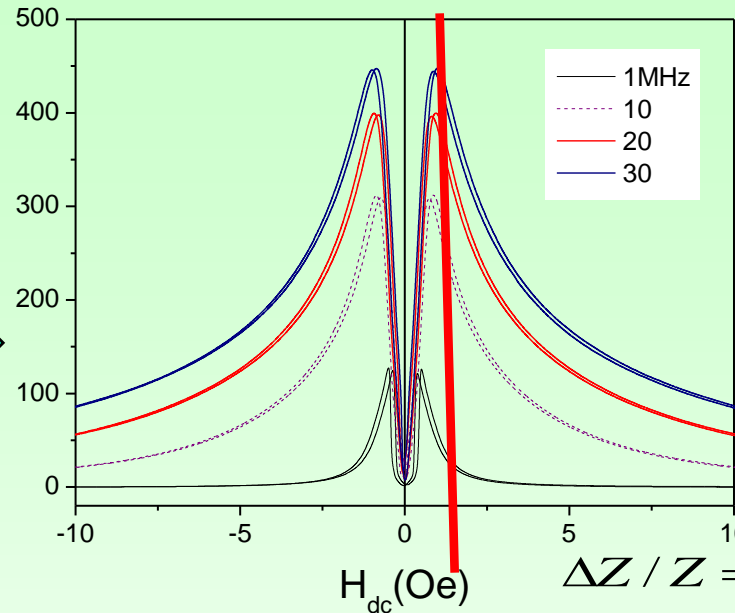
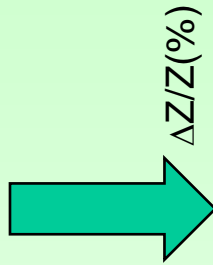
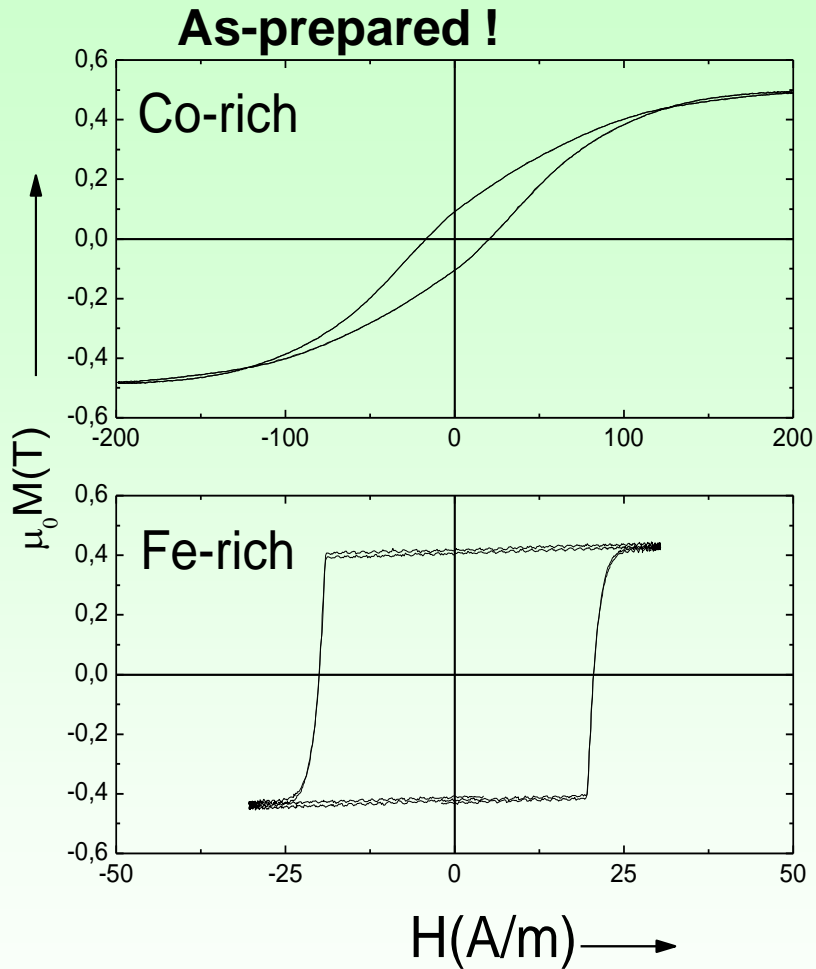
Microwires, typical cross section above $4 - 2 \times 10^3 \mu\text{m}^2$, fast and cheap fabrication, extremely soft magnetic properties, good for microsensors applications



Scale (cross section)

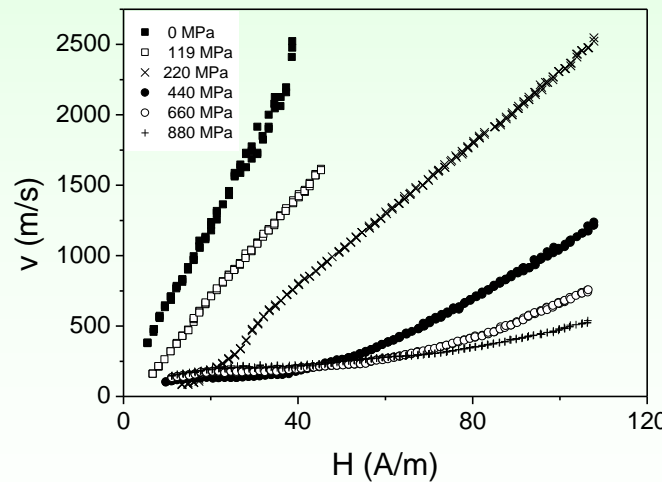
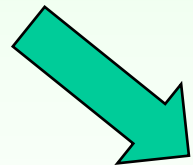


MAGNETIC PROPERTIES OF AMORPHOUS MICROWIRES



GMI effect, high sensitivity
 450%/Oe: 1 Oe = 0,1 mT
 1% MI change $\approx 0,0002$ mT

$$\Delta Z / Z = \{ |Z(H_{ex})| - |Z(H_{max})| \} / |Z(H_{max})|$$



**Fast magnetization switching,
 DW velocity up to 2.5 km/s**

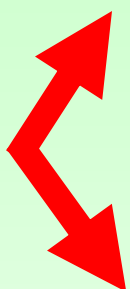
$$v = S (H - H_0)$$

Performance of devices depends on GMI effect value (defined as MI ratio) and DW velocity values.

Engineering of magnetic properties of magnetic microwires

Wire based sensors

Tuneable Parameters



Non-reversible

Reversible

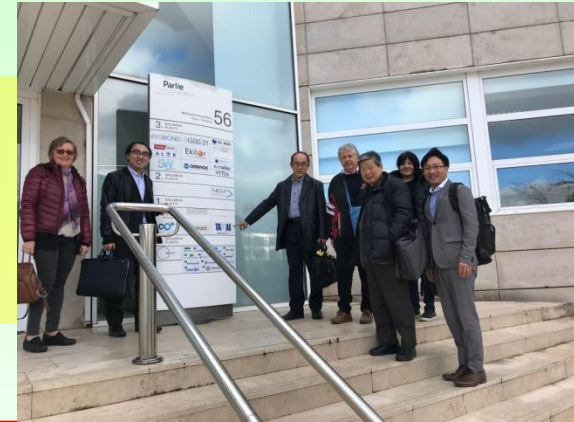
First step

- Composition
- Geometric ratio, ρ
- Conditions of thermal treatment (crystallization)

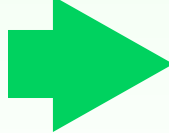
Second step: fine tuning

- Local heating
- Mechanical stress
- Axial-circular crossed magnetic field
- Conditions of thermal treatment (crystallization)

APPLICATIONS



Optimal magnetic properties

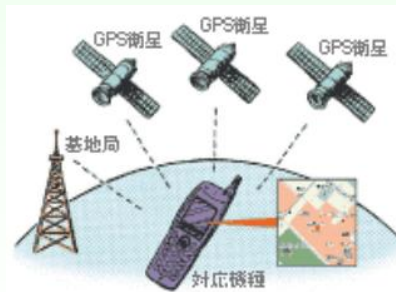


Magnetic microelectronics

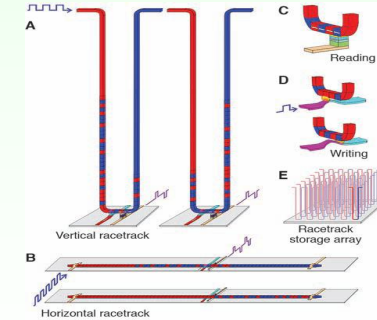
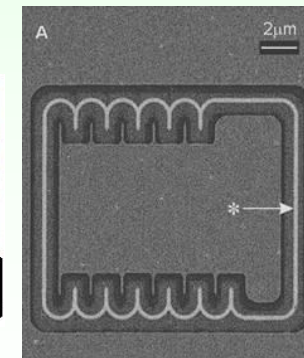
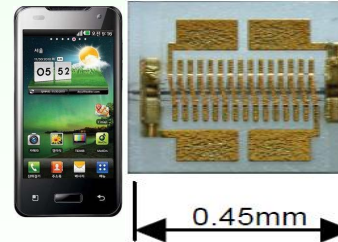


CASIO 2013.June 68250yen

Provided by Prof. K. Mohri



Source: Aichi Micro Intelligent Corporation



S. S. P. Parkin, et al. *Science* **320**, 190 (2008)

Factors affecting soft magnetic properties of amorphous alloys

Amorphous materials do not have defects typical for crystalline materials
(dislocations, point defects...)

H. Kronmüller (1981) contributions in coercivity of amorphous materials:

Local anisotropy fluctuations (10^{-3} –1 me), $H_c(i)$

Clusters and chemical inhomogeneities (< 1 me), $H_c(SO)$

Surface defects and irregularities (< 5 Me), $H_c(surf)$

Local structural defects (0.1-10 me), $H_c(rel)$

Pinning of DW on defects in magnetostrictive alloys (10-100 Me), $H_c(s)$

$$H_c(\text{total}) = [H_c(s)^2 + H_c(\text{surf})^2 + H_c(SO)^2 + H_c(i)^2]^{1/2} + H_c(\text{rel})$$

или

$$H_c(\text{total}) = H_c(s) + H_c(\text{surf}) + H_c(SO) + H_c(i) + H_c(\text{rel})$$

Magnetostriction

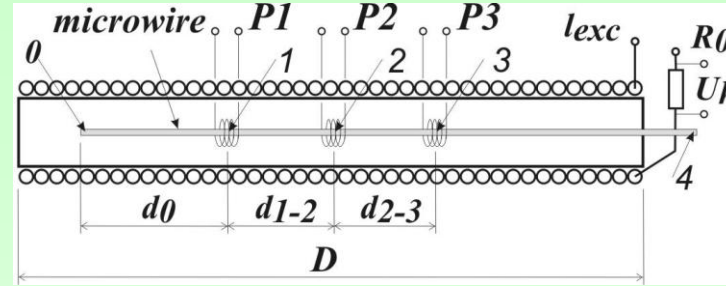
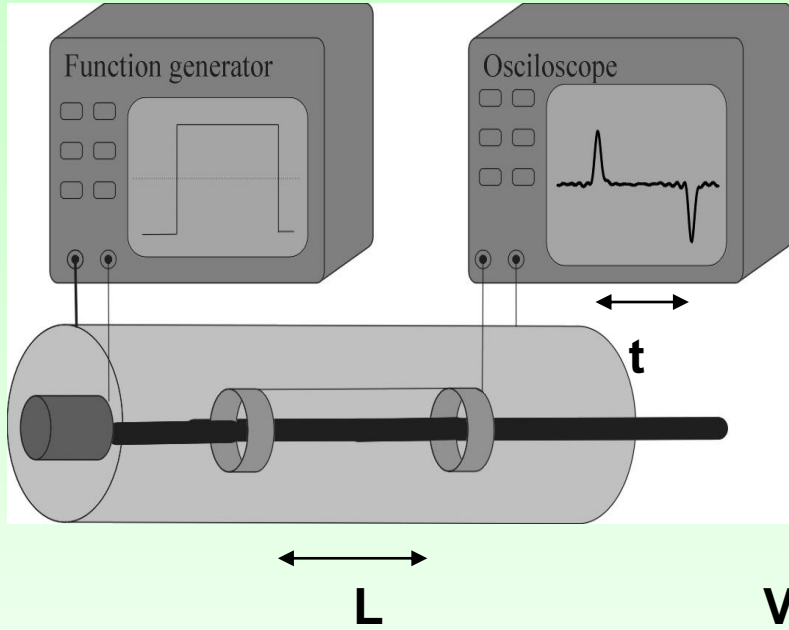
Anisotropy (stresses), **induced anisotropy**

Clusters and chemical inhomogeneities (nanocrystallization)

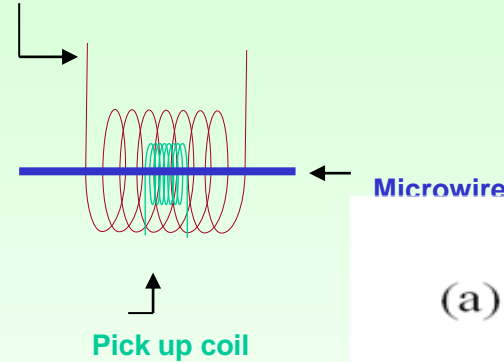
Defects (surface)

Measurements technique

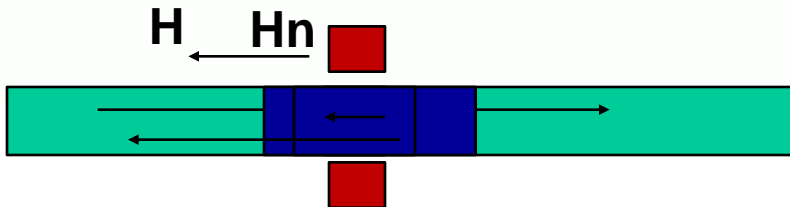
2. Sixtus-Tonks like experiment



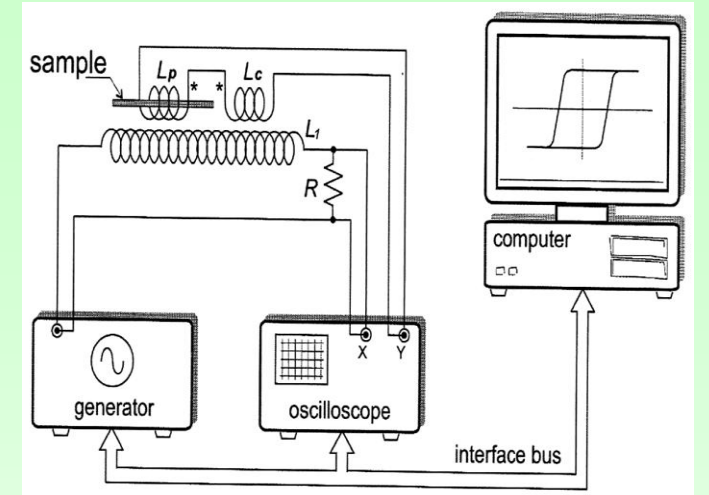
Exciting coil



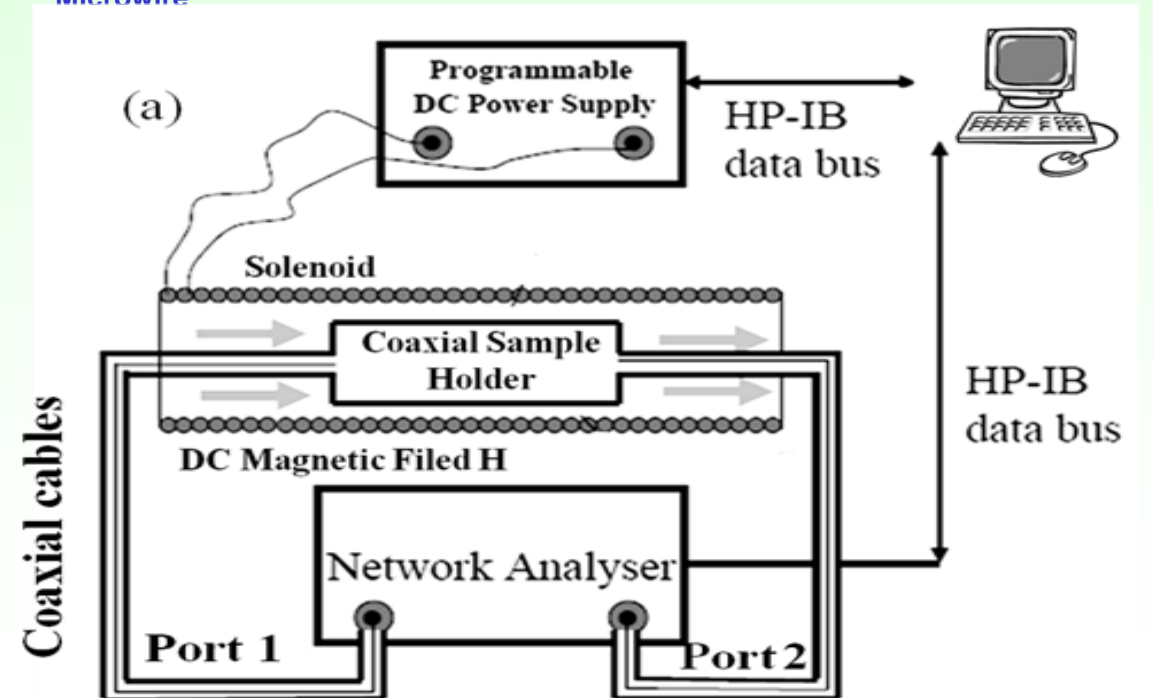
3. Nucleation profile (DW injection)!



1. Hysteresis loops

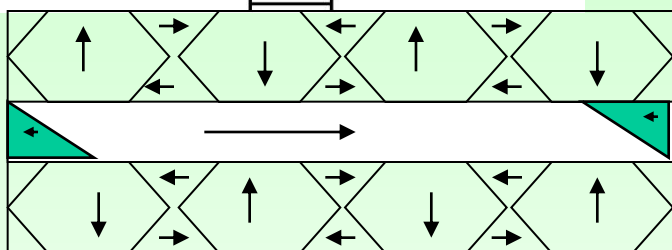
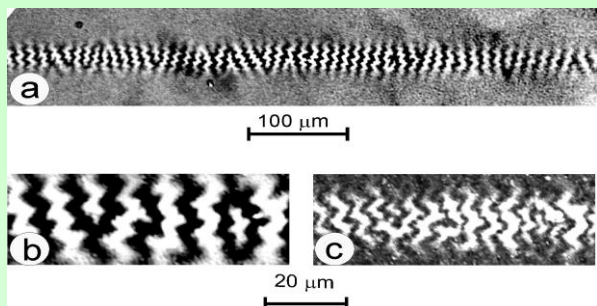


4. Measurements of GMI

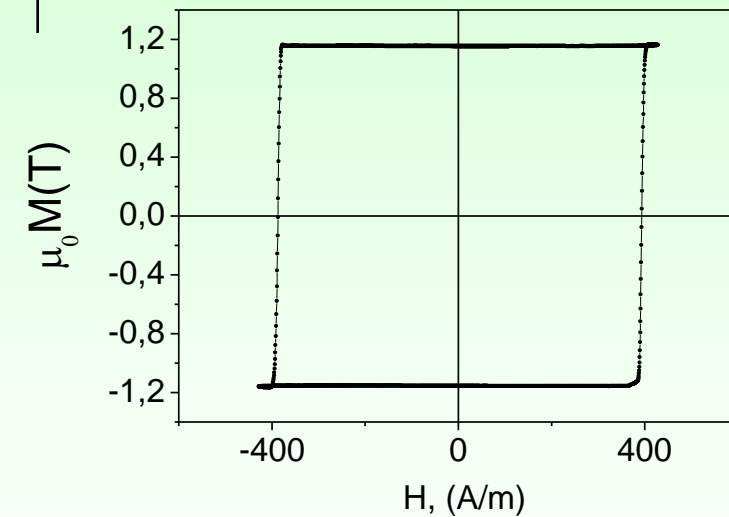
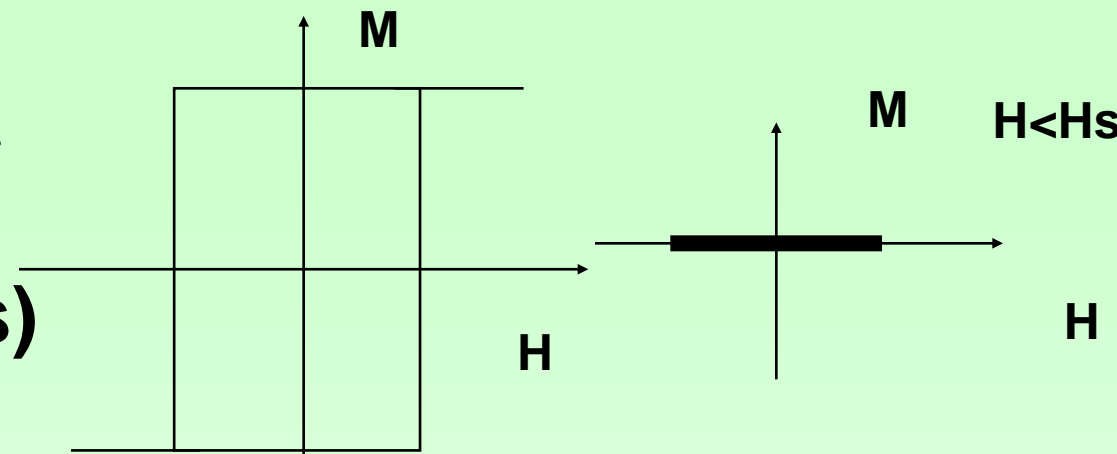
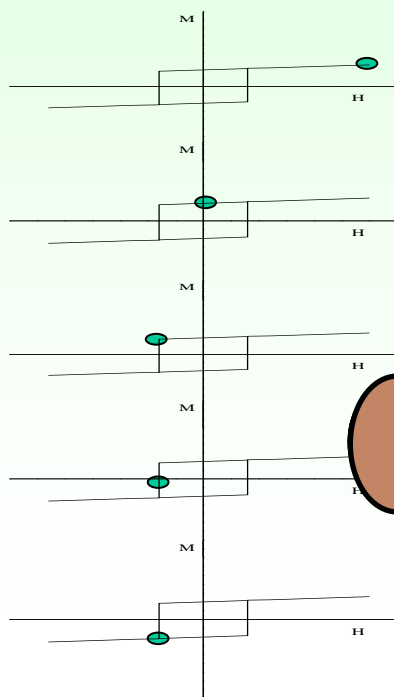


Yu. Kabanov, A. Zhukov, et al,
 Appl. Phys. Lett. 87 (2005) p142507

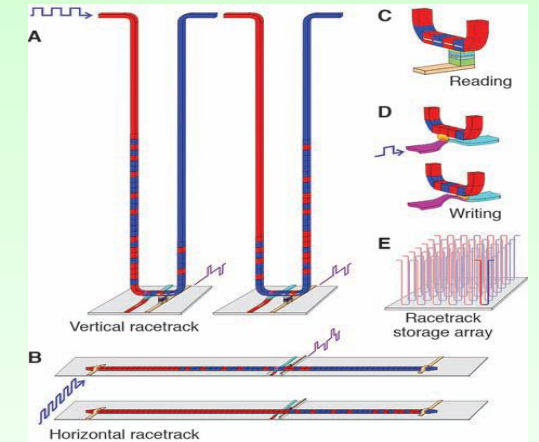
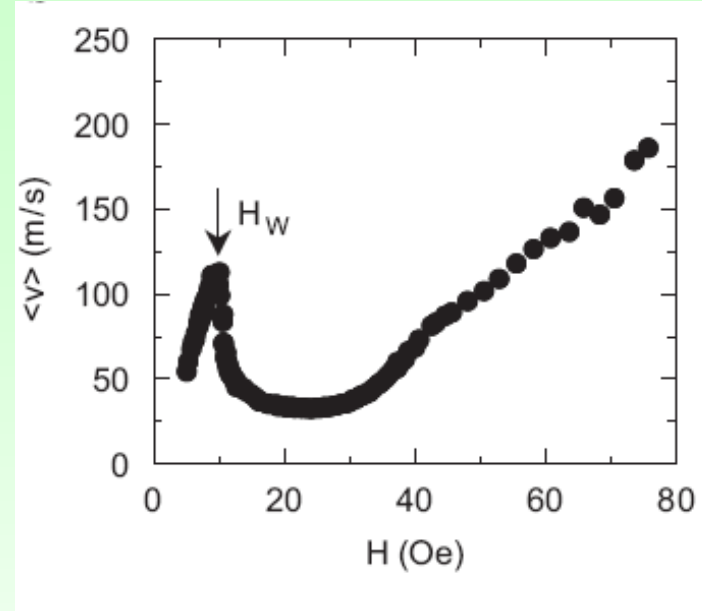
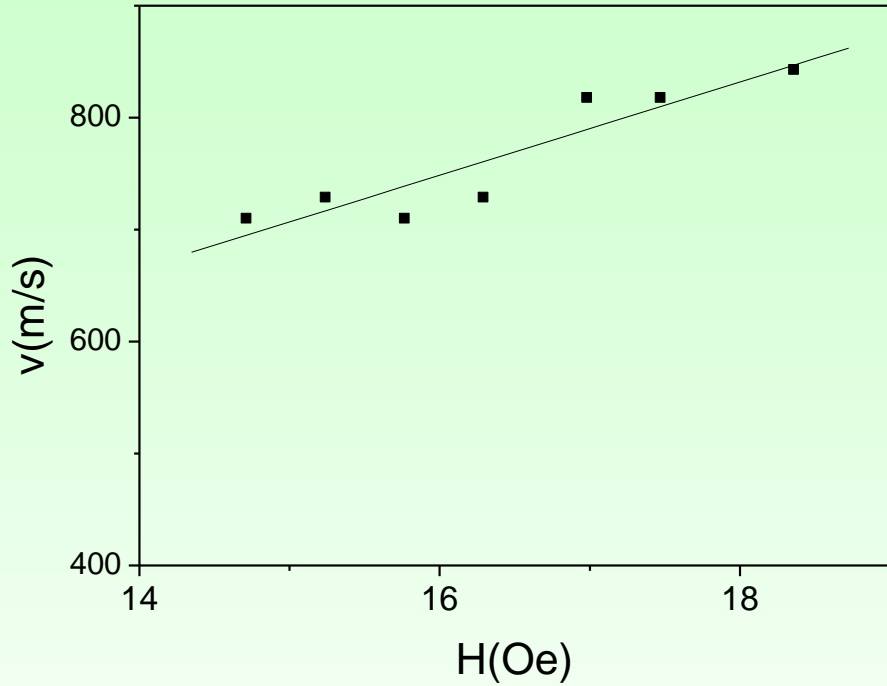
Bistable Loops (Fe-based microwires)



Schematic presentation of the re-magnetization process

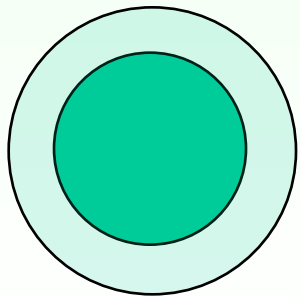


Comparison of domain wall dynamics measured in amorphous Fe-rich microwire and Fe-Ni rich planar nanowires.



Measured mobility curve for a 490nm×20nm Permalloy nanowire
 G.S.D. Beach et al. / J. Magn. Magn. Mater. 320 (2008) 1272–1281
 Experimentally observed maximum $v \approx 110$ m/s at 9 Oe

$d \approx 2,8 \mu\text{m}$ and total diameter $D \approx 9 \mu\text{m}$
 $\rho = 0,31$



DW dynamics measured in Fe-rich microwire and in Fe-Ni rich planar nanowires.

Magnetoelastic energy

Internal stresses in composite microwires

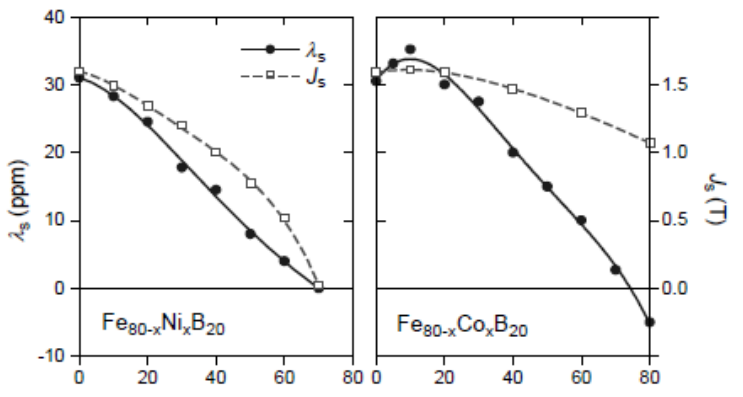
$$K_{me} \approx 3/2 \lambda_s \sigma_i, :$$

Magnetostriction λ_s -determines by the chemical composition

$$\sigma = \sigma_i + \sigma_a$$

σ_a - applied stresses

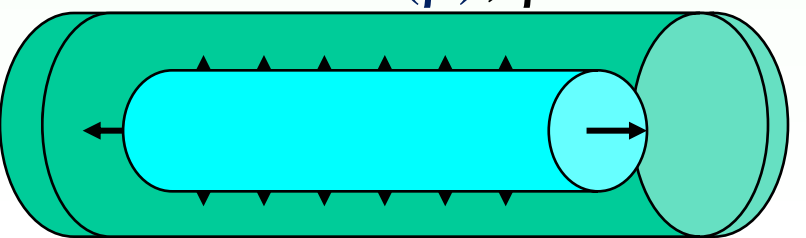
σ_i -determines by the ratio $\rho = d/D$



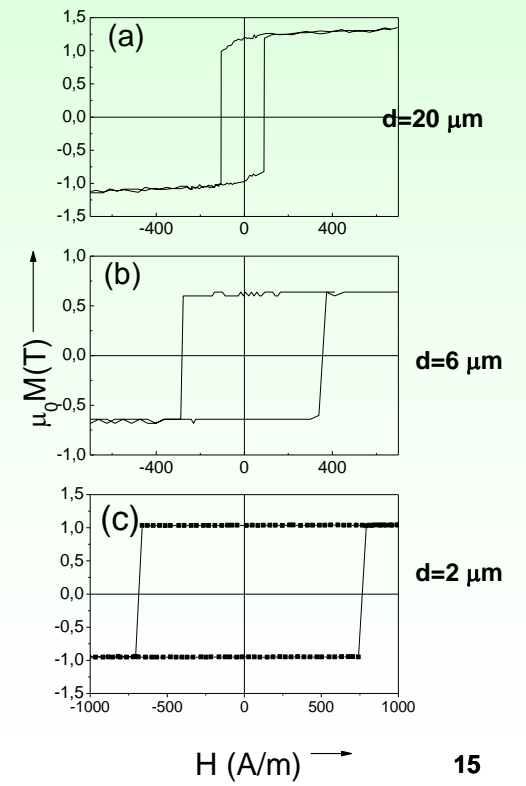
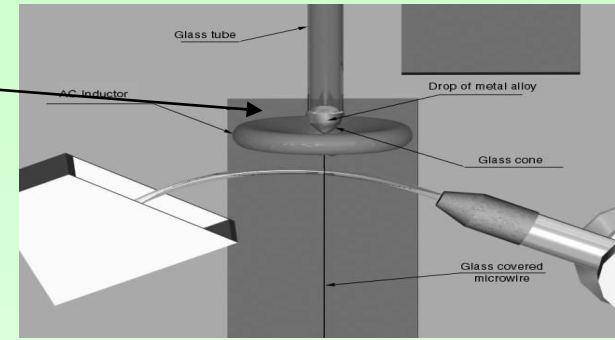
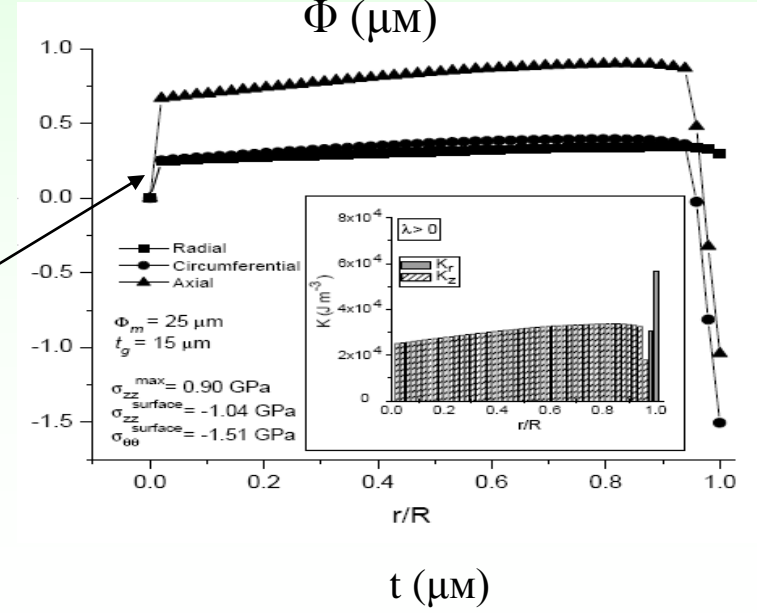
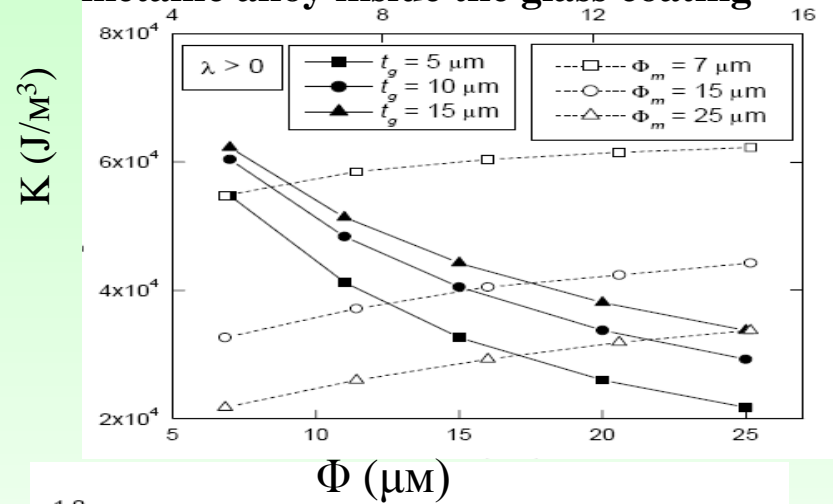
AMORPHOUS AND NANOCRYSTALLINE SOFT MAGNETS

G. Herzer
Vacuumschmelze GmbH & Co KG

$$\sigma = f(\rho), \rho = d/D$$



Stress appears at simultaneous solidification of metallic alloy inside the glass coating



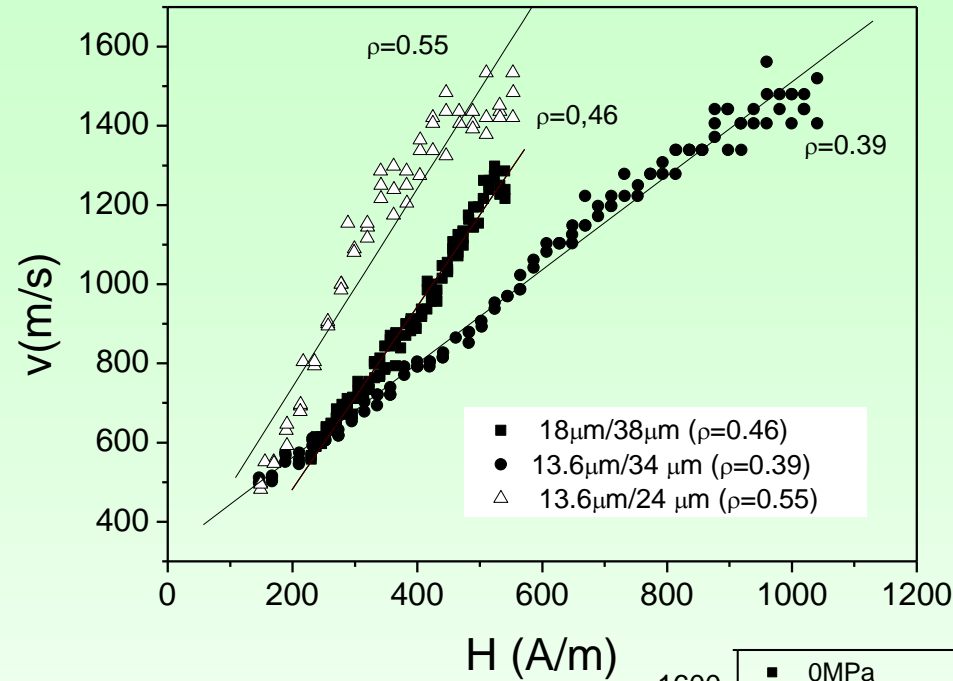
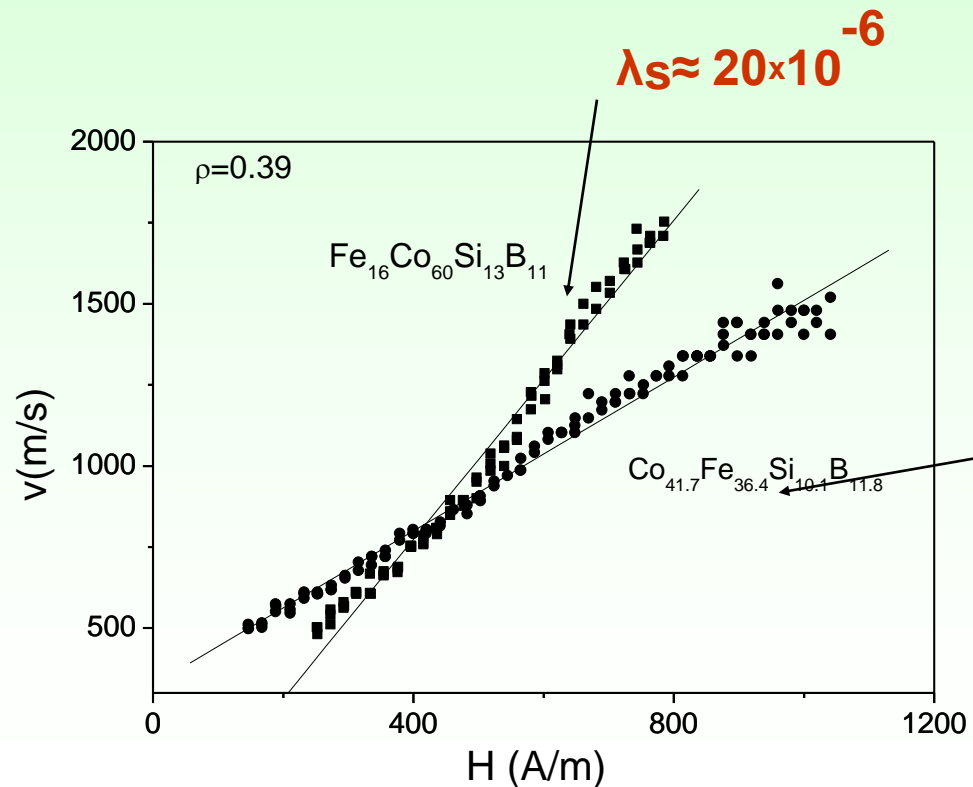
Effect of magnetolastic anisotropy on DW propagation

Fe-Co microwires

$$v = S(H - H_0)$$

where S is the DW mobility, H is the axial magnetic field and H_0 is the critical propagation field.

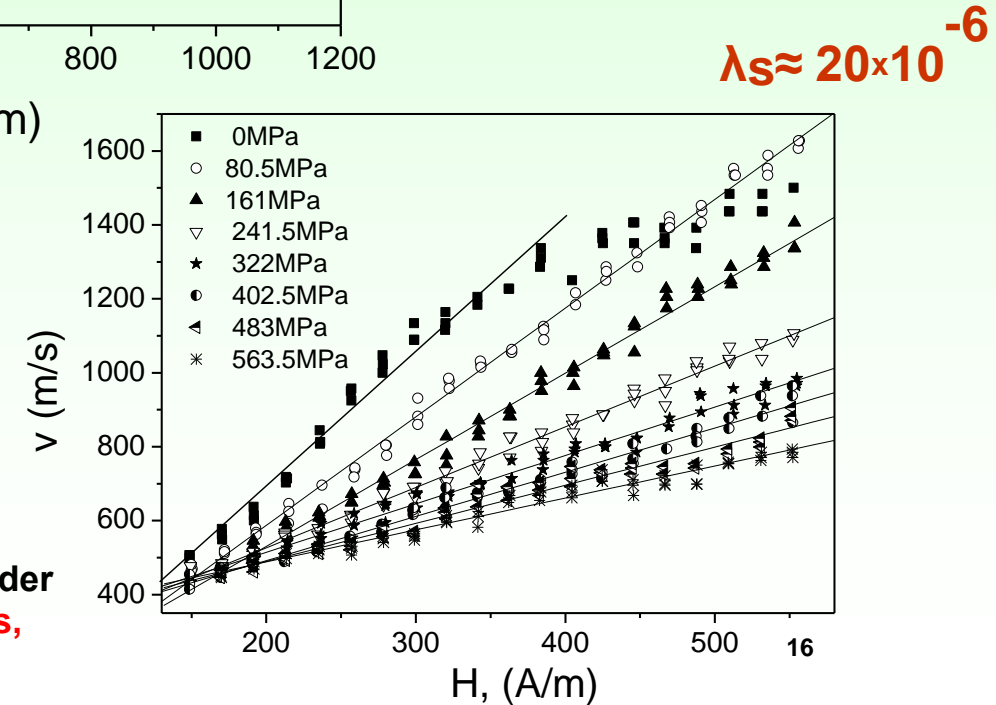
$v(H)$ dependences for Fe₁₆Co₆₀Si₁₃B₁₁ and Co_{41.7}Fe_{36.4}Si_{10.1}B_{11.8} microwires with $\rho=0,39$:
effect of magnetostriction



$v(H)$ dependences for Co_{41.7}Fe_{36.4}Si_{10.1}B_{11.8} microwires with different ratios ρ :
Effect of internal stresses $\sigma = f(\rho)$
Different internal stresses!

$$v = S(H - H_0)$$

$v(H)$ dependences for Co_{41.7}Fe_{36.4}Si_{10.1}B_{11.8} 3 microwires ($d \approx 13,6\mu\text{m}$, $D \approx 24,6\mu\text{m}$, $\rho \approx 0,55$) measured under application of applied stresses, σ_a .

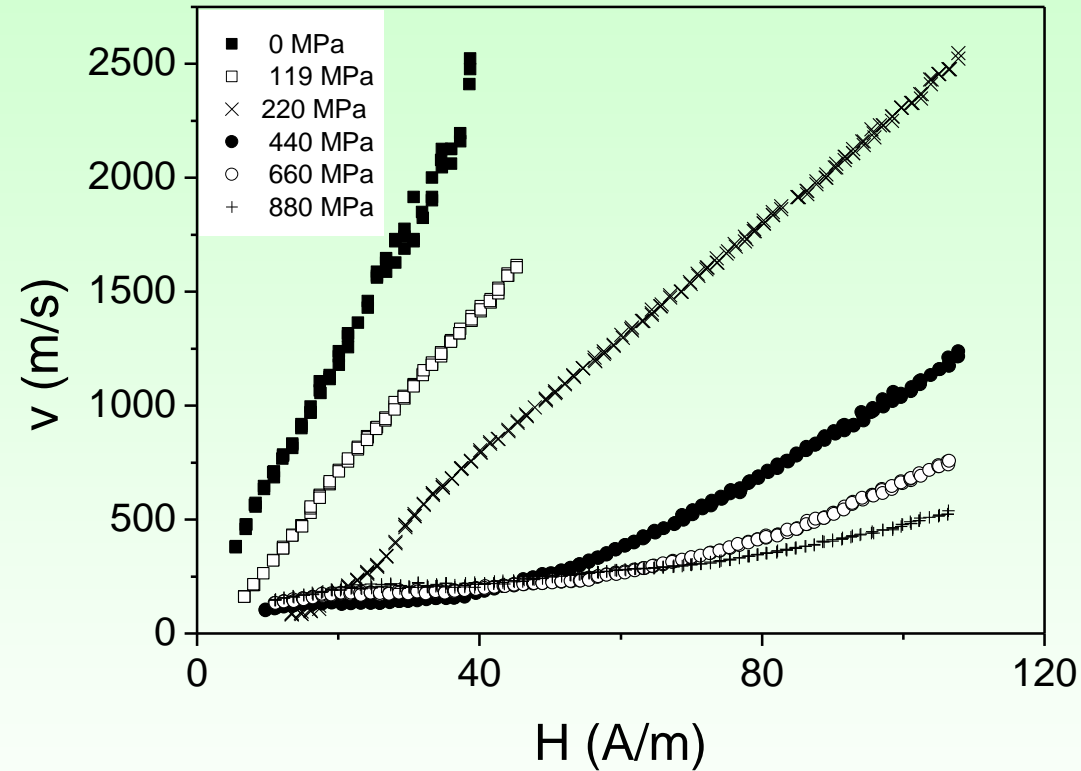


Effect of magnetoelastic anisotropy on DW propagation

$v = S(H - H_0)$, where S is the DW mobility, H is the axial magnetic field and H_0 is the critical propagation field.

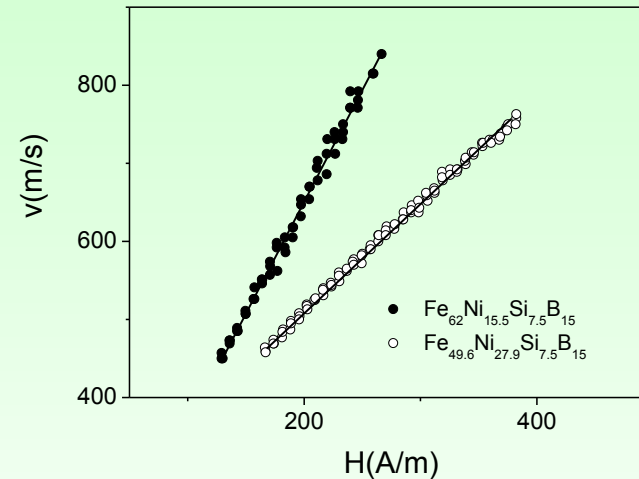
$$\lambda_s, \text{Fe}_{62}\text{Ni}_{15.5}\text{Si}_{7.5}\text{B}_{15} \approx 25 \times 10^{-6};$$

$$\lambda_s, \text{Fe}_{49.6}\text{Ni}_{27.9}\text{Si}_{7.5}\text{B}_{15} \approx 15 \times 10^{-6};$$



$v(H)$ dependences for $\text{Co}_{56}\text{Fe}_8\text{Ni}_{10}\text{Si}_{11}\text{B}_{16}$ microwires measured under application of applied stresses, σ_{app} .

Magnetoelastic energy, K_{me} , is given by $K_{me} \approx 3/2 \lambda_s \sigma$,



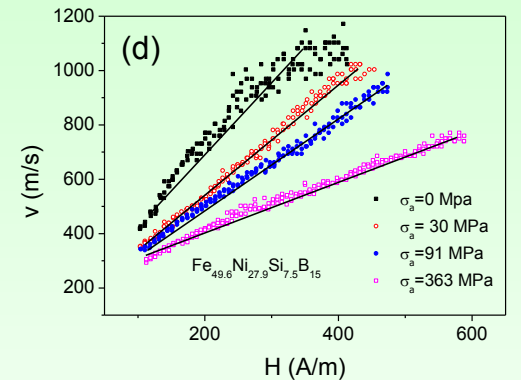
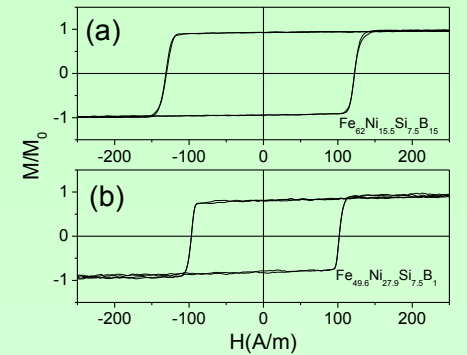
The domain wall mobility, S , is given by:

$$S = 2\mu_0 M_s / \beta$$

This damping is related to the Gilbert damping parameter, α and is inversely proportional to the domain wall width δw ,

$$\beta r \approx \alpha M_s / \gamma \delta w \approx M_s (K_{me} / A)^{1/2}$$

$V(H)$ is affected by K_{me}

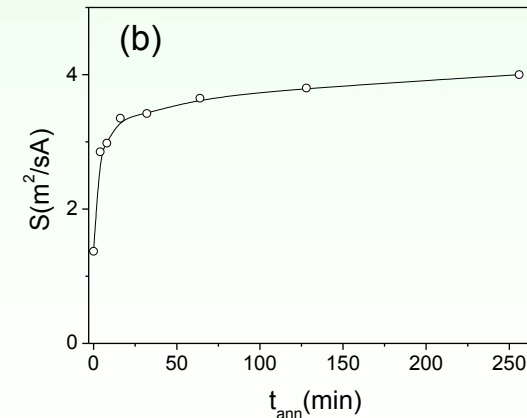
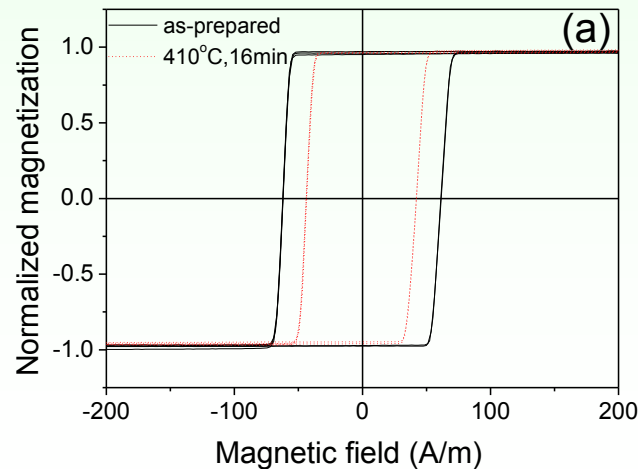
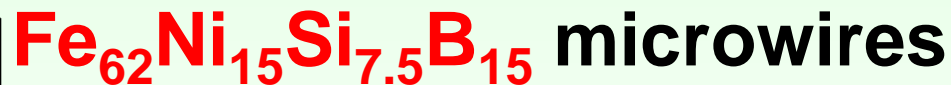
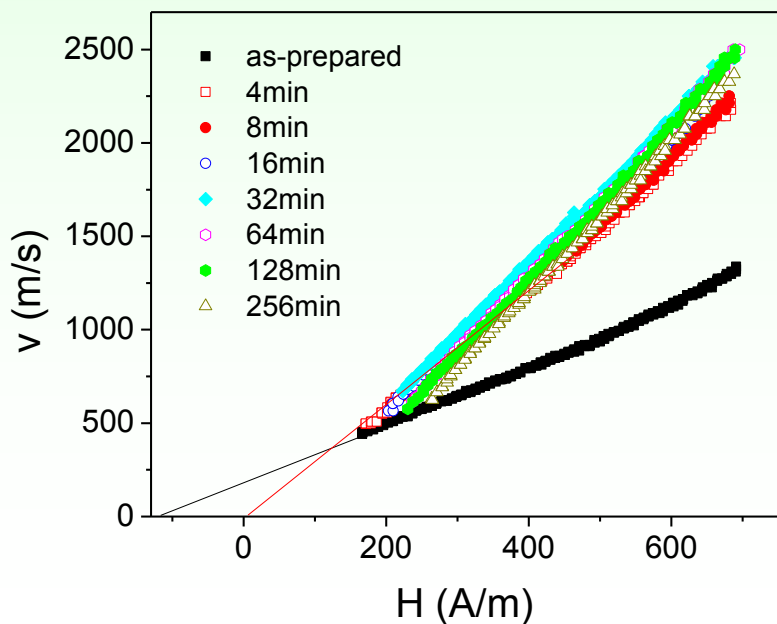
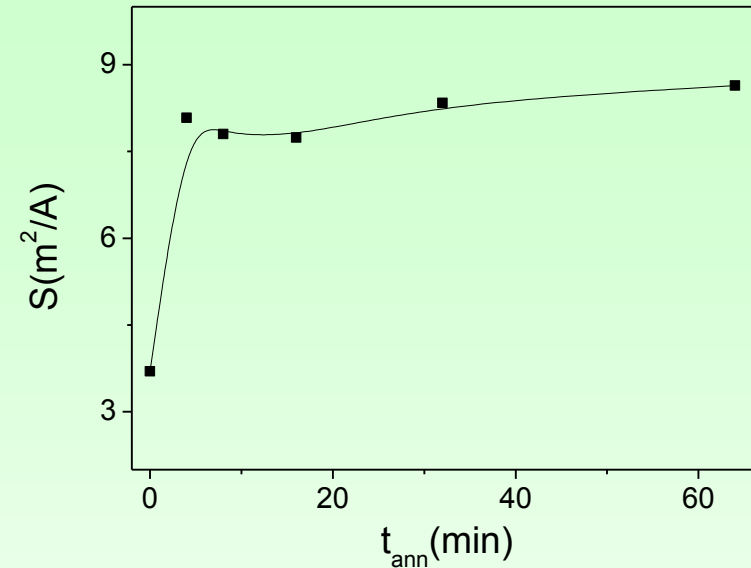
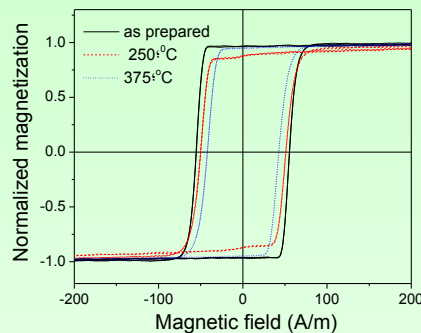
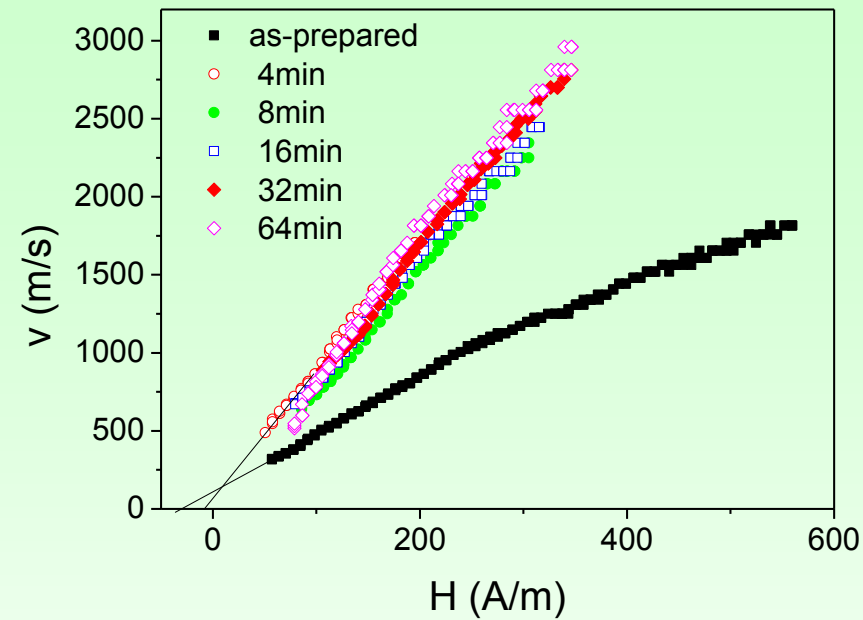


Effect of magnetolastic anisotropy on DW propagation

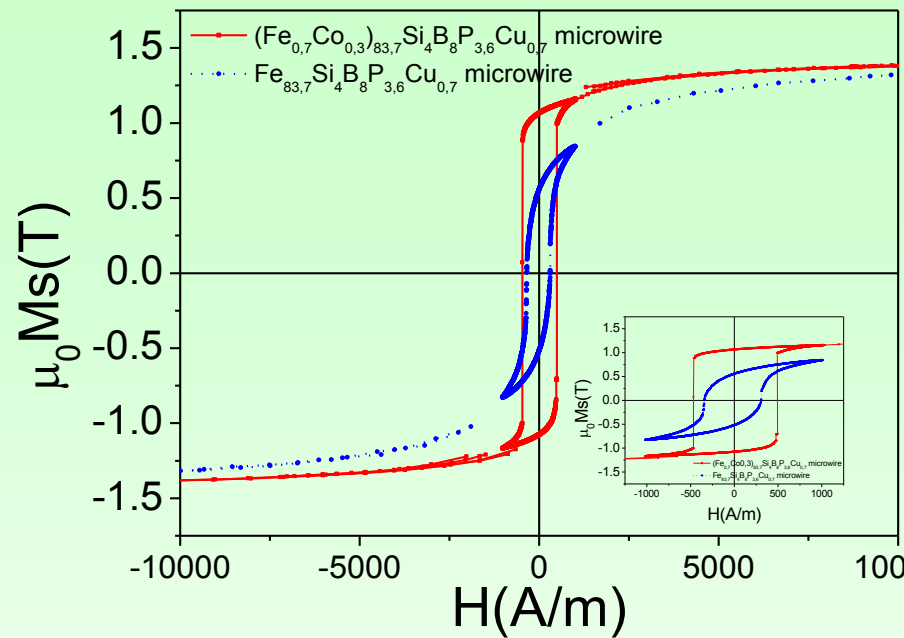
$$K_{me} \approx 3/2 \lambda_s \sigma_i$$



Stress relaxation? $T_{ann} \approx 410^{\circ}C$



Effect of saturation magnetization on DW propagation

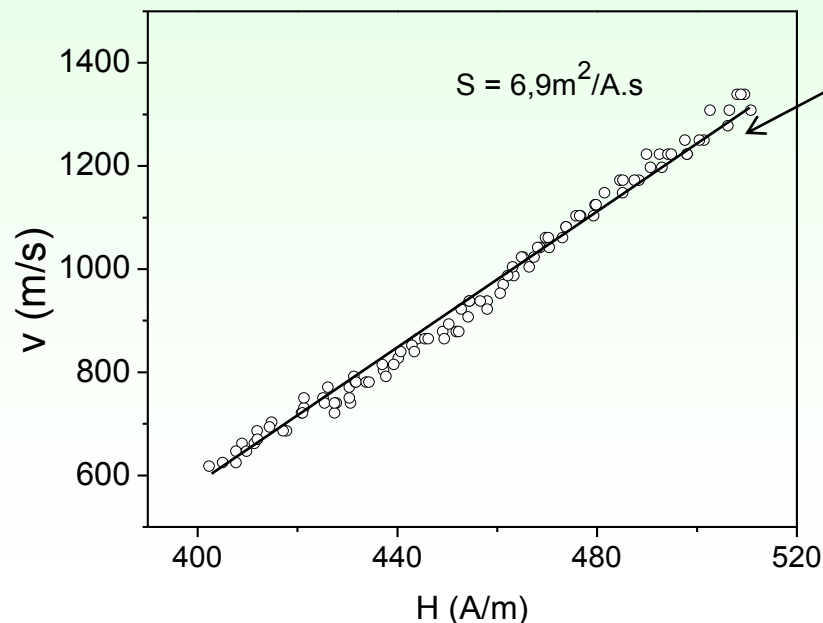


The domain wall mobility, S , is given by:

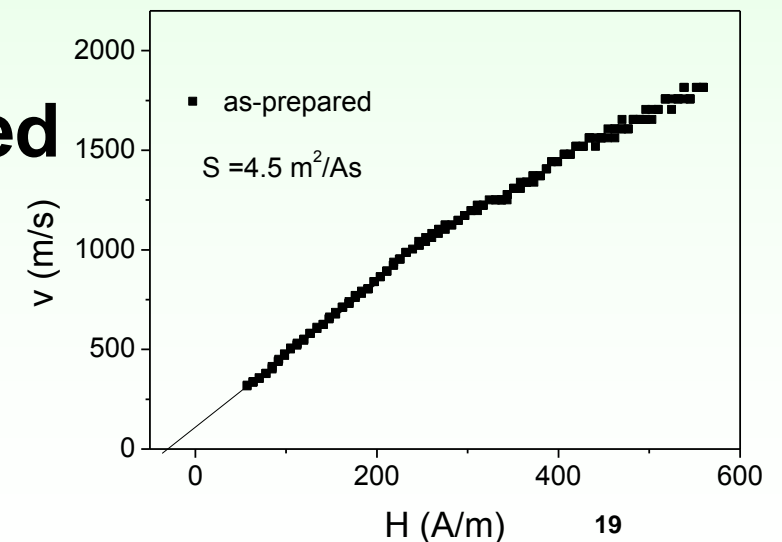
$$S = 2\mu_0 M_s / \beta$$

where, $\mu_0 M_s$ is the saturation magnetization

$$B_r \approx M_s (K_{me}/A)^{1/2}$$

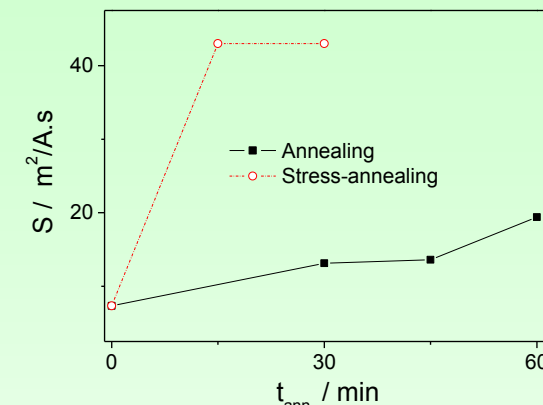
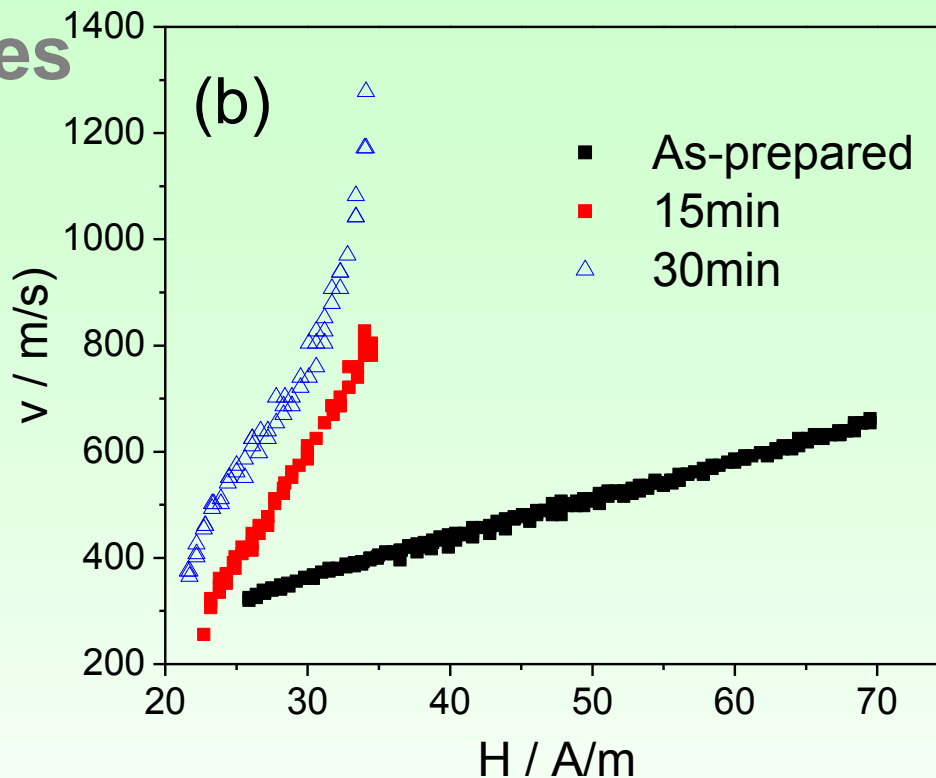
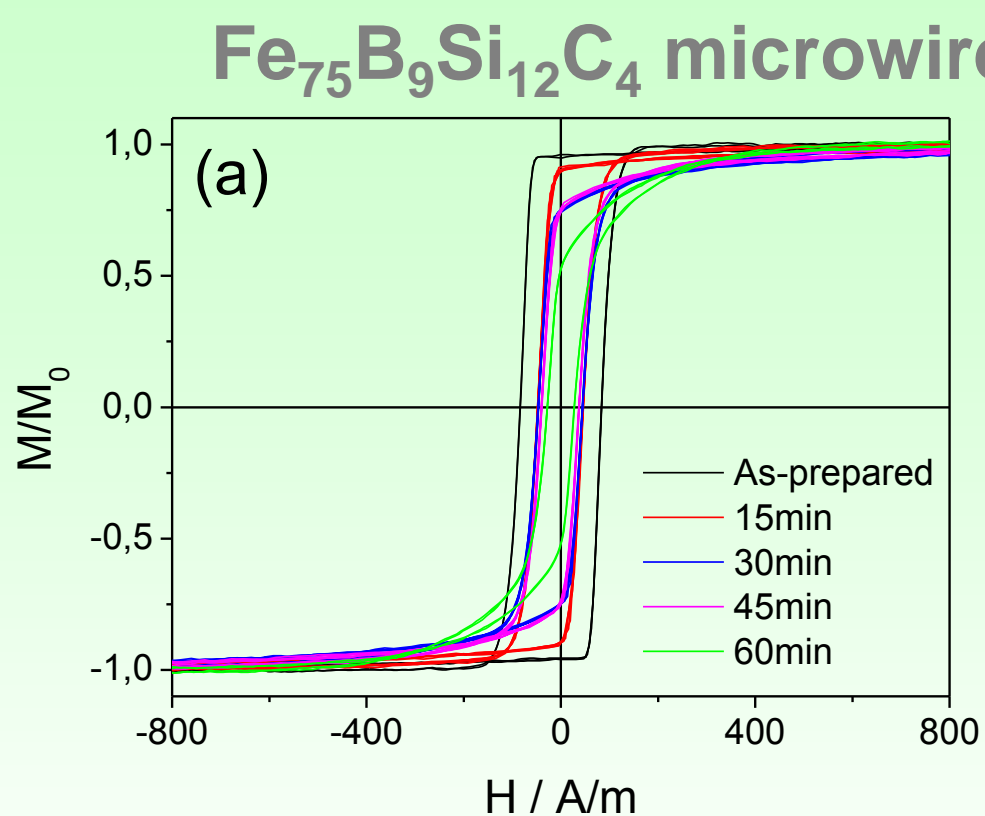


Higher S are observed in new Fe-rich composition with higher $\mu_0 M_s$



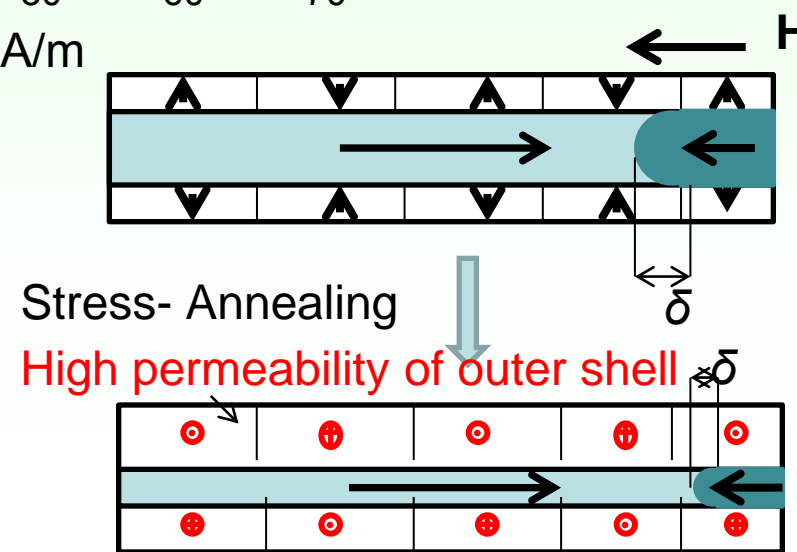
Stress- Annealing

Dependences of DW mobility, S , on annealing time for $\text{Fe}_{75}\text{B}_9\text{Si}_{12}\text{C}_4$ microwires annealed at $T_{ann} = 325$ °C.

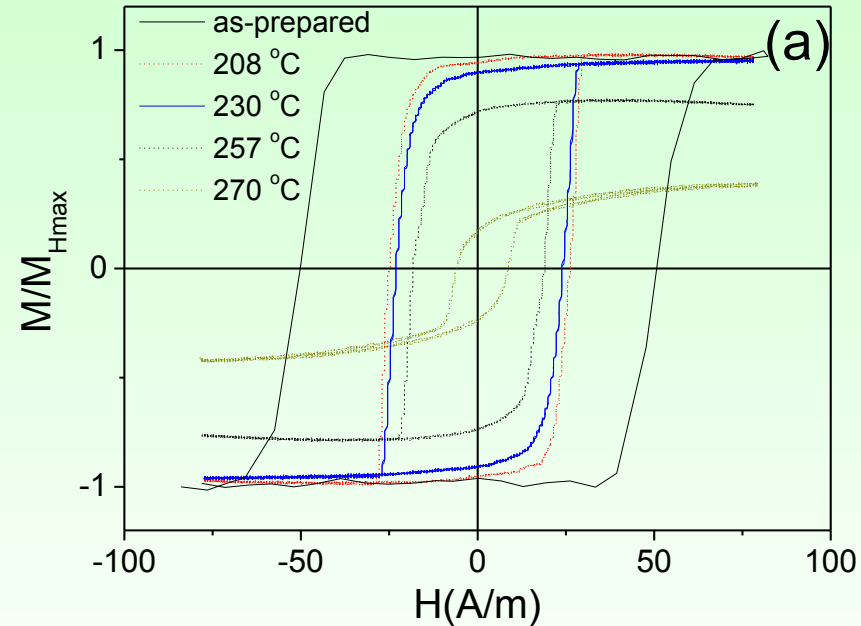
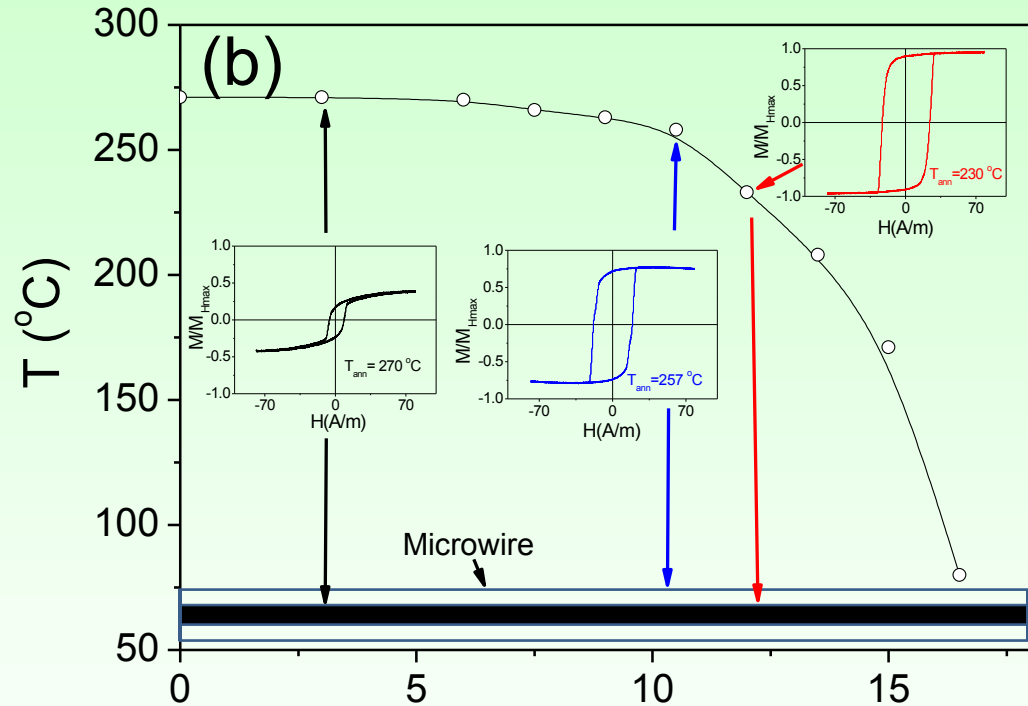


Remarkable DW movility improvement by stress-annealing!

Hysteresis loops (a) and $v(H)$ dependencies (b) of as-prepared and stress- annealed at $T_{ann} = 325$ °C and $\sigma_m=190$ MPa $\text{Fe}_{75}\text{B}_9\text{Si}_{12}\text{C}_4$ microwires.



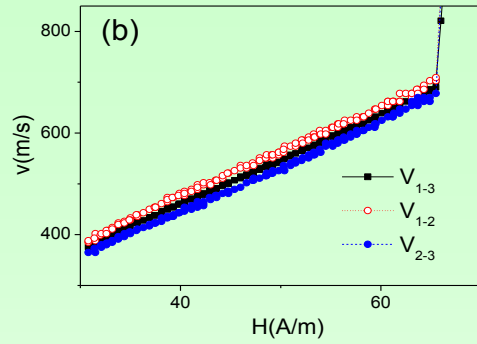
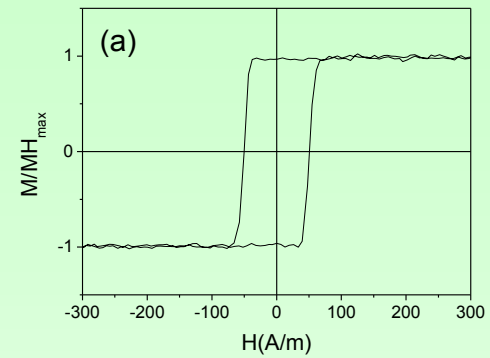
Grading of magnetic anisotropy and engineering of domain wall dynamics in Fe-rich microwires by stress-annealing



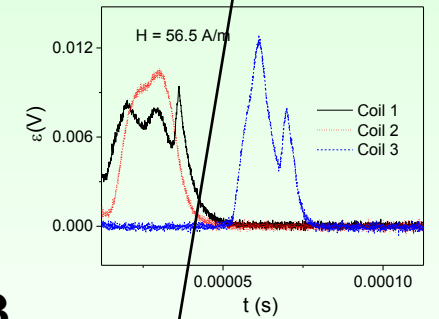
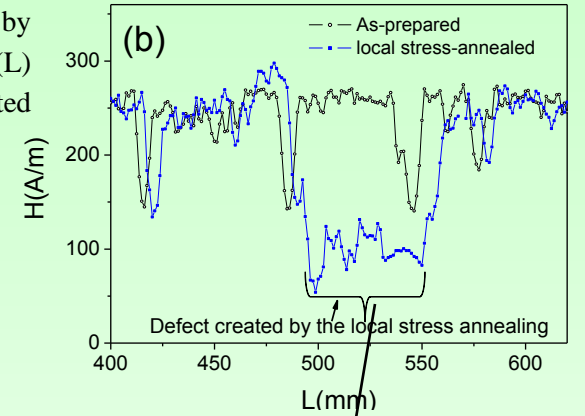
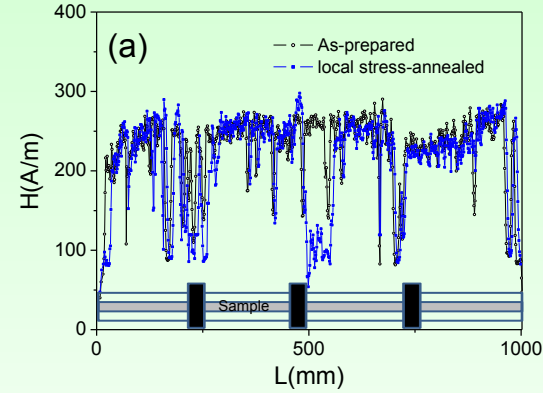
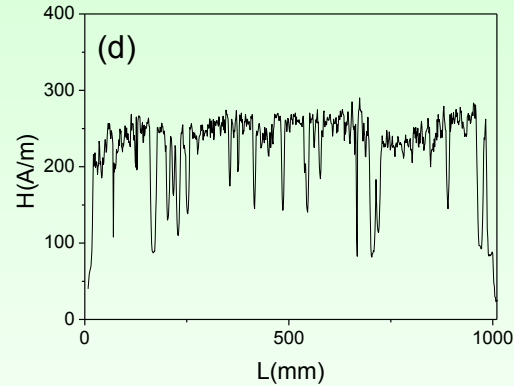
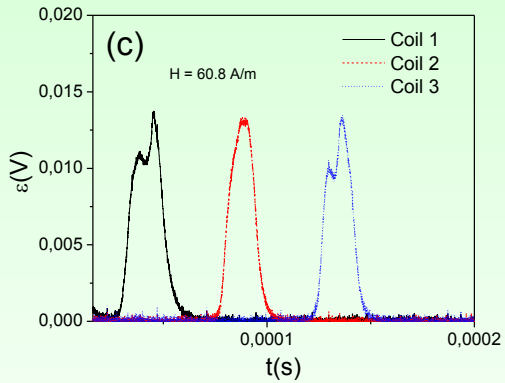
Usually graded anisotropy is obtained varying chemical composition during the sputtering

Hysteresis loops of L (cm) as-prepared and stress-annealed at different T_{ann} $\text{Fe}_{75}\text{B}_9\text{Si}_{12}\text{C}_4$ microwires (a) and graded magnetic properties of $\text{Fe}_{75}\text{B}_9\text{Si}_{12}\text{C}_4$ microwires annealed at variable T_{ann} .

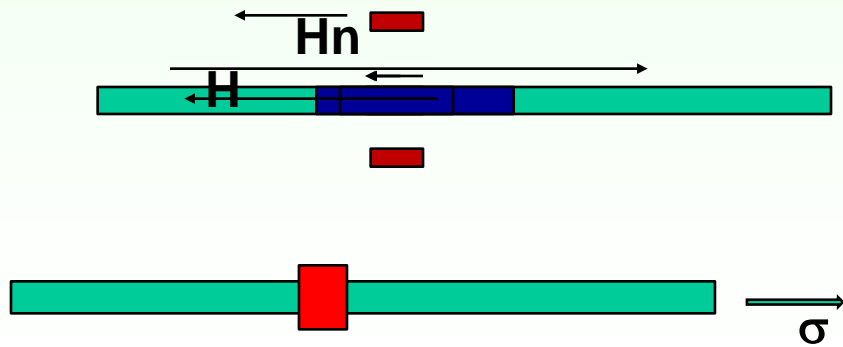
Engineering of domain wall dynamics in Fe-rich microwires by local stress- annealing



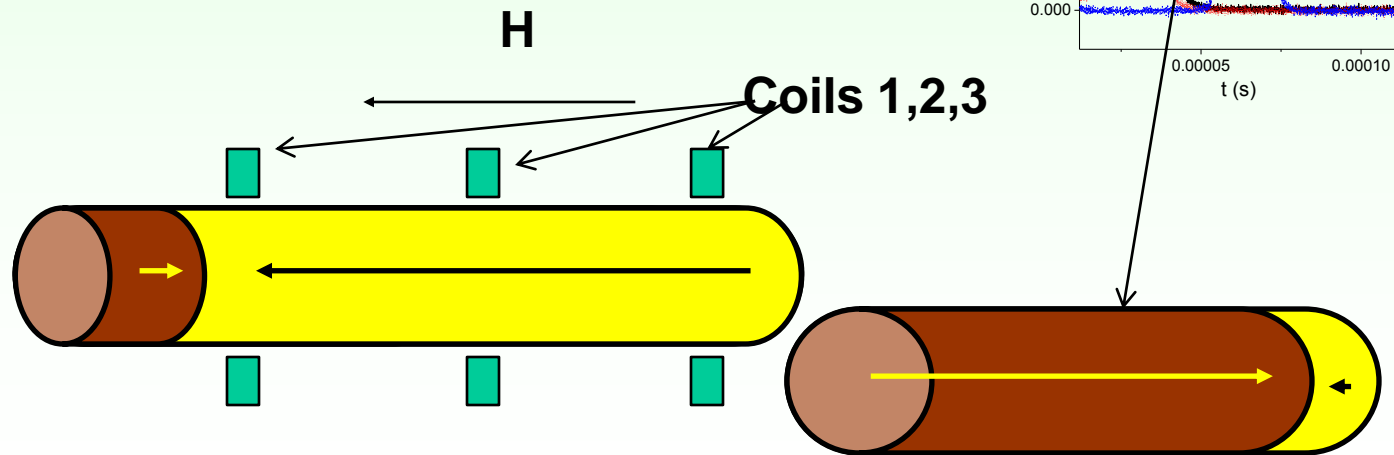
Hysteresis loop (a), $v(H)$ dependence (b), voltage peaks induced by the magnetization change in the pick-up coils (c) and $H_n(L)$ dependence (d) of as-prepared $\text{Fe}_{75}\text{B}_9\text{Si}_{12}\text{C}_4$ amorphous glass-coated microwire.



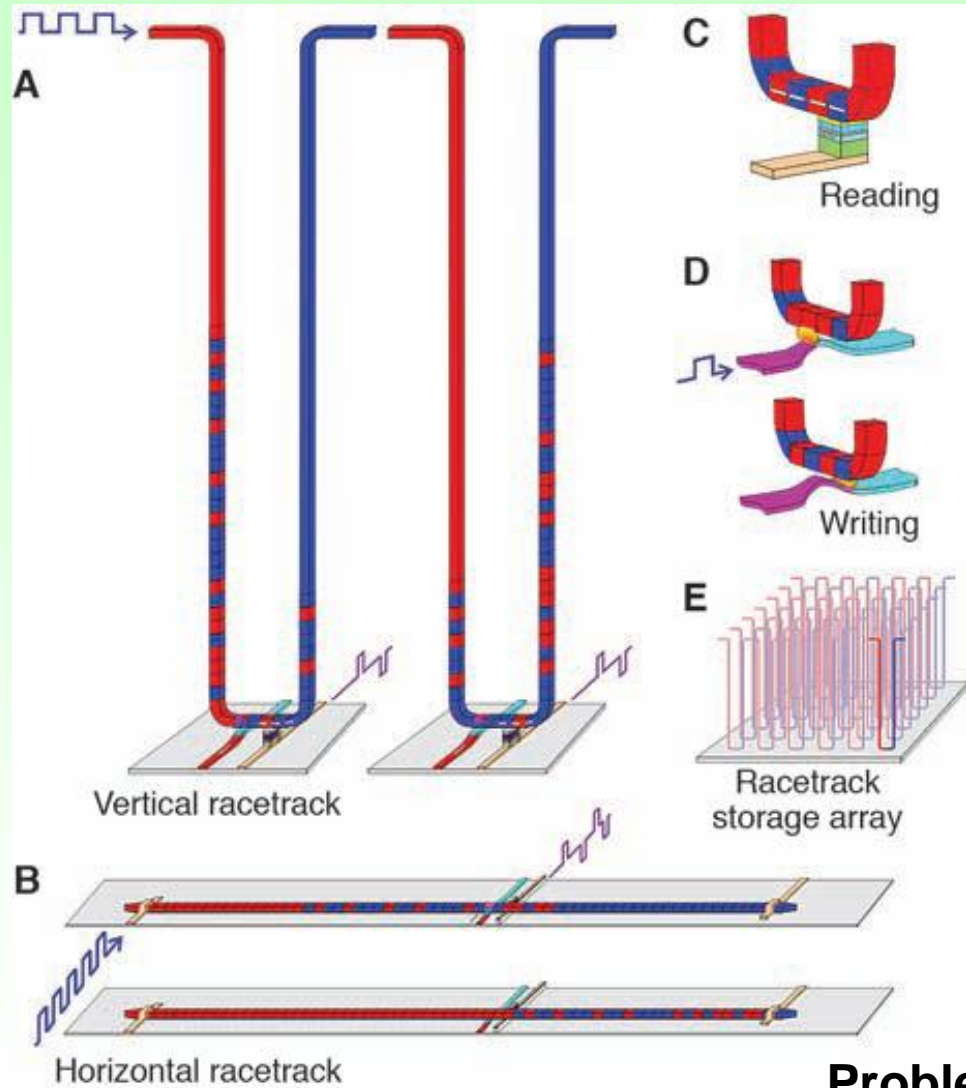
2. Nucleation profile (DW injection)!



Local heating

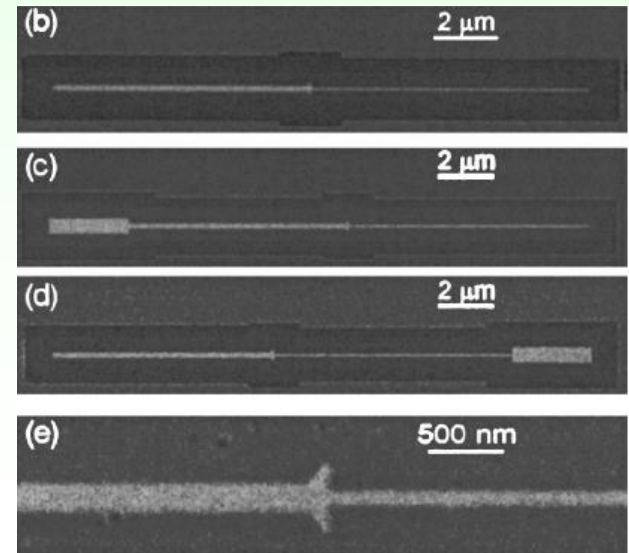
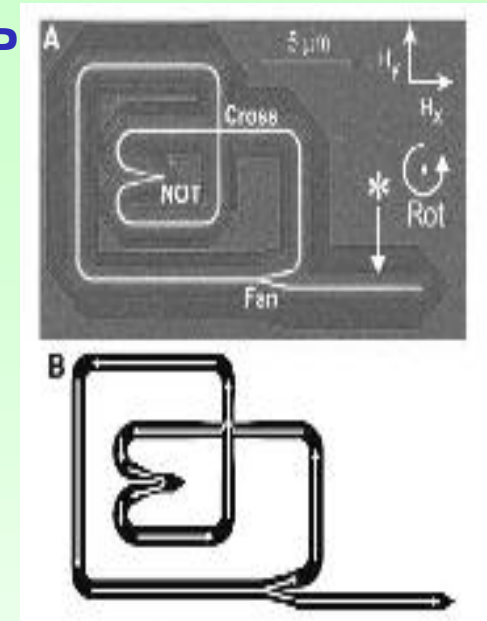


Promising applications: Magnetic memory and logic based on DWP



Requisite: **controllable DWP**

1 of 10 most emerging technologies in 2009
Technology review 2009, published by MIT



Problems:

- 1. Fast DWP (speed)**
- 2. Controlled DW pinning**

Stuart S. P. Parkin, *et al.* *Science* 320, 190 (2008);

APPLICATIONS:

Magnetic codification based on magnetic bistability

Publications

A. Zhukov, J.González, J.M. Blanco, M.Vázquez and V. Larin, J.

Mat. Res 15, (2000), 2107.

Patentes:

1. V. Larin, A. Torcunov, S. Baranov, M. Vázquez, A. Zhukov and A. Hernando, "Method of magnetic codification and marking of the objects", Patent (Spain) N° P 9601993 (1996).

2. M. Vázquez, A. Zhukov, A. Hernando, V. Larin, A. Torcunov, L. Panina, J. Gonzalez and D. Mapps, *TITULO:*

"Microwire and process of their fabrication. AWP/RPS/56672/000, No0108373.2 (UE) 01.11.2001

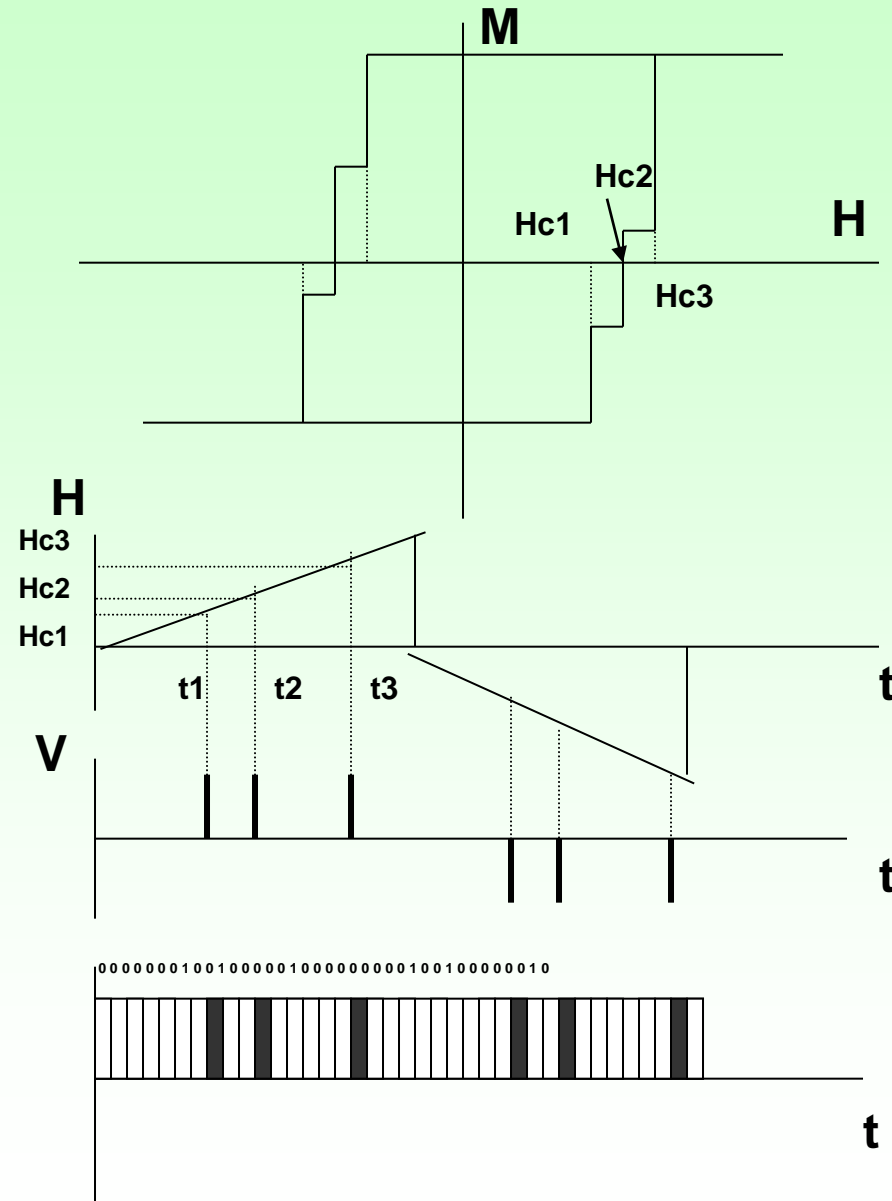
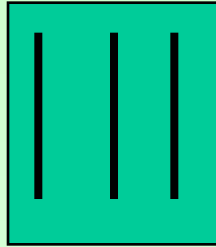
"Four wnds", Amotec" and "Tamag Iberica. S.L."

3. A. Zhukov, V. Zhukova, M. Vázquez, J. González, V. S. Larin y A.V. Torcunov "Amorphous microwires as an element of magnetic sensor based on magnetic bistability, magneto-impedance and

material for the radiation protection".

P200202248 (Span) 02.10.2002 "Tamag Iberica. S.L."

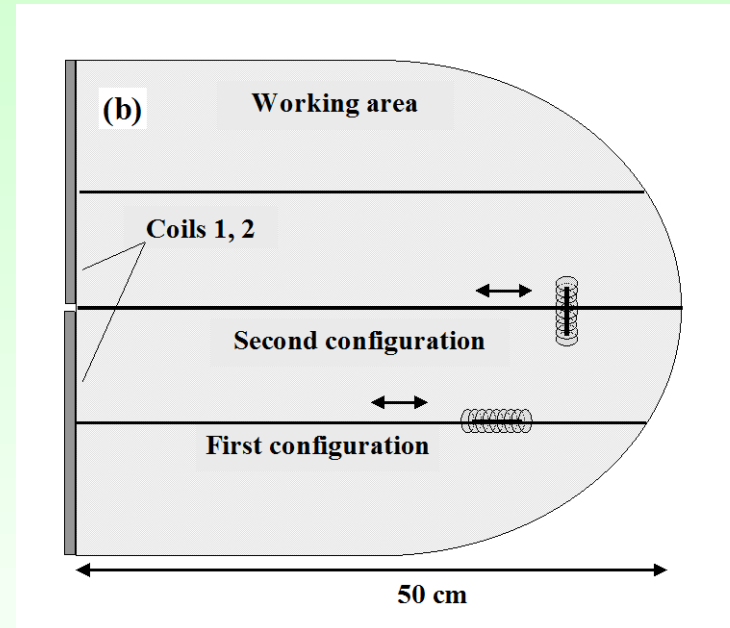
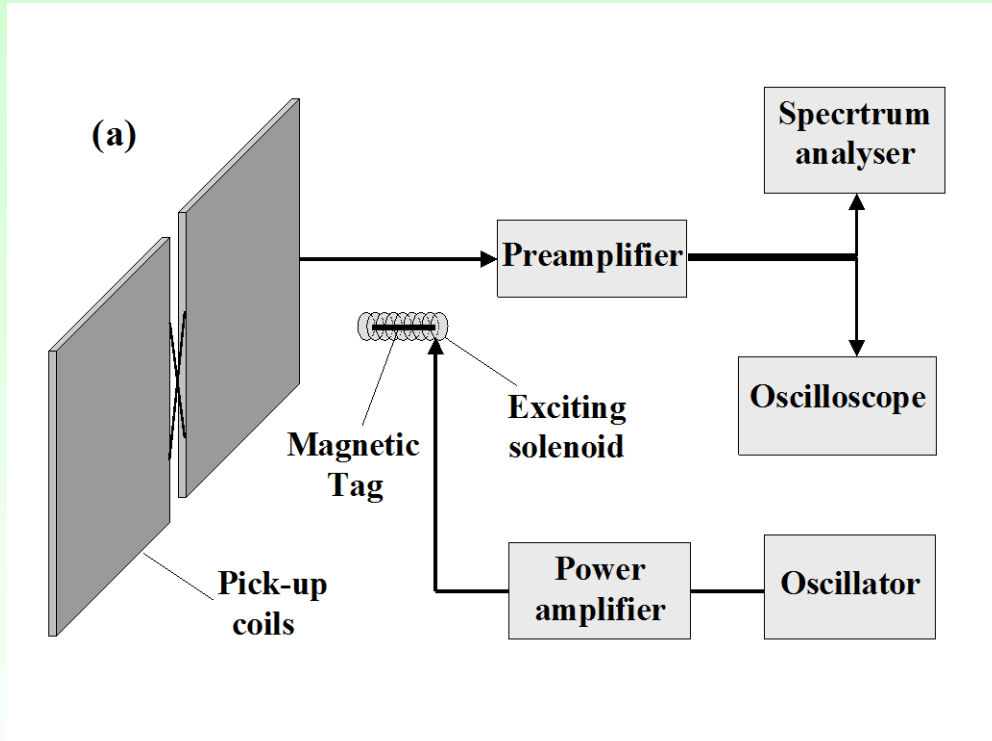
4 A. Zhukov, V. Zhukova, J. González, V. S. Larin y A.V. Torcunov "Ultra-thin glass-coated microwires with GMi effect at elevated frequencies." PCT Es/2006/000434 (USA)



APPLICATIONS:

Scheme of the installation to record the EMF signals of magnetic tags;

(b) geometry of the working area near the receiving coils.

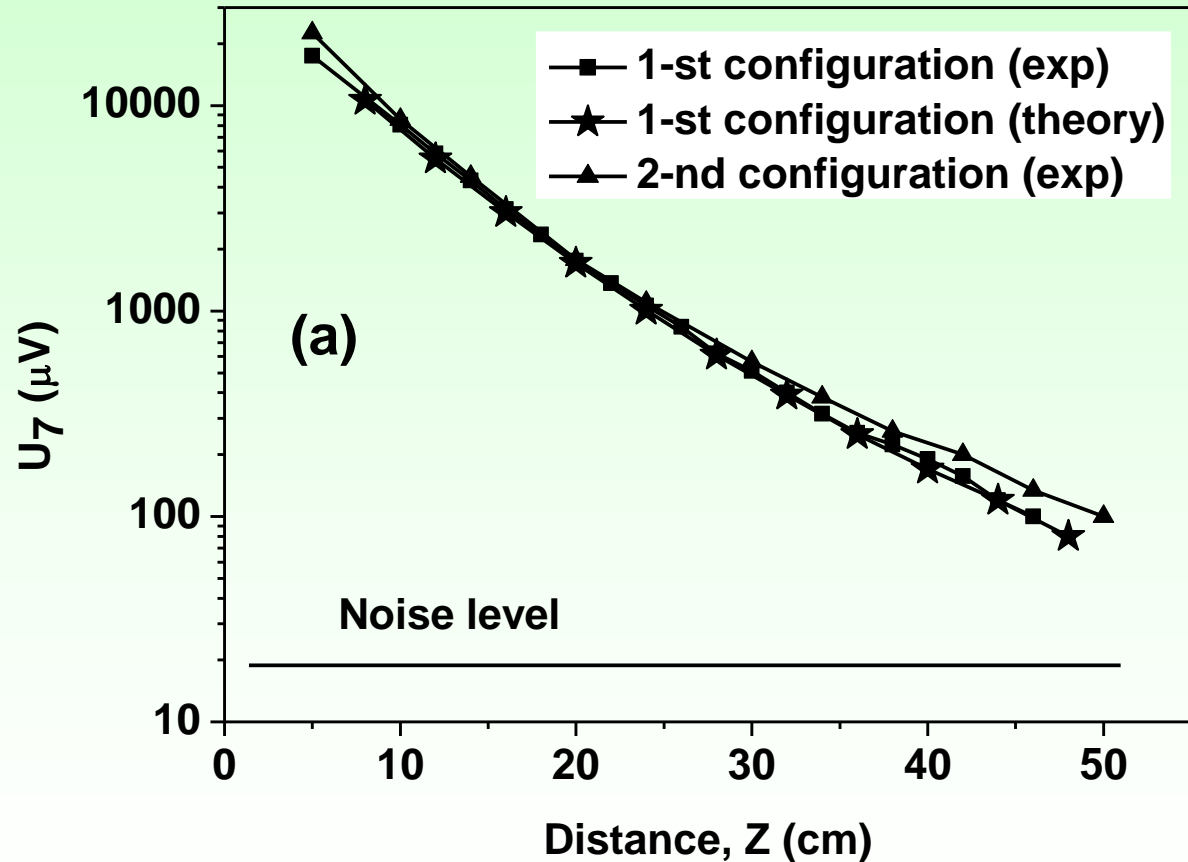


- receiving coils with a side of $a = 20$ cm were made of 20 turns of thin copper wire.

- small solenoid with a length 5 cm has been used to excite the magnetic tags by alternating magnetic field with a frequency $f = 327$ Hz and amplitude $H_0 = 5$ Oe.

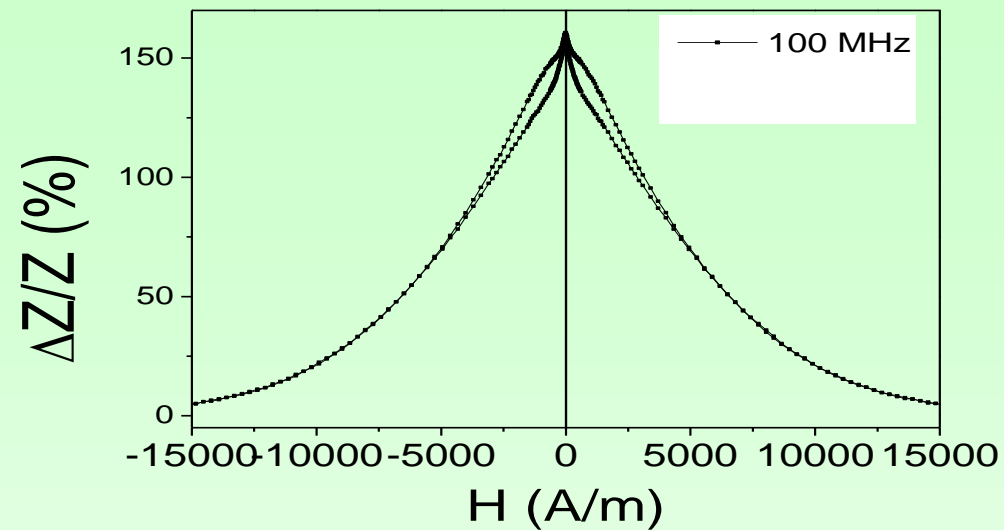
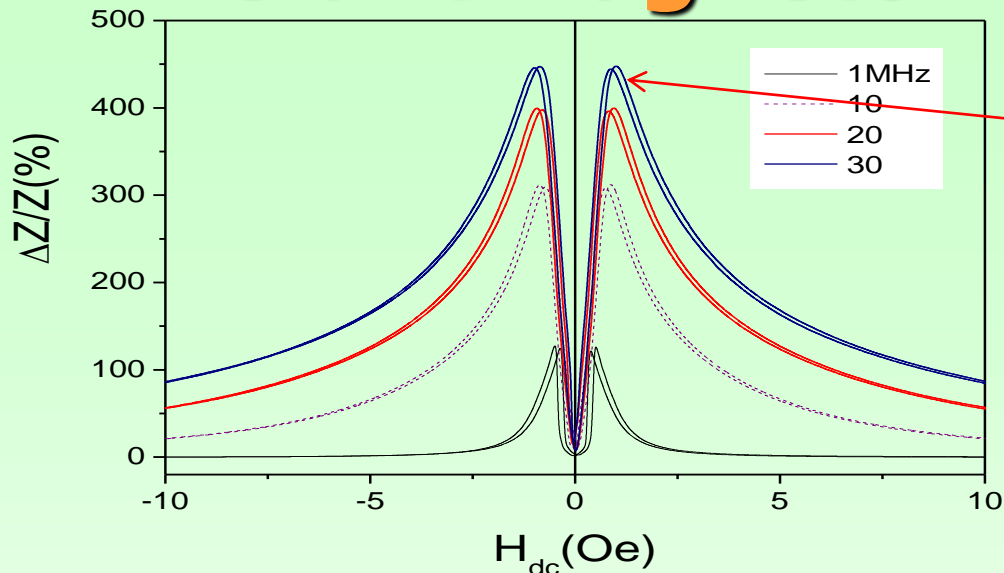
APPLICATIONS:

The measured amplitude of 7-th harmonics of the magnetic tag EMF signals as a function of the distance of the tag from the receiving coil plane for the cases when the tag is oriented perpendicular (squares) or parallel (triangles) to the coil plane.



For the given size of the receiving coils the magnetic tag having $\sim 100 \mu m$ magnetic core diameter can be detected at the distances higher than 45 cm, irrespective of the magnetic tag orientation with respect to the receiving coil plane.

Giant Magneto-impedance effect



Magnetic field dependence and value are affected by magnetic anisotropy

■ Skin Effect of the Magnetic Conductor

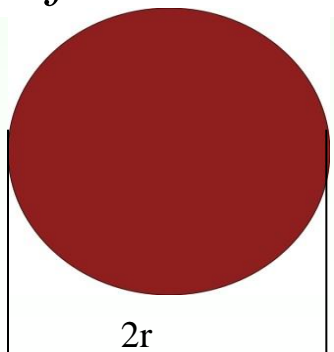
AC current frequency



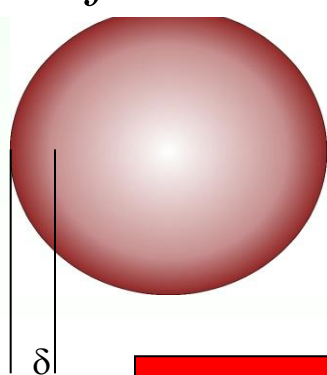
$$\mu_{\phi} \Downarrow \rightarrow \delta \Uparrow$$

$$\delta = \sqrt{\frac{\rho}{\pi \mu_{\phi} f}}$$

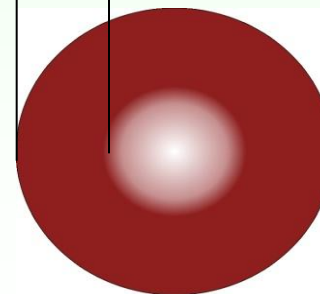
$f \approx \text{kHz}$



$f \approx \text{MHz}$



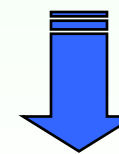
δ



$\mu_{\phi}(H, f)$

$\delta < r$

(at high enough f)



$Z(H)$

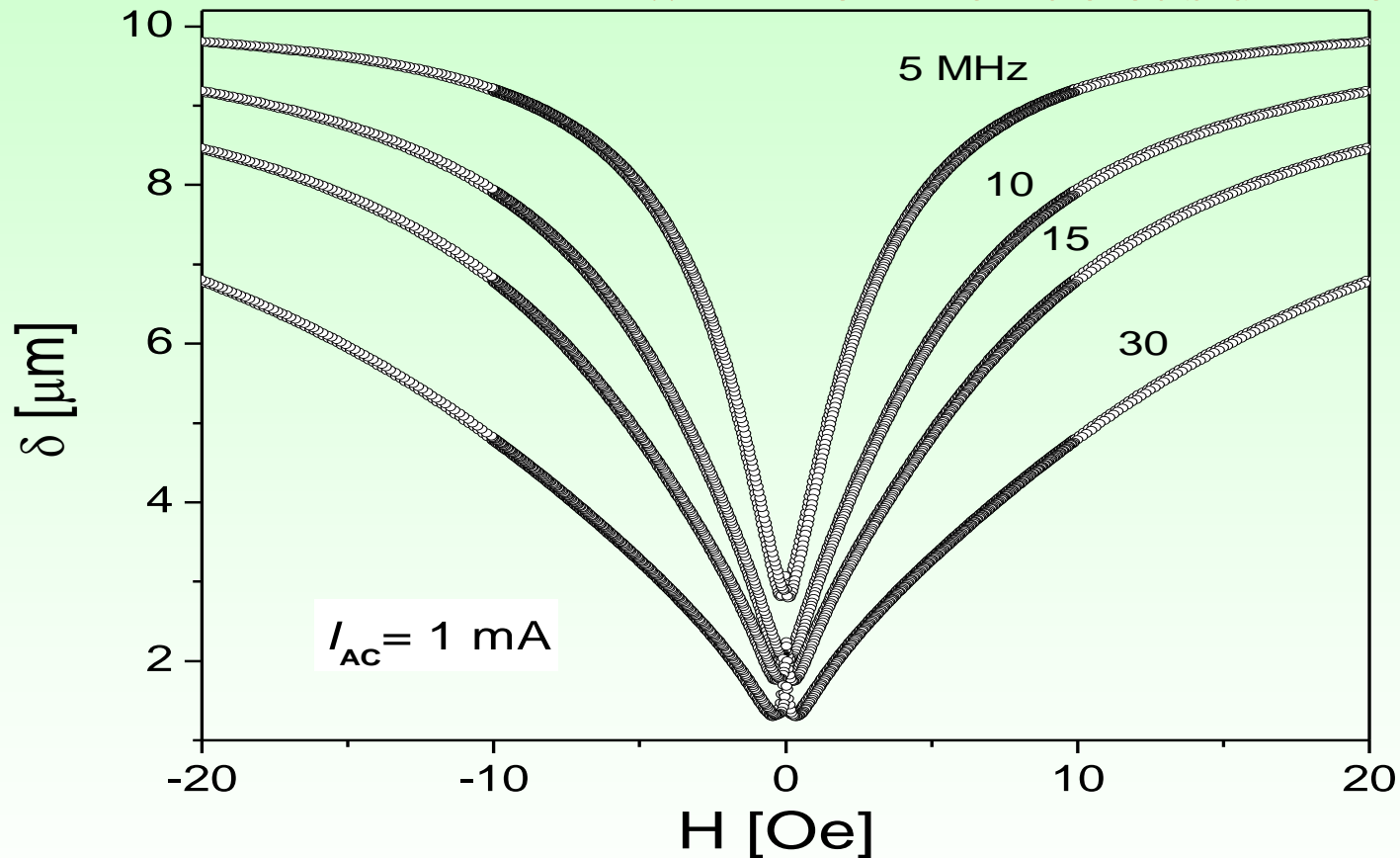
Magnetic field



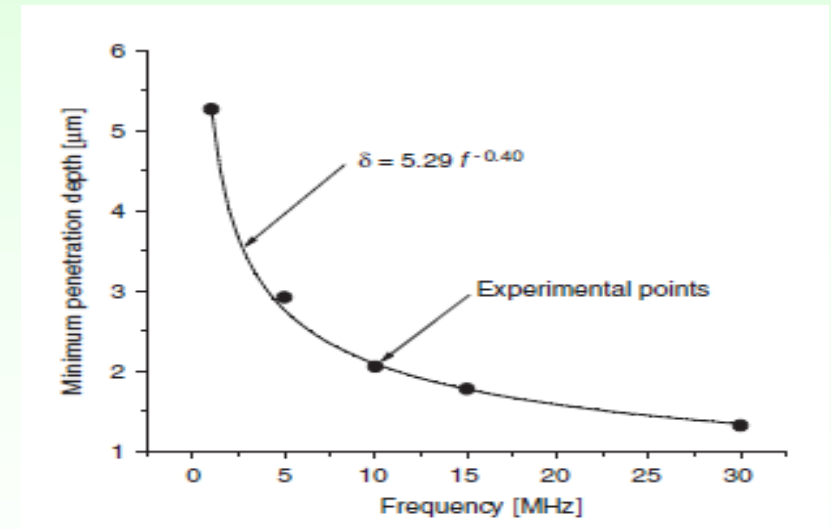
$$\Delta Z / Z = \{ |Z(H_{ex})| - |Z(H_{max})| \} / |Z(H_{max})|$$

GMI effect

Calculated penetration depth vs. axial dc-field at various frequencies of ac-current in $\text{Co}_{67}\text{Fe}_{3.85}\text{Ni}_{1.45}\text{Mo}_{1.7}\text{Si}_{14.5}\text{B}_{11.5}$ microwire with metallic nucleus diameter $22.4\ \mu\text{m}$

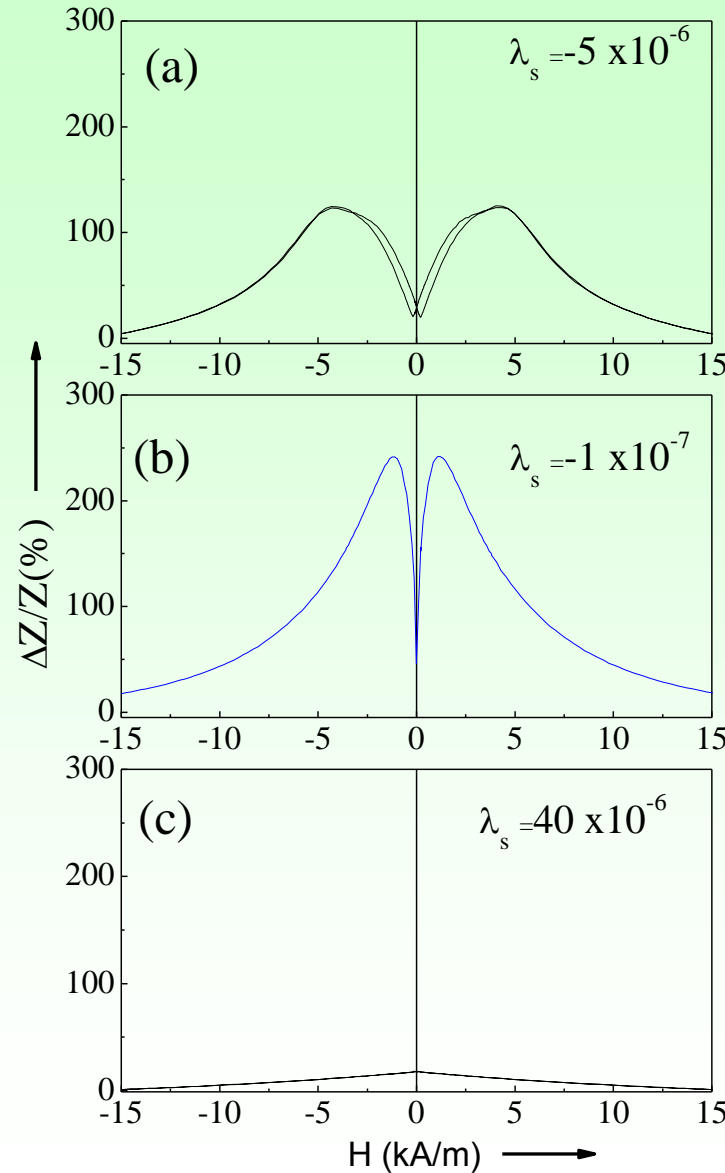
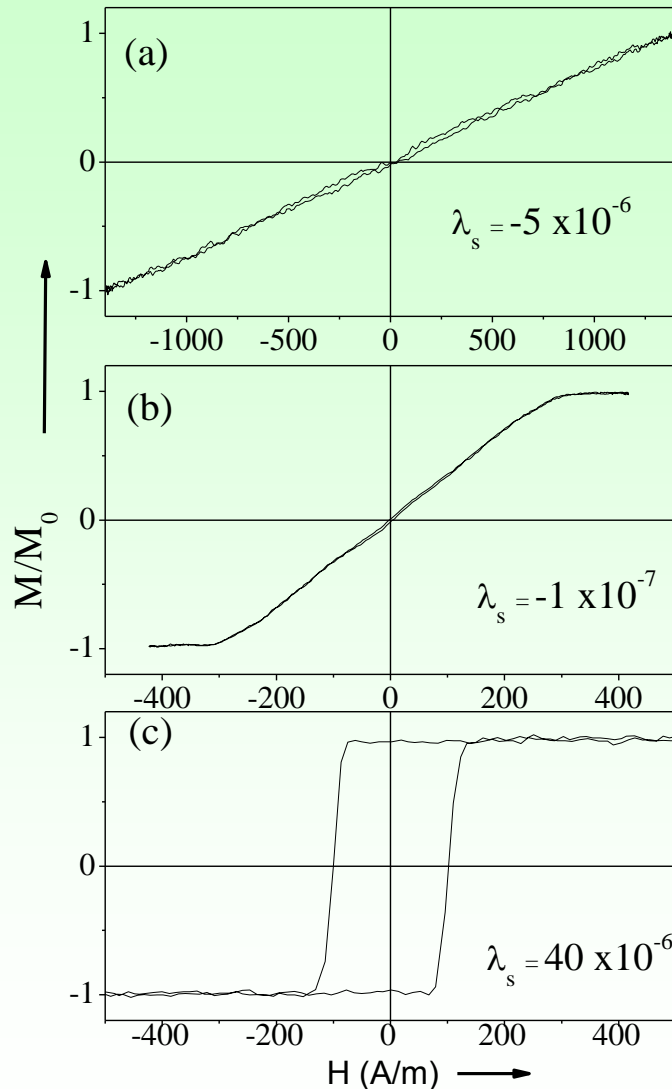


Essentially surface effect. Thin surface layers are involved in the GMI process



H. Lachowicz, M. Kuzminski, K.L. García, A. Zhukov and M. Vázquez, A. Krzyzewski, "Influence of Alternative circular magnetic field strength on magnetoimpedance of glass-coated micro-wire", J. Magn. Magn. Mater. 300 (2006), e88-e-92

Magnetic properties and GMI effect of magnetic microwires



$\lambda_s \approx -5 \times 10^{-6}$
Co_{77.5}Si₁₅B_{7.5} (a),

$\lambda_s \approx -1 \times 10^{-7}$
Co₆₇Fe₄Ni_{1.4}Si_{14.5}B_{11.5}Mo_{1.7} (b)

$\mu = \Delta M / \Delta H$
High μ , low H_c
Good candidate for GMI

and

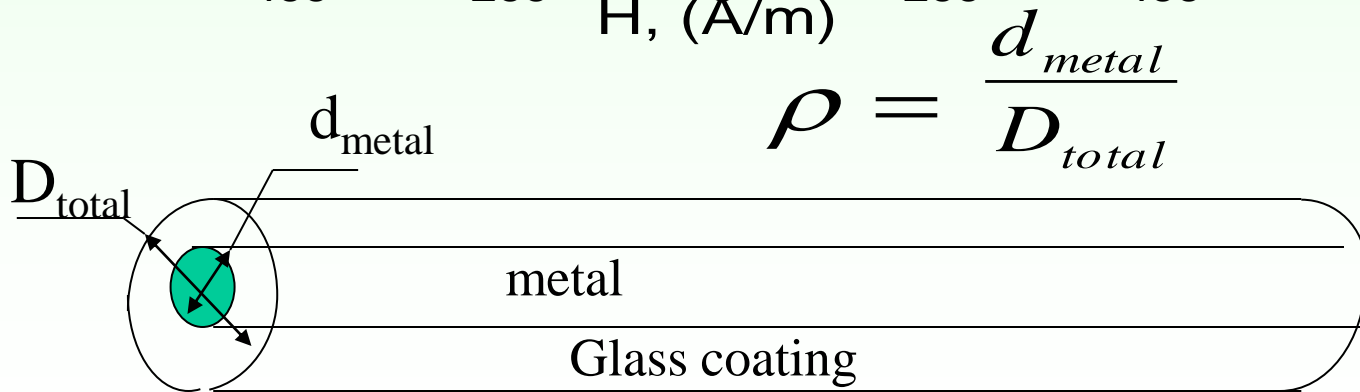
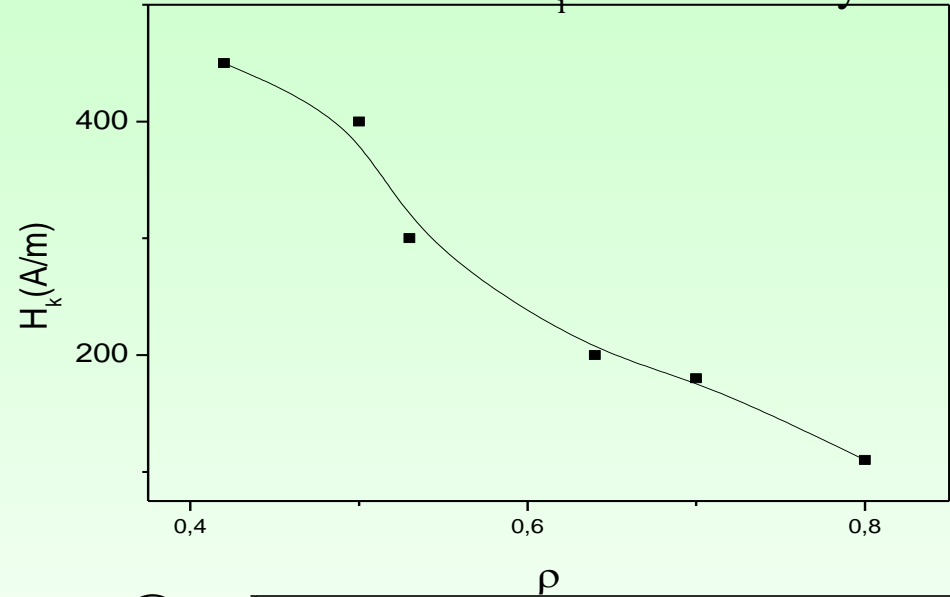
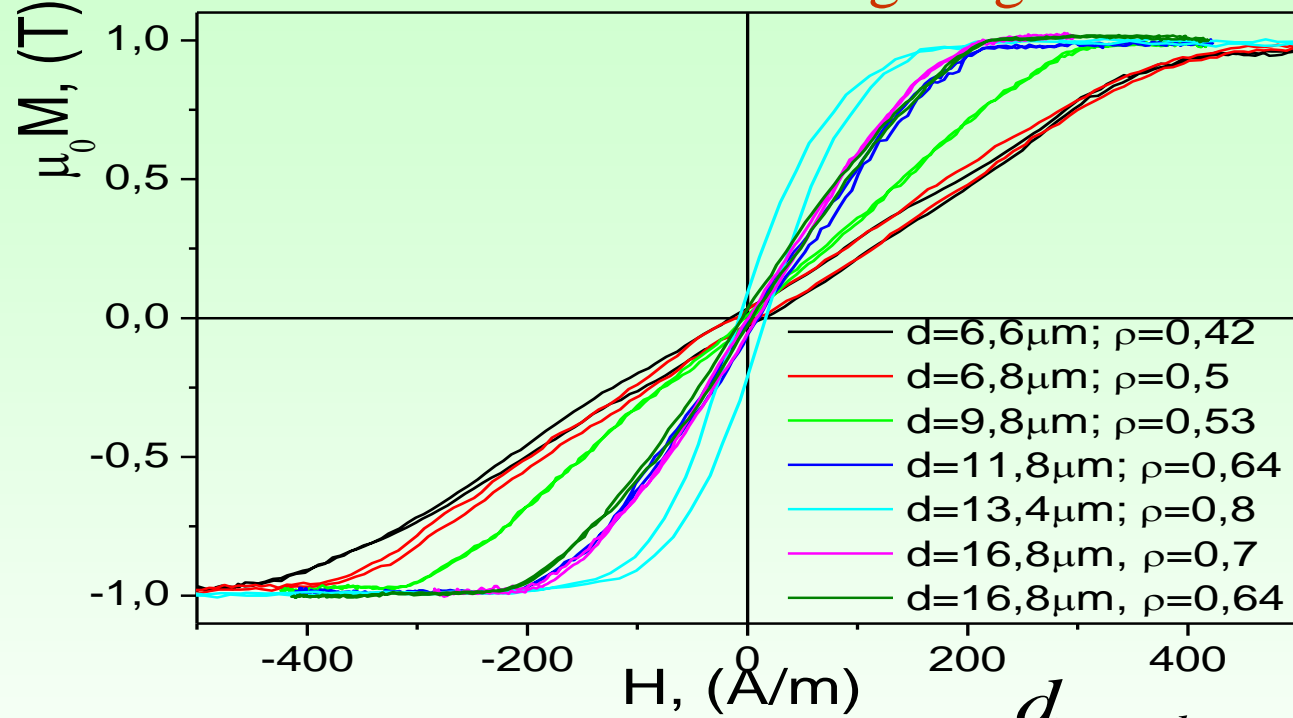
$\lambda_s \approx 40 \times 10^{-6}$
Fe₇₅B₉Si₁₂C₄ (c)
microwires

Hysteresis loops, shape and value of GMI ratio are different

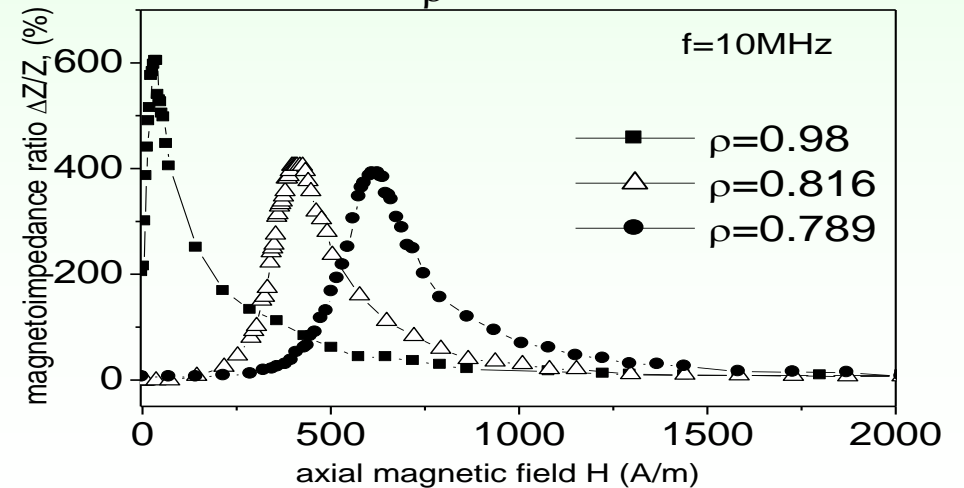
TAILORING OF GMI EFFECT AND MAGNETIC PROPERTIES

Effect of the samples geometry on the hysteresis loops of Co-rich microwires with vanishing magnetostriction constant.

$K_{me} \approx 3/2 \lambda_s \sigma_i$:
Magnetostriction λ_s -determines by the chemical composition
 σ_i -determines by the ratio $\rho = d/D$



$$\rho = \frac{d_{metal}}{D_{total}}$$



Correlation with magnetic anisotropy

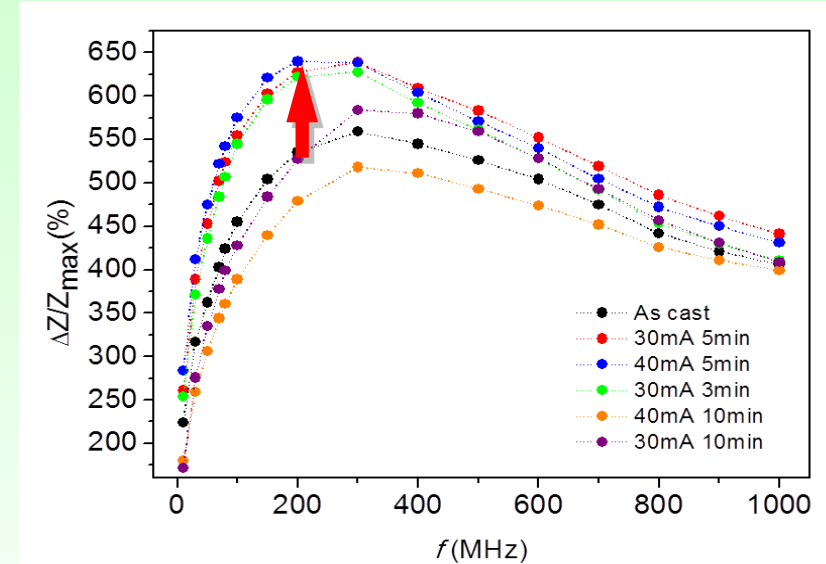
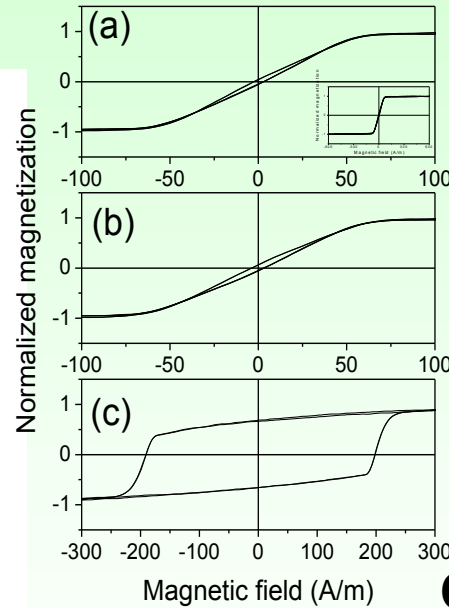
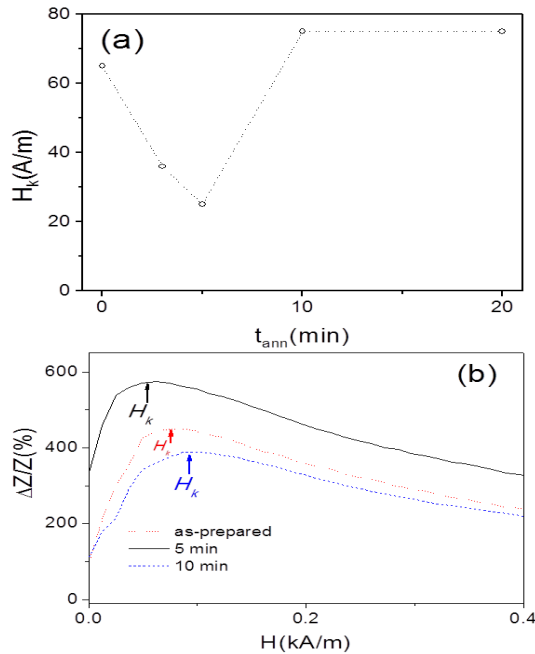
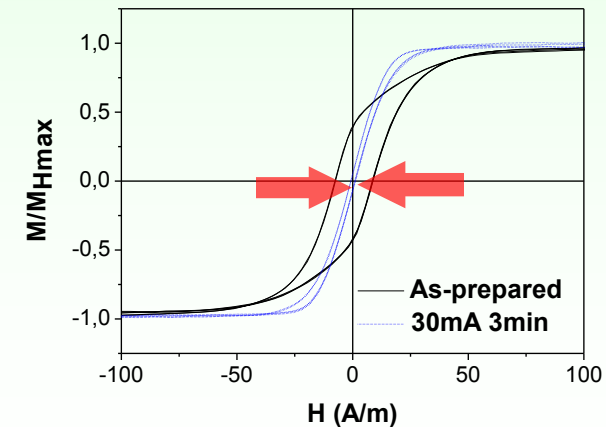
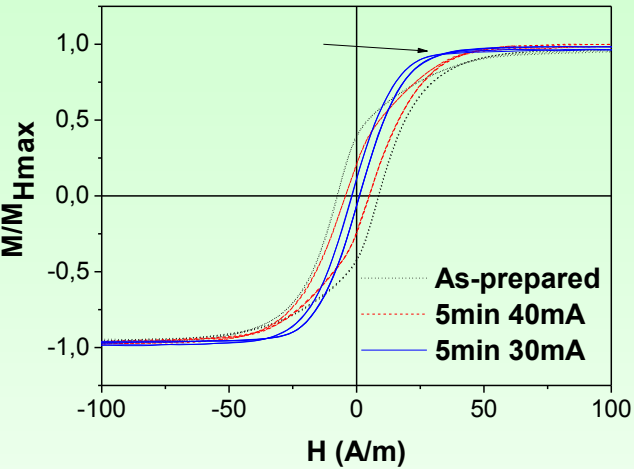
Theoretical GMI ratio value is about 3000%

Tailoring by Joule heating

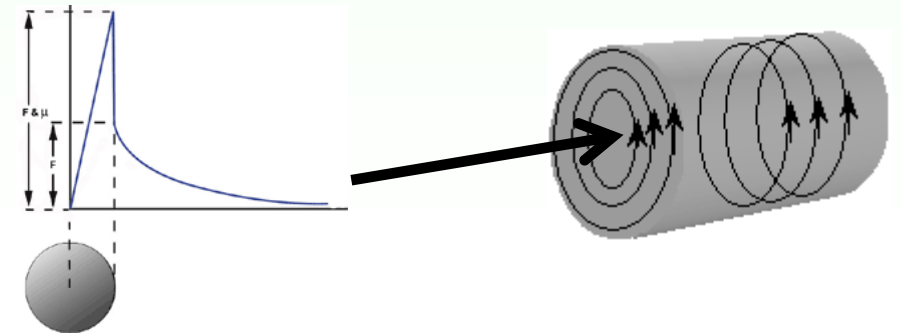
- Internal stresses relaxation
- Induced magnetic anisotropy

GMI ratio up to 650%

$$H_k = 25 \text{ A/m}$$



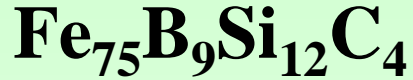
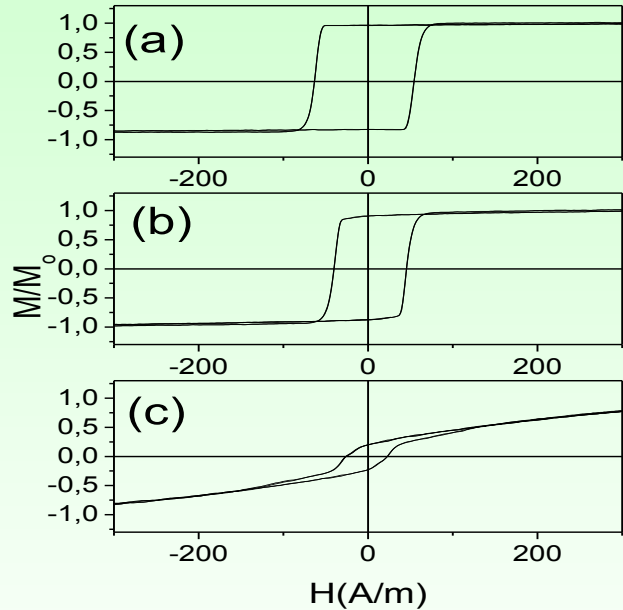
Circular magnetic field by current:



$$H_c = 2 \text{ A/m}$$

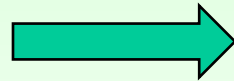
Stress-annealing induced Anisotropy and GMI in Fe-rich microwires

Motivation: Co-critical element!

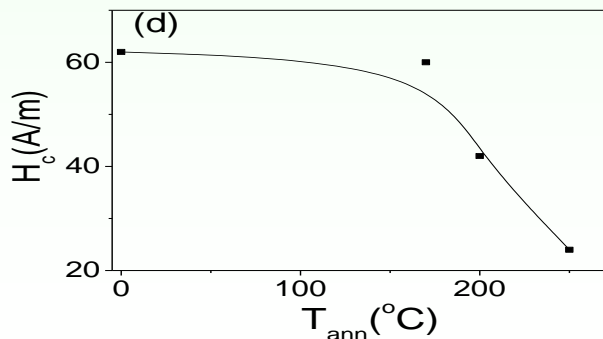
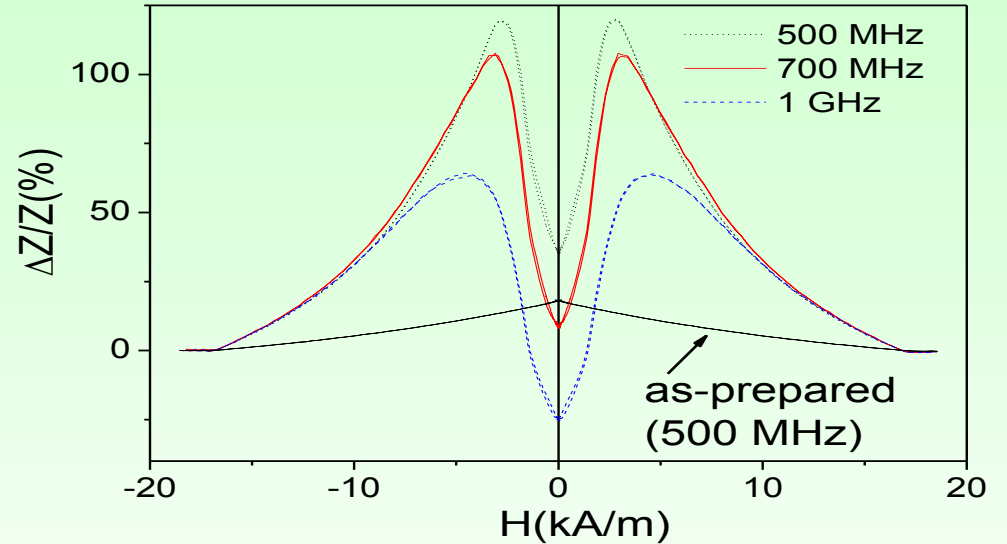


As-prepared

Stress annealed 200 °C



Stress annealed 250 °C



i) considerable transversal magnetic anisotropy and magnetic softening and GMI enhancement

ii) existence of maximum on $\Delta Z/Z(H)$ dependences reflects transversal magnetic anisotropy of stress-annealed

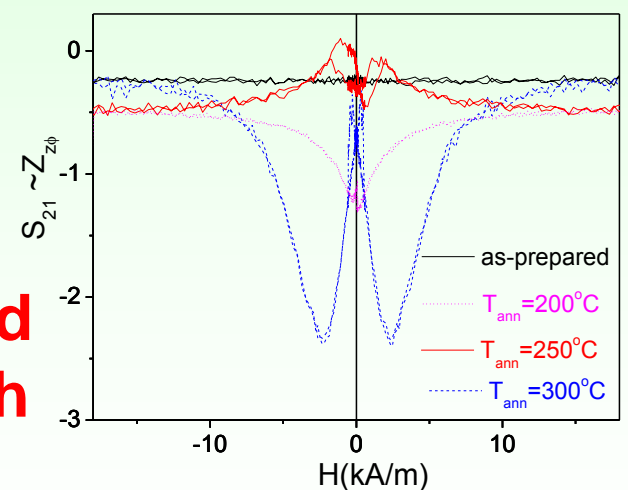
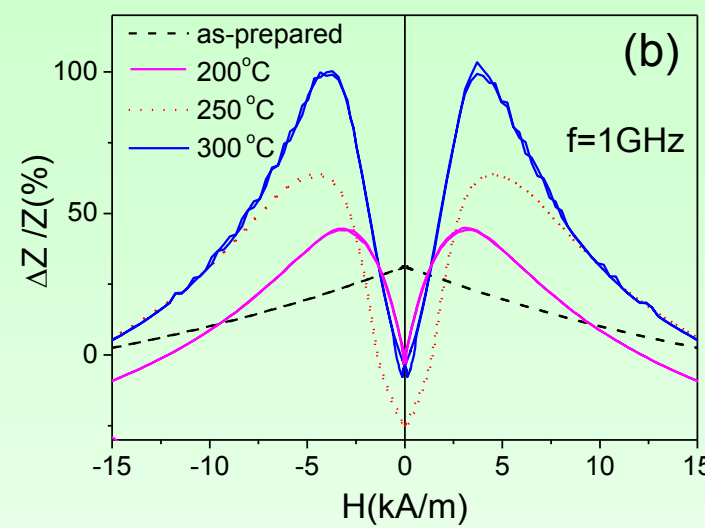
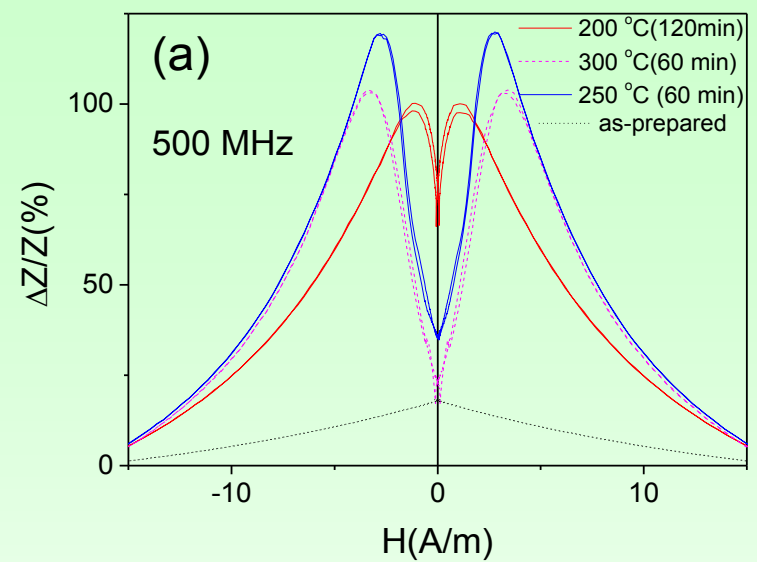
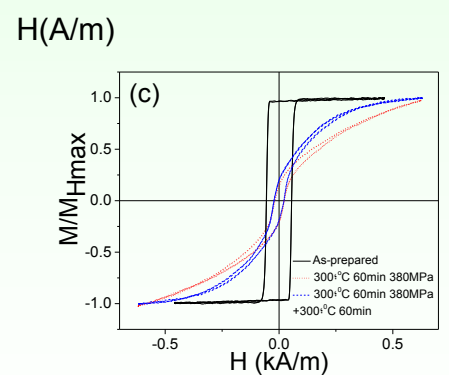
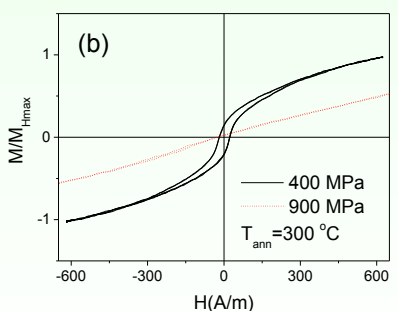
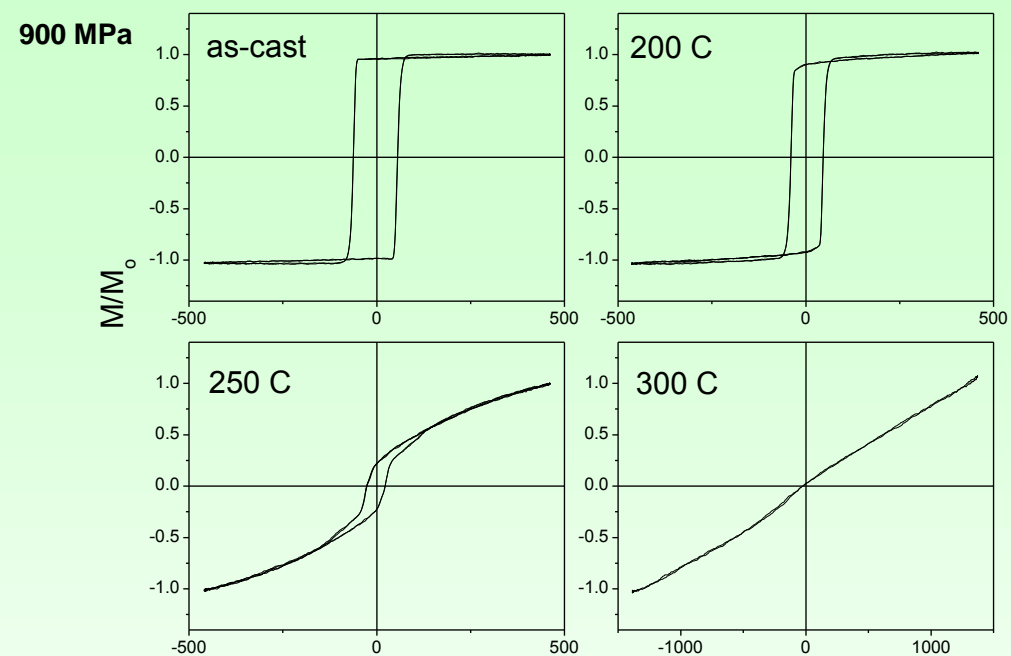
iii) Excellent mechanical properties (amorphous material)

V. Zhukova, M. Ipatov, A. Talaat, J. M. Blanco, M. Churyukanova, S. Taskaev and A. Zhukov, "Effect of stress-induced anisotropy on high frequency magnetoimpedance effect of Fe and Co-rich glass-coated microwires" J. Alloys Compound. 735 (2018) 1818-1825;

V. Zhukova, J.M. Blanco, M. Ipatov, J. Gonzalez, M. Churyukanova A., Zhukov, Scripta Materialia, Vol. 142, (2018) 10–14, doi: 0.1016/j.scriptamat.2017.08.014

Ways to improve GMI in Fe-rich microwires

Effect of stress annealing on GMI of Fe-rich microwires



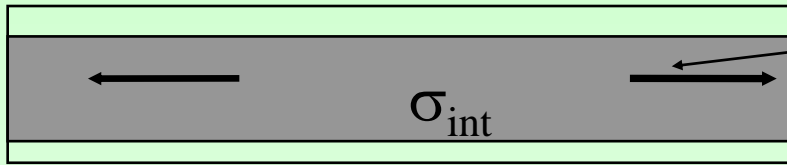
1. Depend on T, σ
2. Only partially reversible
3. SA is a promising method for MI optimization in Fe-rich microwires

V. Zhukova, M. Ipatov, A. Talaat, J. M. Blanco, M.Churyukanova, S. Taskaev and A. Zhukov, "Effect of stress-induced anisotropy on high frequency magnetoimpedance effect of Fe and Co-rich glass-coated microwires" J. Alloys Compound. 735 (2018) 1818-1825

V. Zhukova, J. M. Blanco, M. Ipatov, M.Churyukanova, S. Taskaev and A. Zhukov, Tailoring of magnetoimpedance effect and magnetic softness of Fe-rich glass-coated microwires by stress- annealing, Sci. Reports 8 (2018) 3202

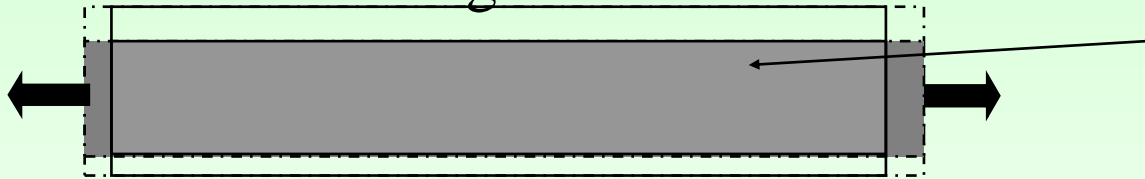
Origin of stress-induced anisotropy 1

As-prepared microwire



Internal stresses with mainly axial component

Stress Annealing



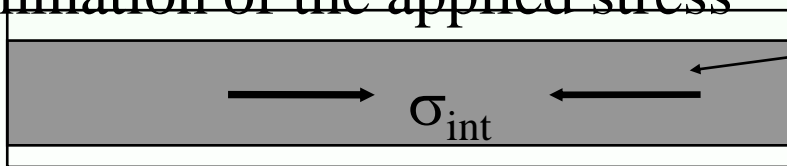
Induction of magnetic anisotropy during stress annealing

Slow Cooling under stress



Stress relaxation in the stressed state at room temperature

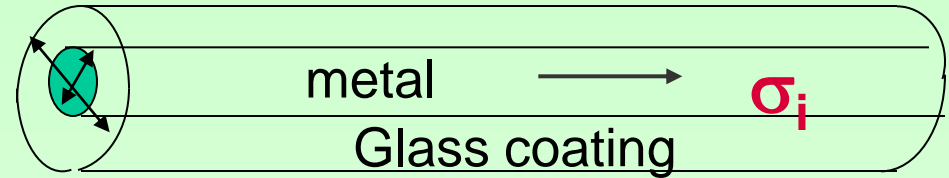
Elimination of the applied stress



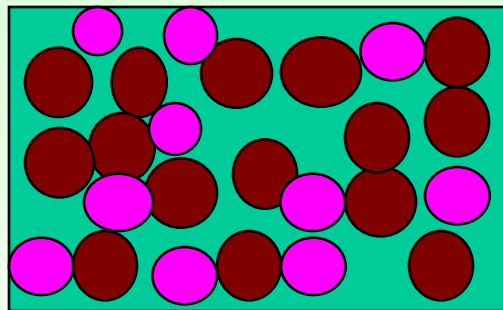
Induction of the compressive stresses at room-temperature (so-called “Back stresses”)

Origin of induced anisotropy 2

**Possible origin:
-Stress induced anisotropy
(stress from glass coating)?**

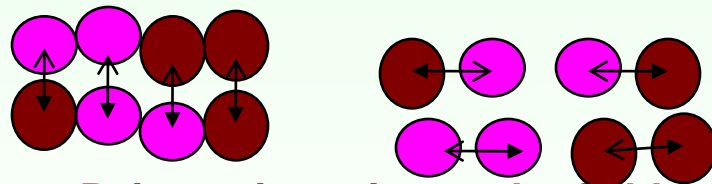


Origin: Pair ordering usually considered



TM1 (Co)
TM2 (Fe)

H or/and σ



Pair reorientation under field and/or stress annealing (after Neel)

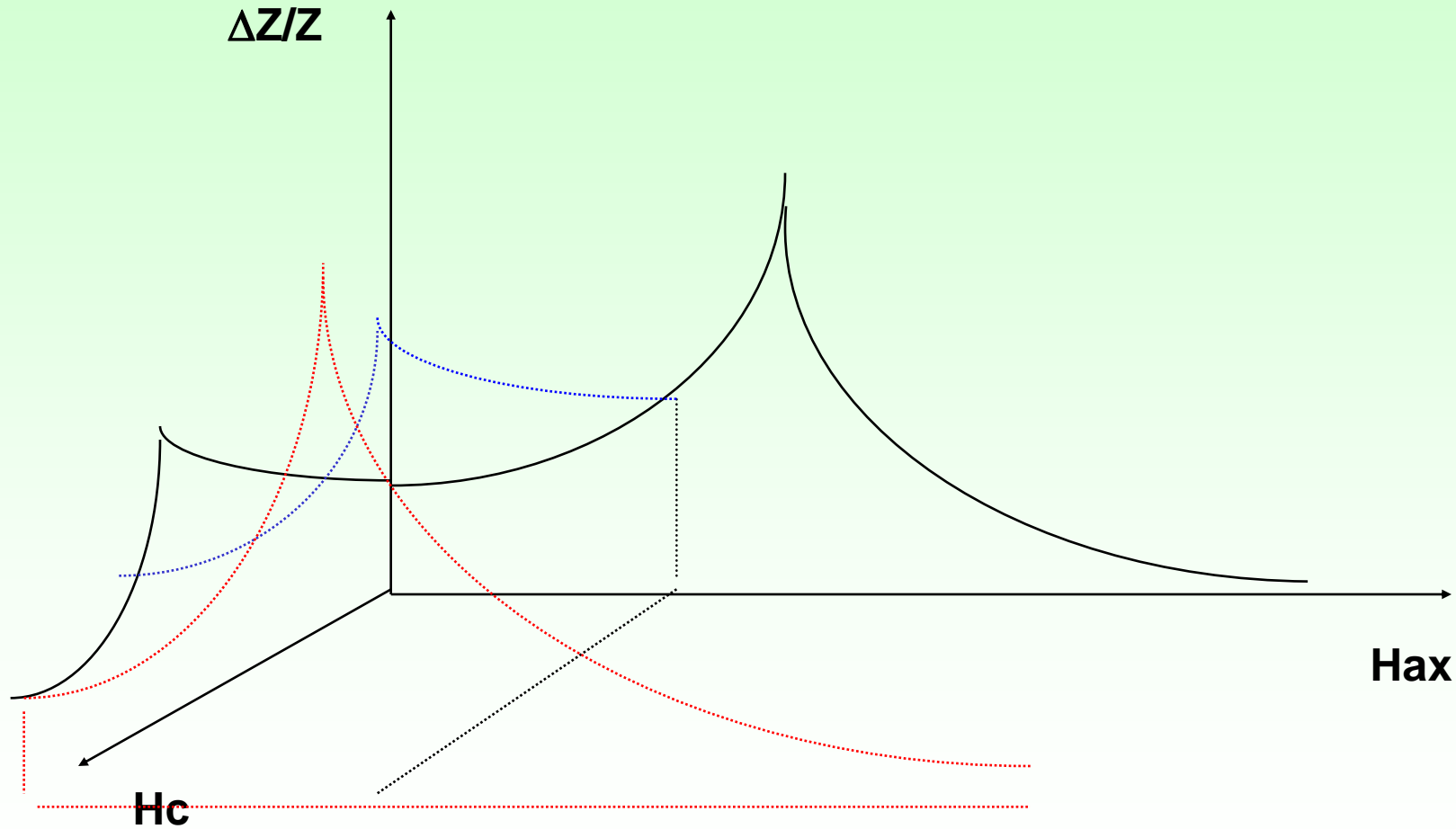
**Possible origin 3:
The topological short range ordering (also known as structural anisotropy) can play an important role. This involves the angular distribution of the atomic bonds and small anisotropic structural rearrangements at temperature near the glass transition temperature**

[1] F. E. Luborsky and J. L. Walter, "Magnetic Anneal Anisotropy in Amorphous Alloys", *IEEE Trans. Magn.* Vol.13 (2), pp.953-956, 1977.

[2] J. Haimovich, T. Jagielinski, and T. Egami, "Magnetic and structural effects of anelastic deformation of an amorphous alloy", *J. Appl. Phys.* Vol. 57, pp. 3581-3583, 1985.

Tensor character of GMI

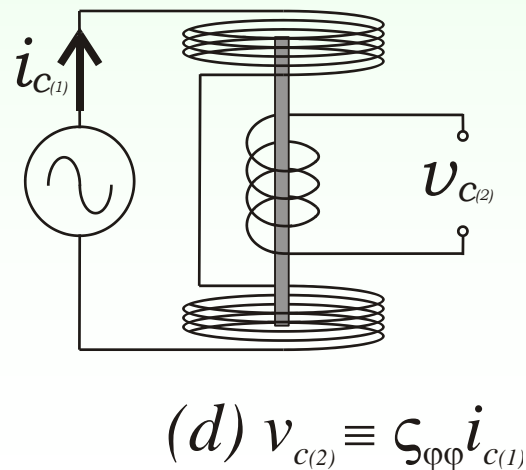
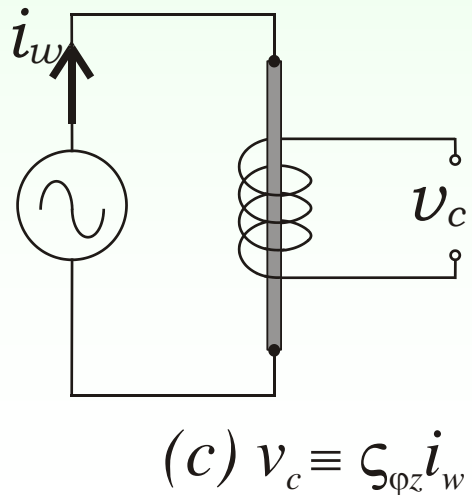
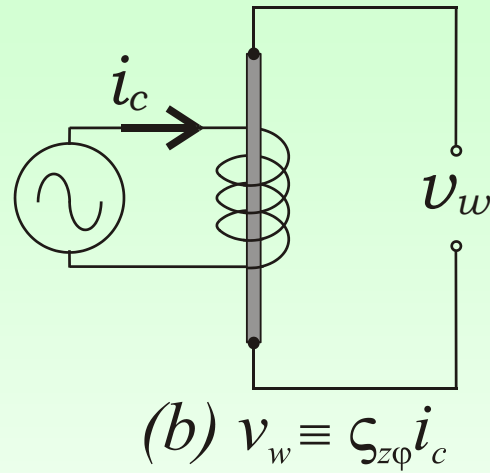
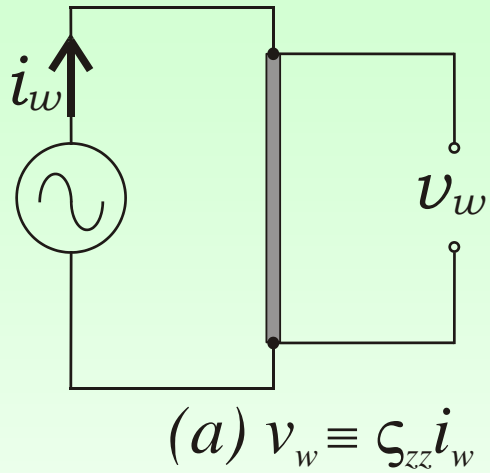
Schematic representation



A.S. Antonov, I.T. Iakubov, A.N. Lagarkov, J. Magn. Magn. Mat. 187 (1998), 252

P. Aragonese, A. Zhukov, J. Gonzalez, J.M. Blanco and L. Dominguez, Sensors and Actuators A, 81/1-3 (2000) 86-90

Methods for revealing the impedance matrix elements: (a) ζ_{zz} , (b) $\zeta_{z\varphi}$, (c) $\zeta_{\varphi z}$, (d) $\zeta_{\varphi\varphi}$



D.P.Makhnovskiy, L.V. Panina and D.J. Mapps, Phys Rev B 63 (2001), 1444241.

Or

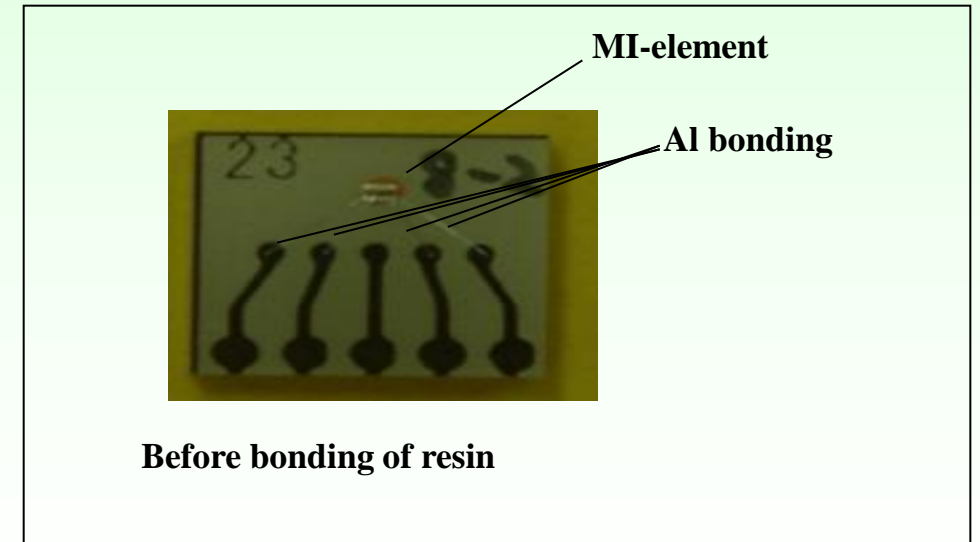
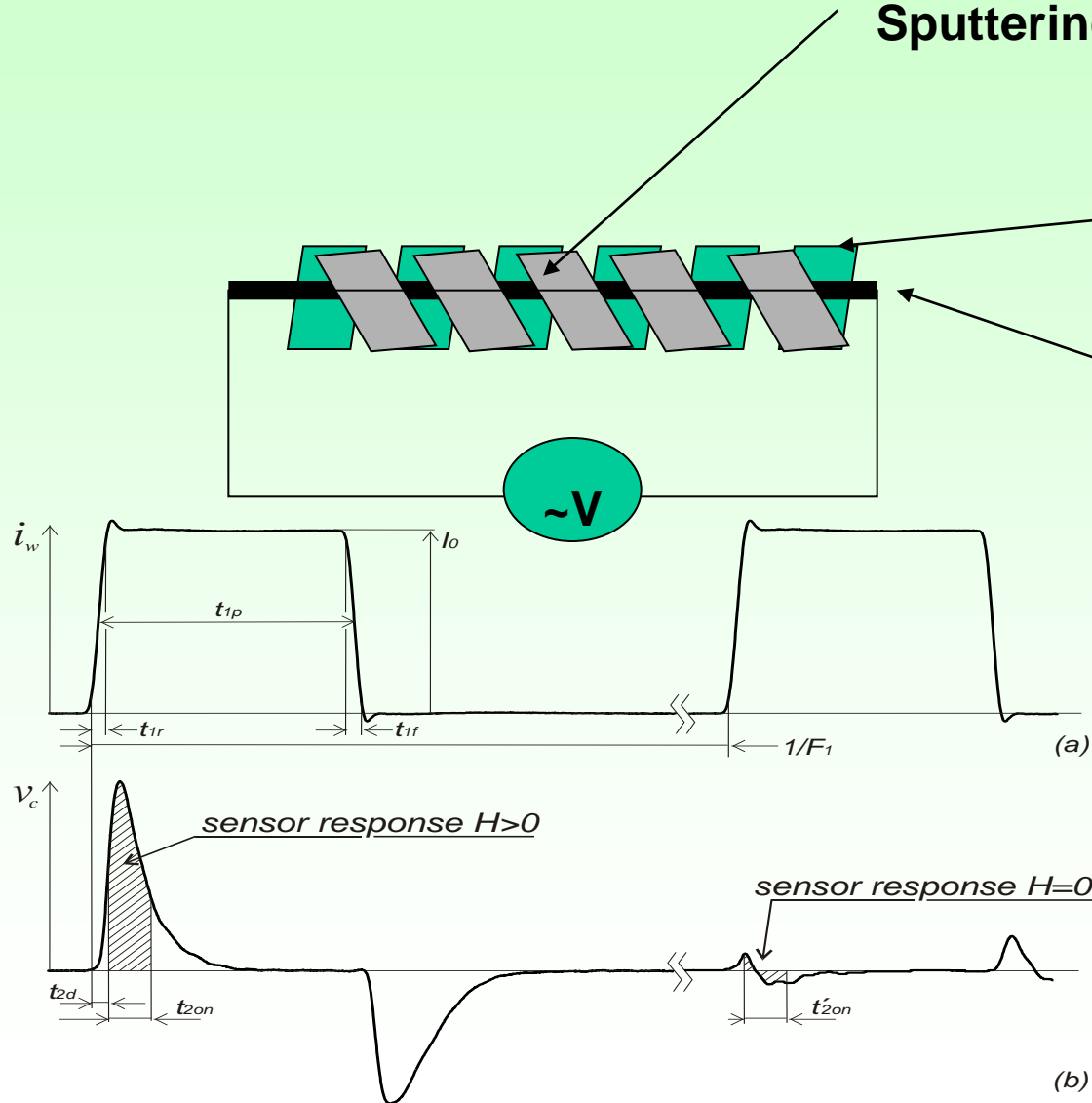
V. A. Zhukova, A.B. Chizhik, J.Gonzalez , D.P. Makhnovskiy, L.V. Panina, D.J. Mapps and A.P. Zhukov, J Magn Magn Mat. 249 (2002), 3124.

MI element

Sputtering of 2-nd Cu layer

Sputtering of Cu

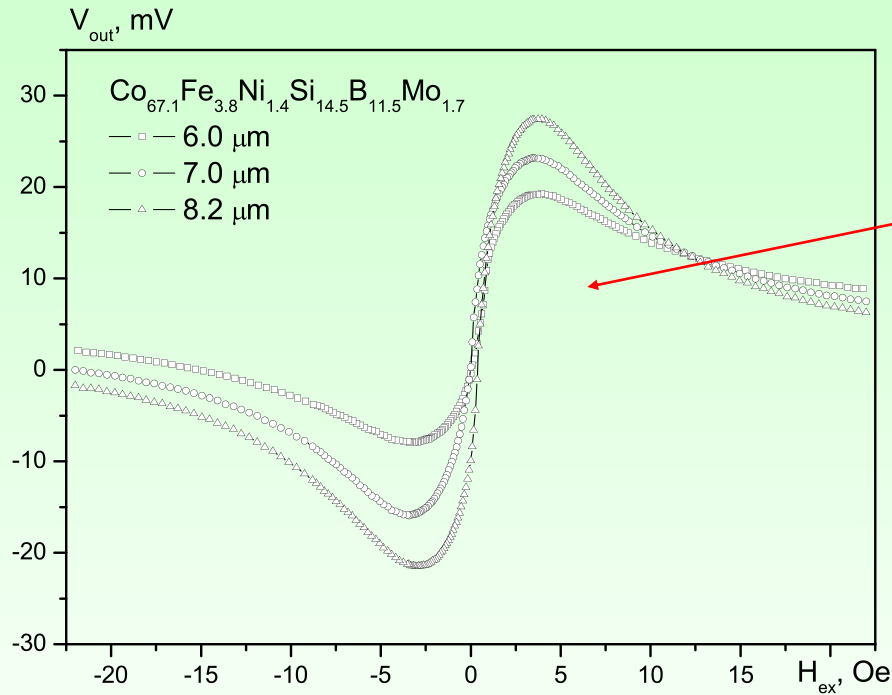
Microwire with GMI



Excitation current pulse in the wire (a) and voltage induced in the pickup coil (b).

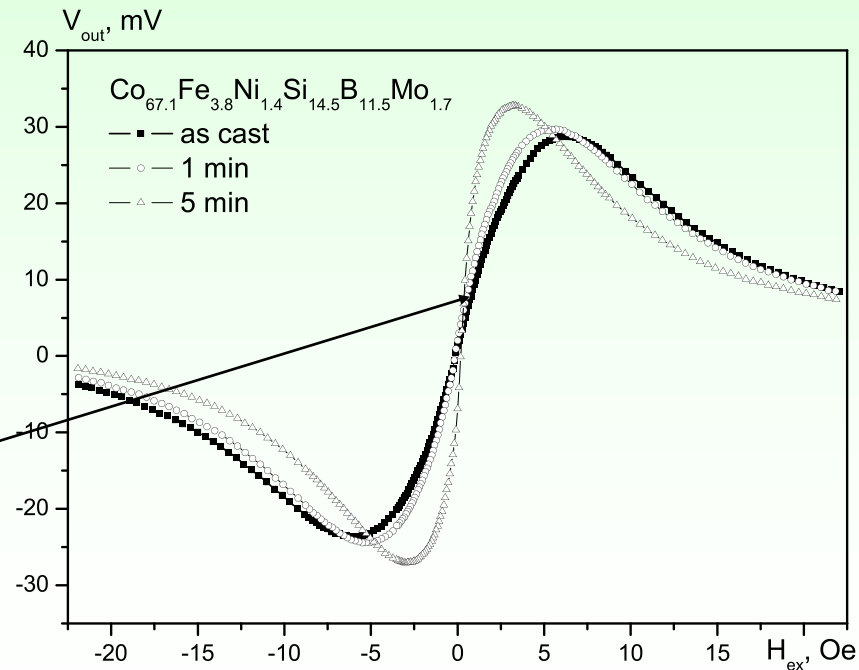
Off-diagonal GMI of nearly zero magnetostriction

$\text{Co}_{67,1}\text{Fe}_{3,8}\text{Ni}_{1,4}\text{Si}_{14,5}\text{B}_{11,5}\text{Mo}_{1,7}$ microwires



**Asymmetrical shape,
Almost linear region**

**Linear region and maximum
Position depends on geometry**



Tailoring of GMI by heat treatment

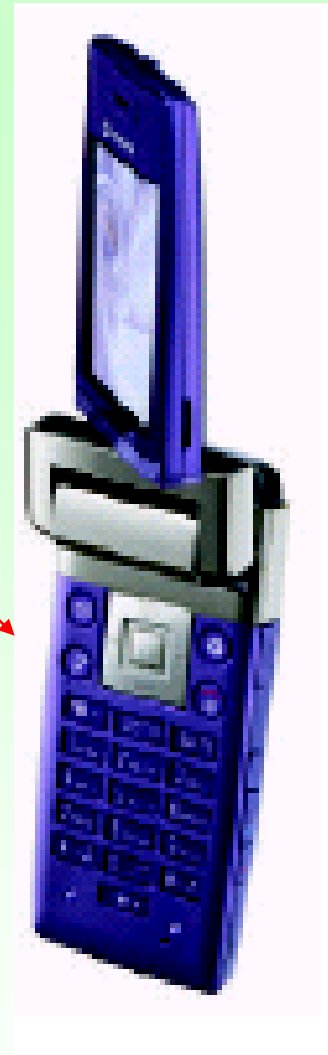
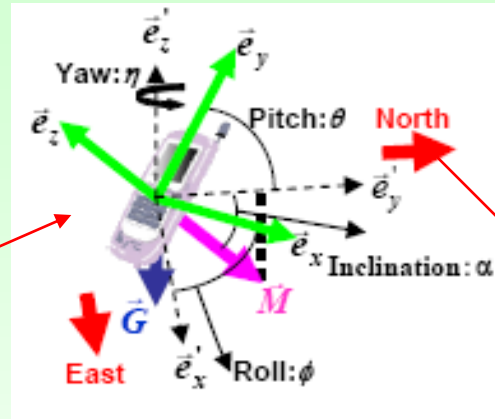
APPLICATIONS:

m-wires –GMI Since 2010

■ AMI601 Appearance



Dimensions: 5.2 × 6.0 × 1.5 mm



Size – 1 mm

AMI 601 –Aichi Steel Corp.

6-axis sensor

3 axis of magnetic earth sensing

3 axis acceleration sensing

APPLICATIONS: Application for MI effect - Sensors

❖ High sensitive electronic compass

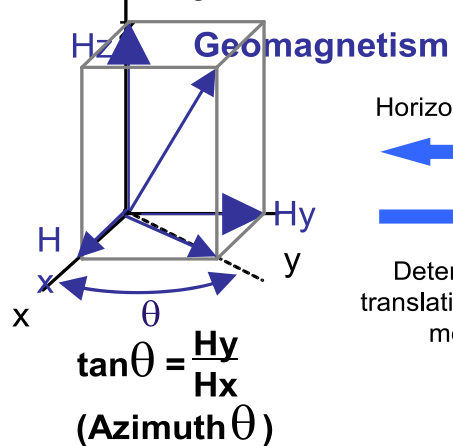
❖ Positional sensor ❖ Motion-sensing controllers ❖ Operating attitude automated control.

Motion Sensor = 3D magnetic sensor + 2/3D accelerometer

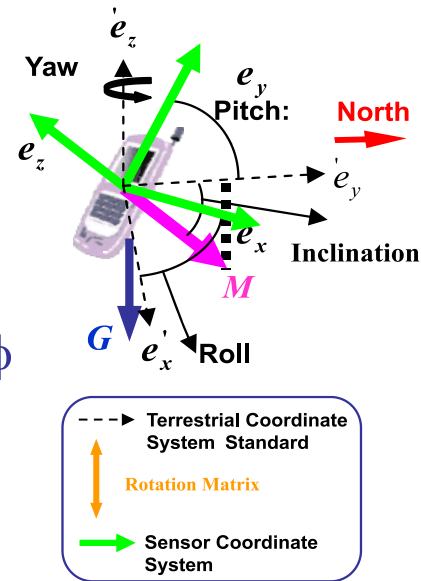
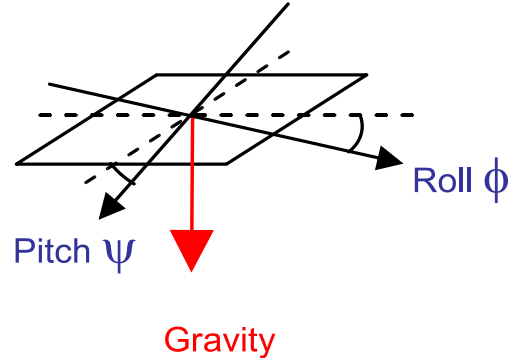
It determines the attitude of mobile devices relative to geomagnetism and gravity, and by analyzing the attitude and speed, other aspects of movement such as acceleration, translational speed and rotational speed can be calculated.

Attitude Detection Principles

3-Axis Magnetic Sensor



2-Axis Accelerometer

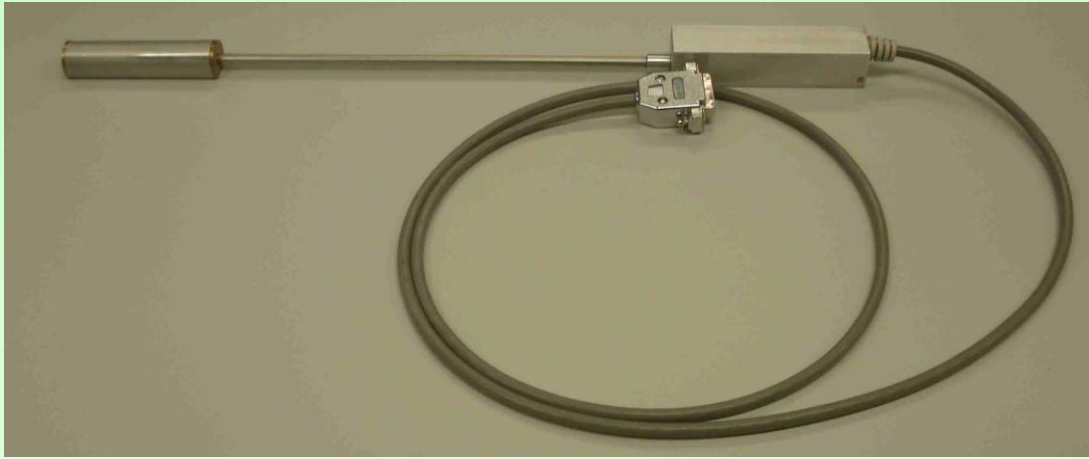


Source: Aichi Micro Intelligent Corporation

❖ Navigation functions combining the motion sensor with a GPS:
Intelligent Transportation System,
Control of operating attitude in unmanned helicopters, robots, automobiles, etc.

Requirements: high sensitivity at low H (up to few Oe)

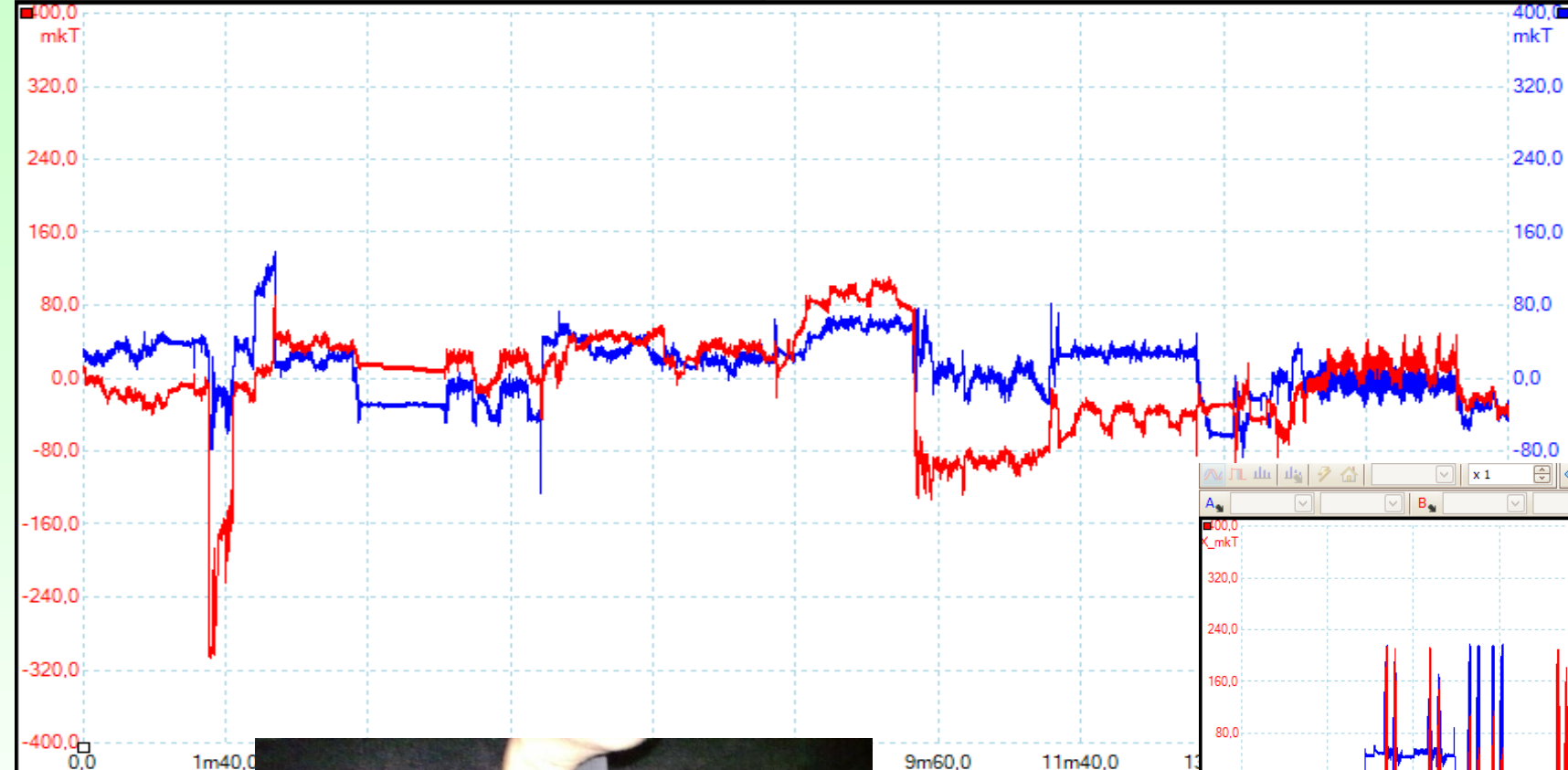
Designed by us magnetometer



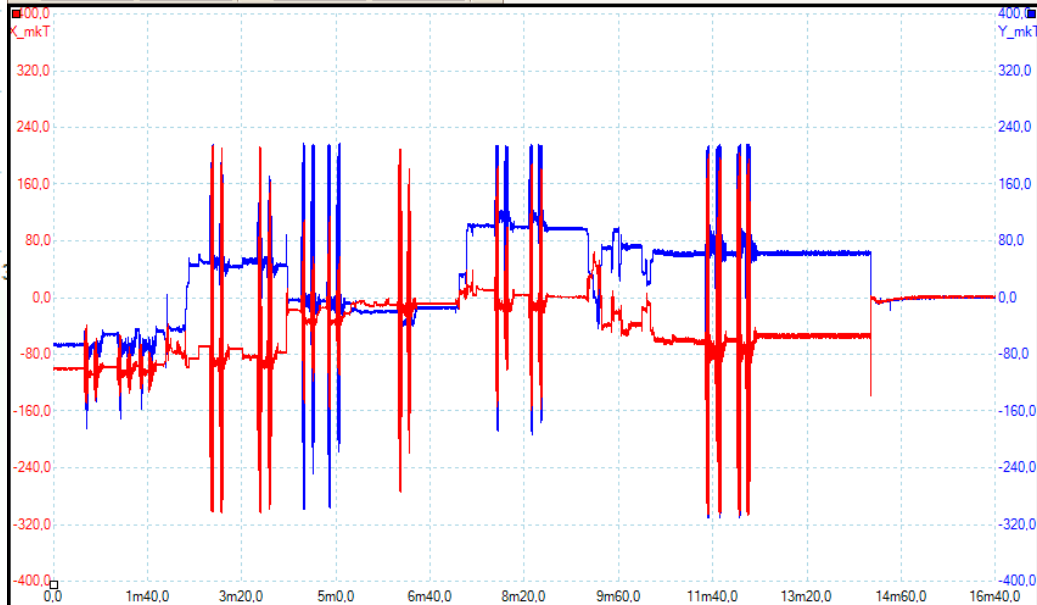
Technical characteristics

Channel number	3 (X, Y, Z components);
Size of the 3-component sensing element	cube with 14 mm edge;
Input voltage of the channel, not less	± 4.5 V;
Dynamic range, not less	± 2.5 Oe;
Frequency range, not less	1 kHz;
Power voltage	0 + 5.5V;
Consuming current	~ 250 mA;
<u>Transmission coefficient of the channels</u>	
Channel X	1.58V per 1Oe;
Channel Y	1.57V per 1Oe;
Channel Z	1.69V per 1Oe.
Noise level (resolution)	≈ 10 nT

MAGNETIC FIELD MEASUREMENTS WITH GMI MAGNETOMETER inside the electric car (FIAT Turin Nov. 2012) (FP7 project)



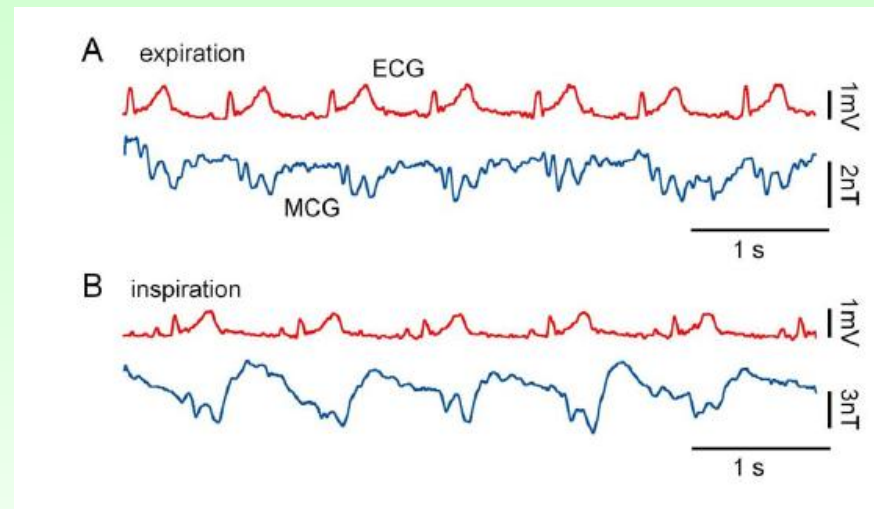
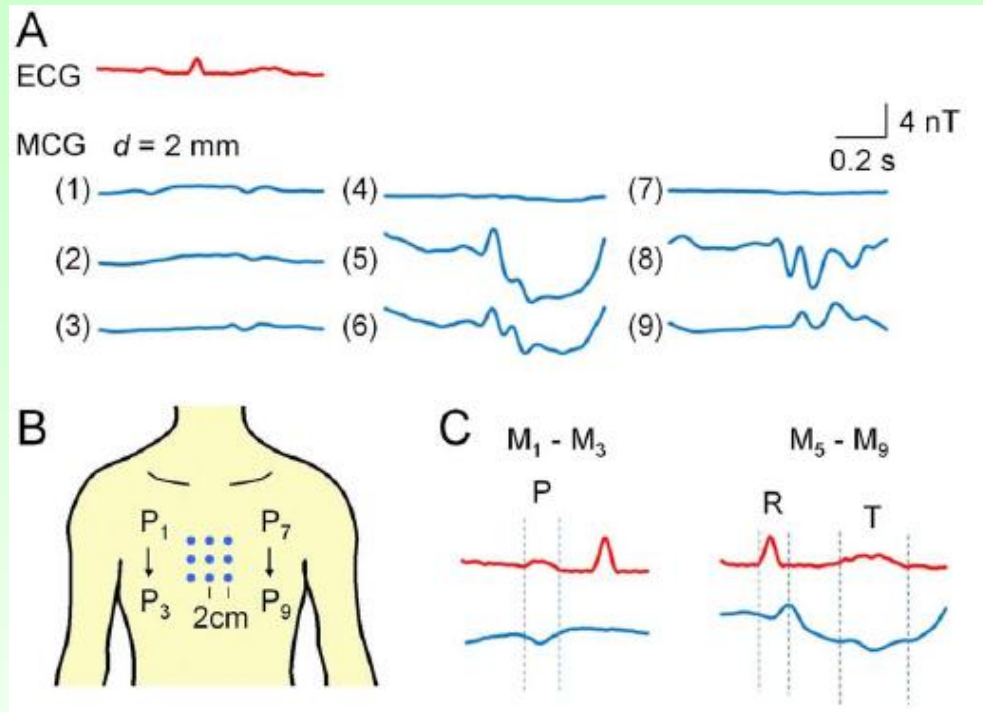
Properties	
Sample interval	
Sample rate	9.9
No. samples	9.3
Channel	
Range	
Coupling	
Channel	
Range	
Coupling	
Capture Date	27/11/2012
Capture Time	16:04:29



Properties	
Sample interval	101 μ s
Sample rate	9,901 kS/s
No. samples	9,900,996
Channel A	
Range	± 5 V
Coupling	DC
Channel B	
Range	± 5 V
Coupling	DC
Capture Date	27/11/2012
Capture Time	16:04:29
Saved with	PicoScope 4224 AQ529/020



Prospective applications of GMI magnetic field sensors



OPEN ACCESS Freely available online

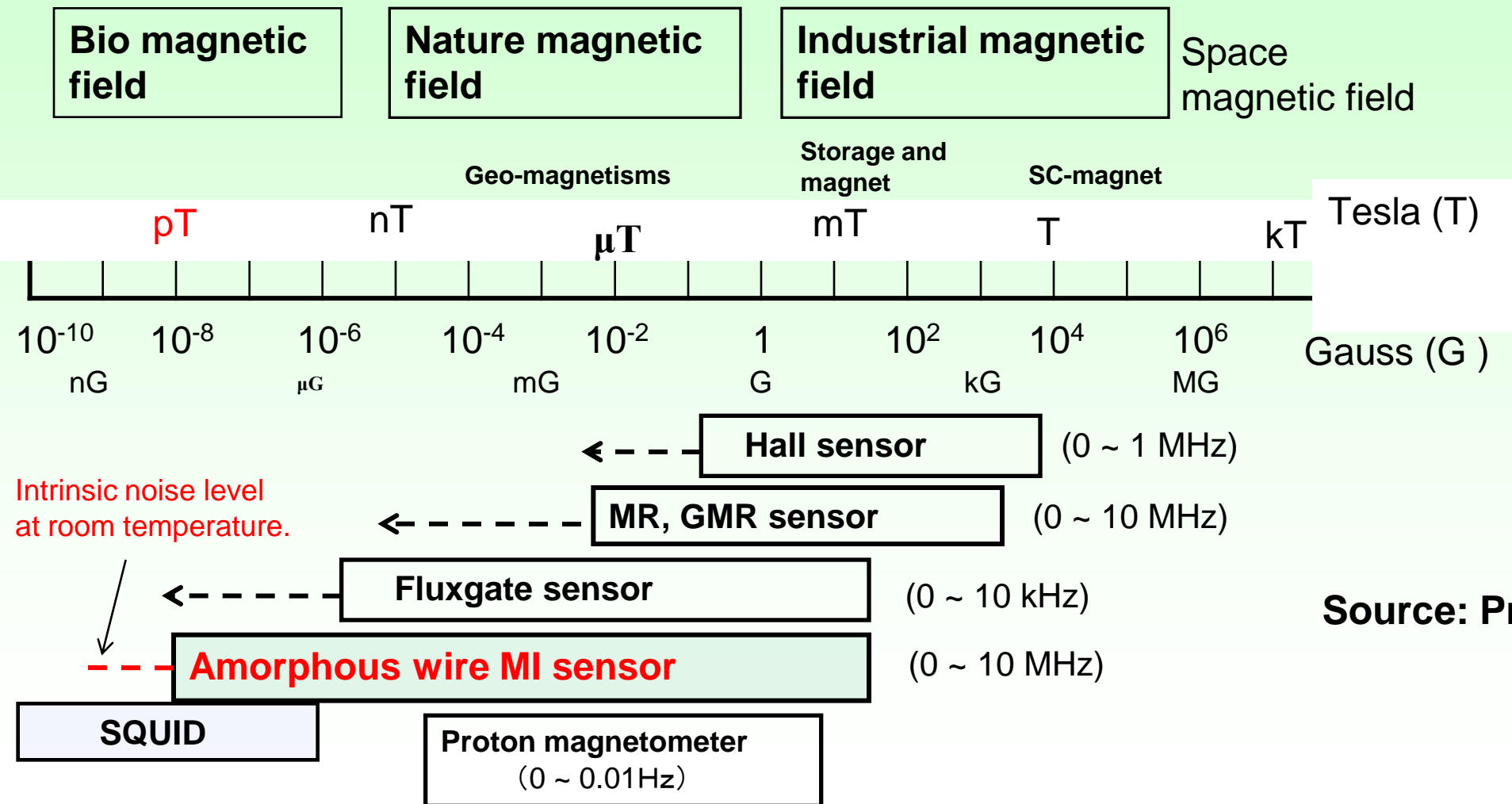
PLoS one

Pulse-Driven Magnetoimpedance Sensor Detection of Cardiac Magnetic Activity

Shinsuke Nakayama¹, Kenta Sawamura¹, Kaneo Mohri², Tsuyoshi Uchiyama^{2*}

¹ Department of Cell Physiology, Nagoya University Graduate School of Medicine, Nagoya, Japan, ² Department of Electronics, Nagoya University of Graduate School of Engineering, Nagoya, Japan

Magnetic Field and Magnetic Sensors



Source: Prof. K. Mohri

Tuneable composites with ferromagnetic wires

Magneto-impedance effect (MI)
in ferromagnetic wires

Composite materials with metallic wires

MI at Radio Frequencies
(MHz)

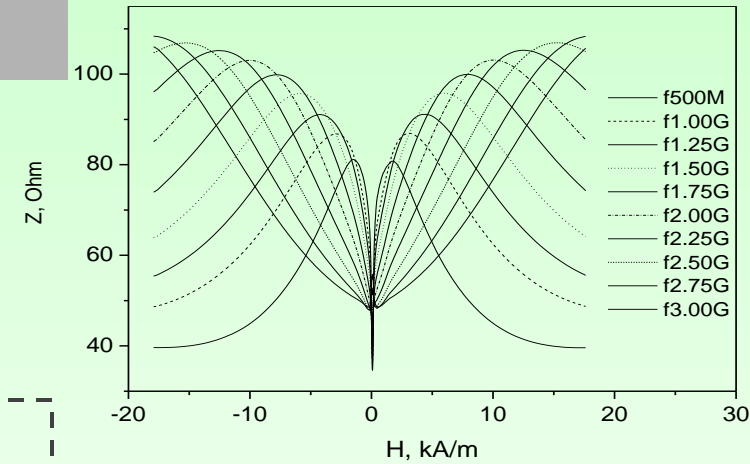
Strong dispersion of the
effective permittivity

High sensitivity
magnetic,
stress,
temperature
sensors

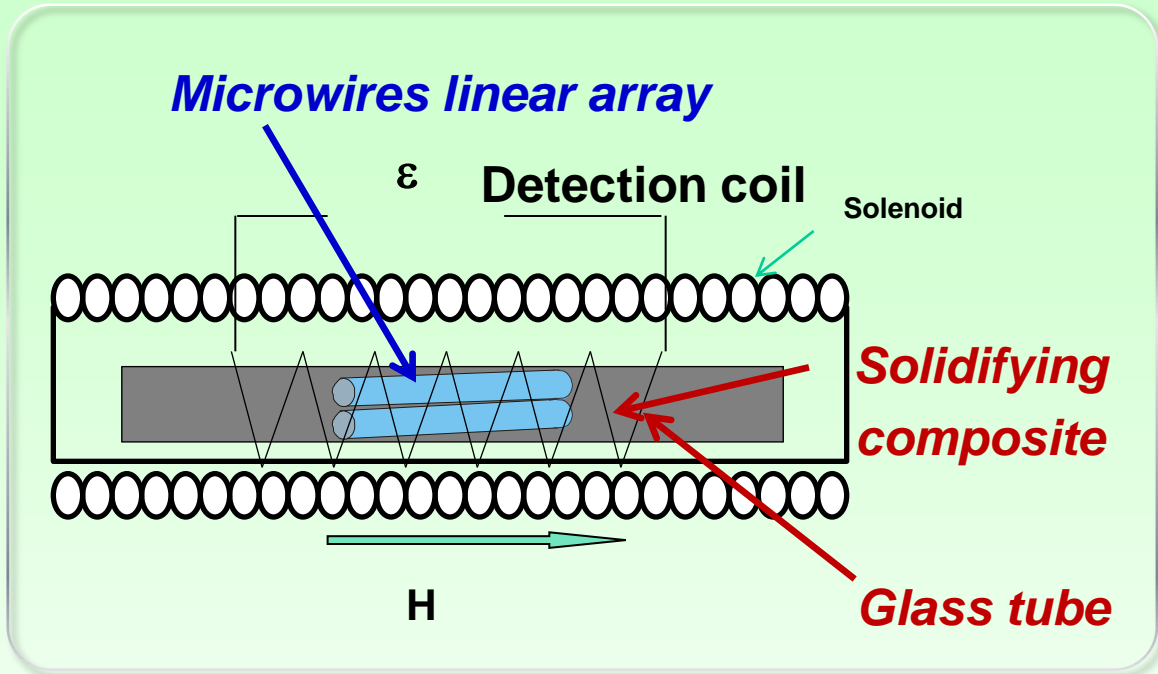
MI at GHz

Magnetically tuneable
composite

- 1) Tuneable selective microwave coatings
- 2) Stress-sensitive media for remote non-destructive health monitoring.
- 3) Temperature monitoring composites

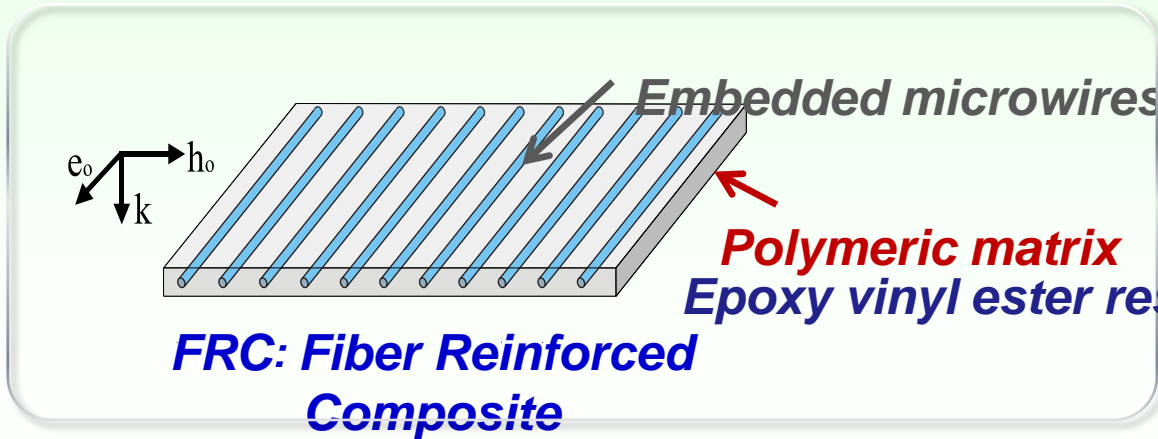


Composite structures



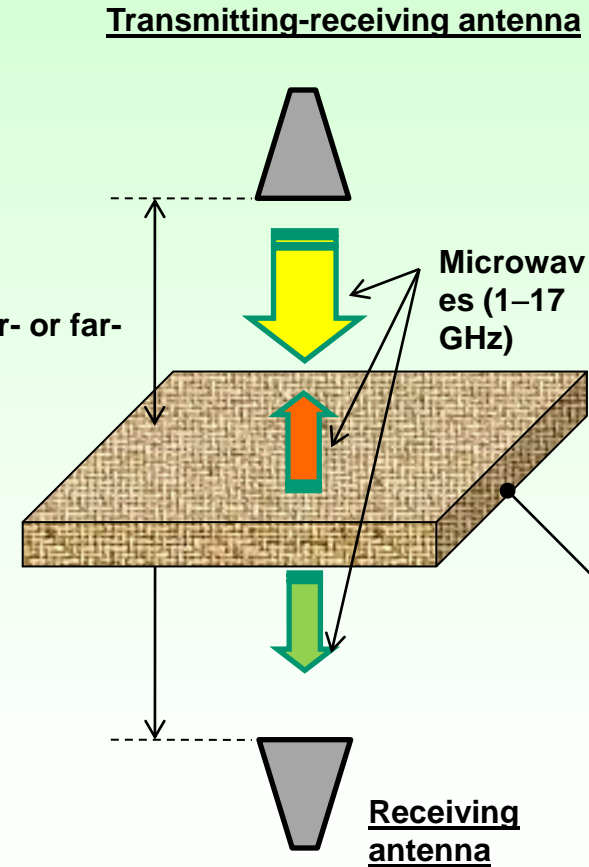
Microwires in a thermoset matrix during polymerization

Hysteresis loops Measurements



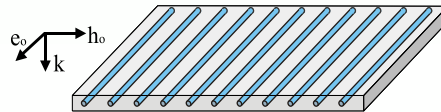
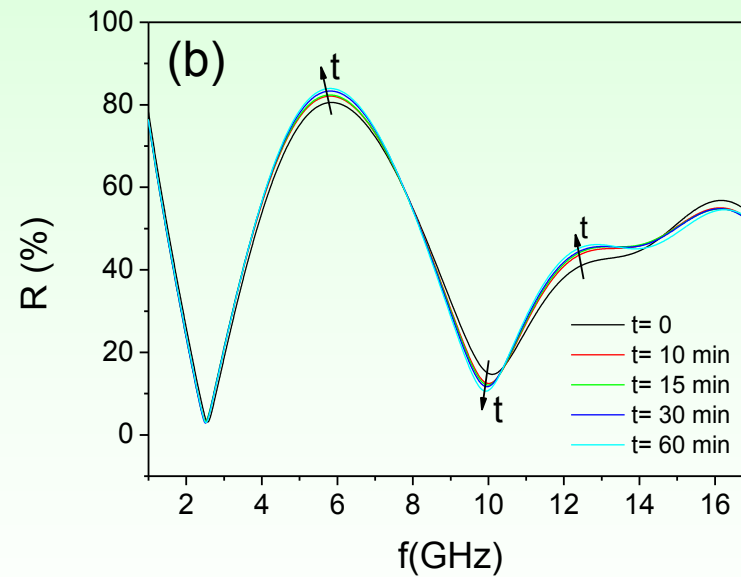
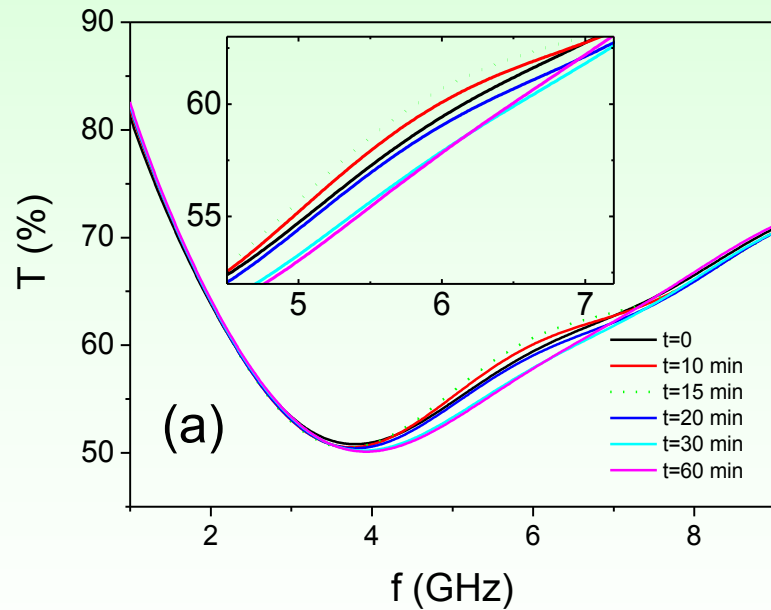
Composite during polymerization

Free-space Measurements

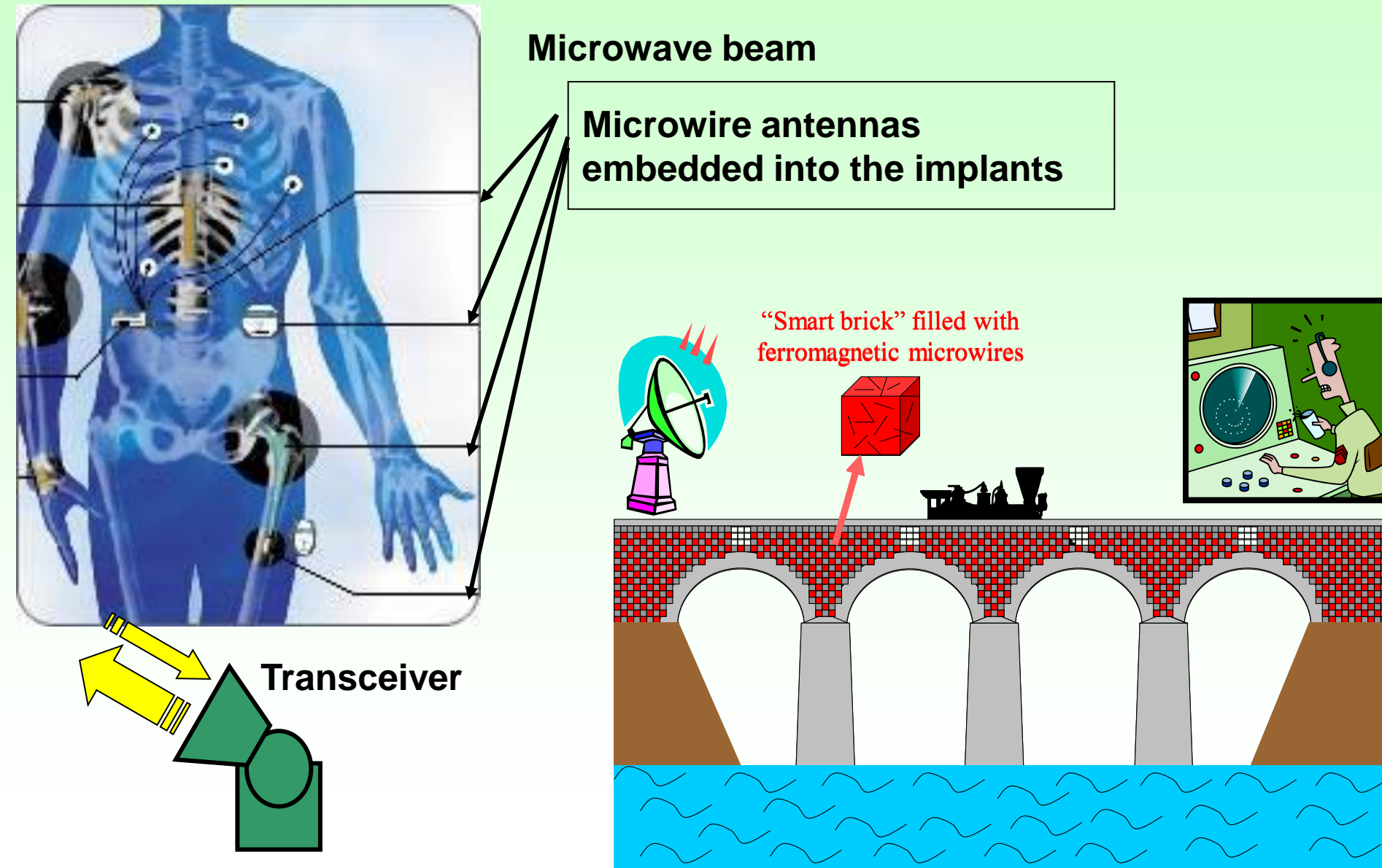


Electromagnetic properties of composites with glass-coated microwire inclusions

The Transmission, T (a) and reflection, R (a) parameters measured using free-space system during the composite solidification.



Potential application for stress-sensitive microwires:
remote local stress control



Existing and proposed applications

1. Mobile phones (navigation and games)
2. Bio- and medical applications
3. Tags
4. Smart composites

3070

IEEE TRANSACTIONS ON MAGNETICS, VOL. 47, NO. 10, OCTOBER 2011

Measurement of Spontaneous Oscillatory Magnetic Field of Guinea-Pig Smooth Muscle Preparation Using Pico-Tesla Resolution Amorphous Wire Magneto-Impedance Sensor

Tsuyoshi Uchiyama¹, Kaneo Mohri², *Life Fellow, IEEE*, and Shinsuke Nakayama³

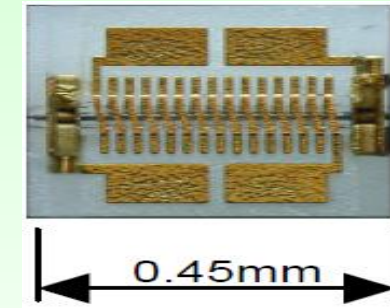
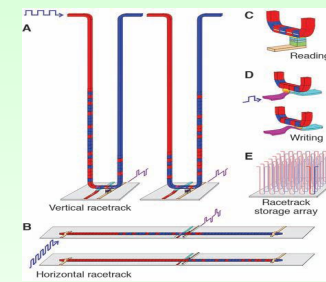
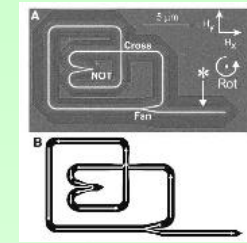
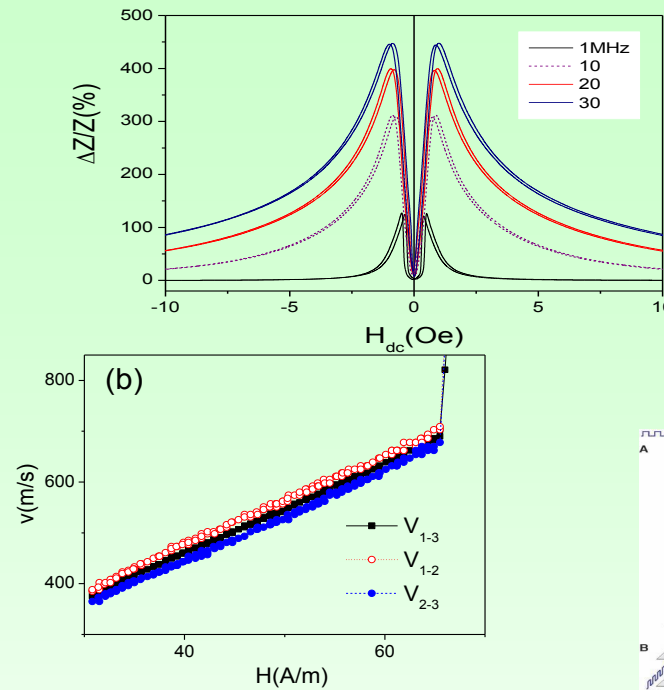
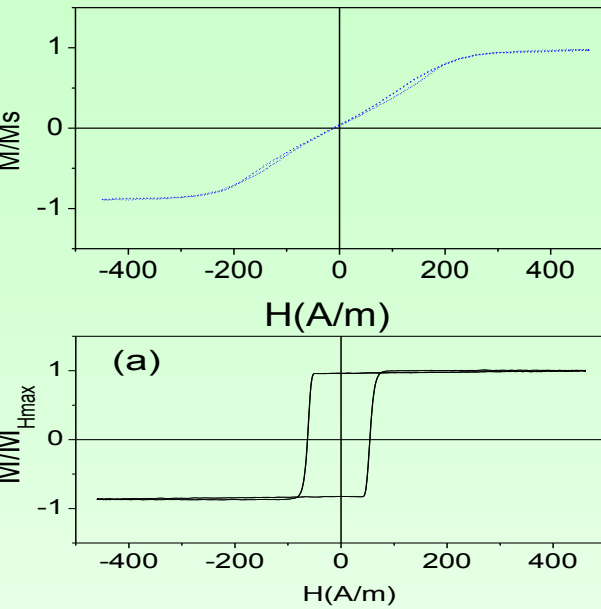
240

PIERS Proceedings, Kuala Lumpur, MALAYSIA, March 27–30, 2012

Health Recovery Effect of Physiological Magnetic Stimulation on Elder Person's Immunity Source Area with Transition of ECG and EEG

K. Mohri¹, Y. Inden², M. Yamada³, and Y. Mohri⁴

Present talk : magnetic softness and GMI effect of amorphous microwires

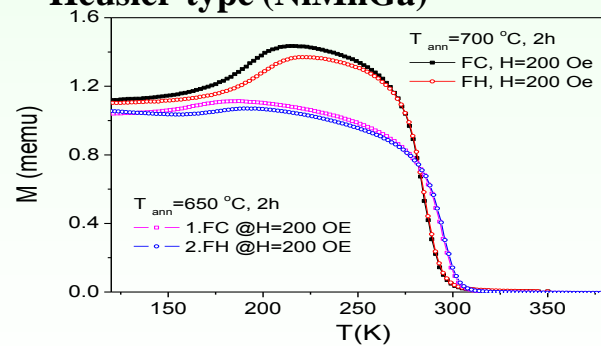


1. A. Zhukov, J.M. Blanco, M. Ipatov, A. Talaat, V. Zhukova, "Engineering of domain wall dynamics in amorphous microwires by annealing", *J. Alloys Compounds*, Volume 707, 15 (2017), p. 35–40
2. V. Zhukova, J. M. Blanco, A. Chizhik, M. Ipatov, A. Zhukov, "AC-current-induced magnetization switching in amorphous microwires", *Front. Phys.* 13(2), 137501 (2018)
3. V. Zhukova, J. M. Blanco, M. Ipatov, M. Churyukanova, S. Taskaev and A. Zhukov, Tailoring of magnetoimpedance effect and magnetic softness of Fe-rich glass-coated microwires by stress-annealing, *Sci. Reports* 8 (2018) 3202
4. V. Zhukova, J.M. Blanco, M. Ipatov, J. Gonzalez, M. Churyukanova A., Zhukov, "Engineering of magnetic softness and giant magnetoimpedance effect in Fe-rich microwires by stress-annealing", *Scripta Materialia* Vol. 142, 1 January 2018, 10–14,

Other features of amorphous microwires:

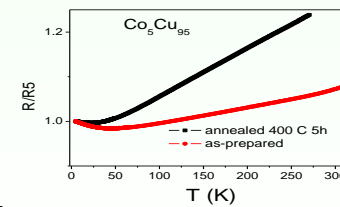
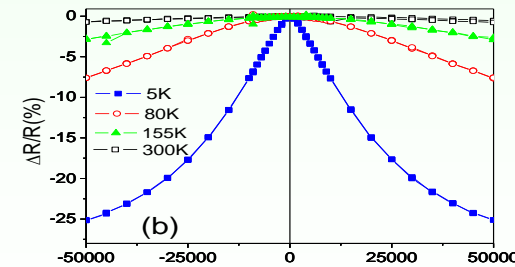
Crystalline microwires:

Heusler-type (NiMnGa)

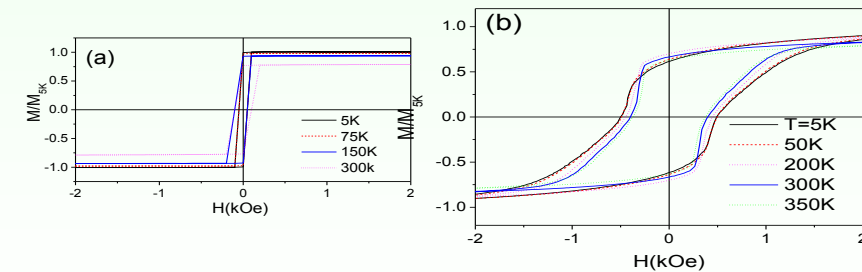


Granular microwires

Co-Cu



Magnetic hardening: FePt



A. Zhukov, M. Ipatov, A. Talaat, A. Aronin, G. Abrosimova, J.J. del Val and V. Zhukova, Magnetic hardening of Fe-Pt and Fe-Pt-M (M=B, Si) microwires, *J. Alloys Compound.*, Volume 735, (2018) pp.1071–1078

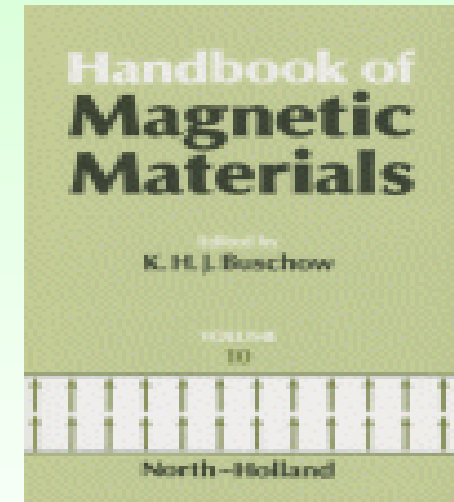
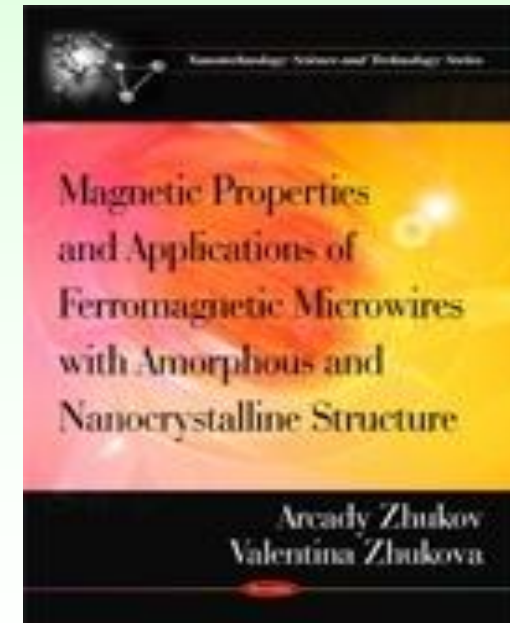
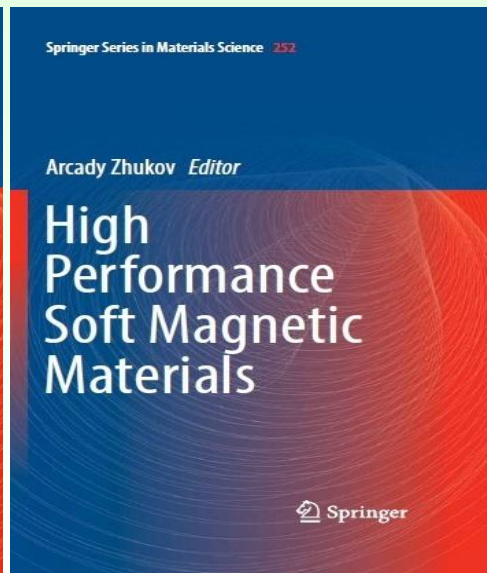
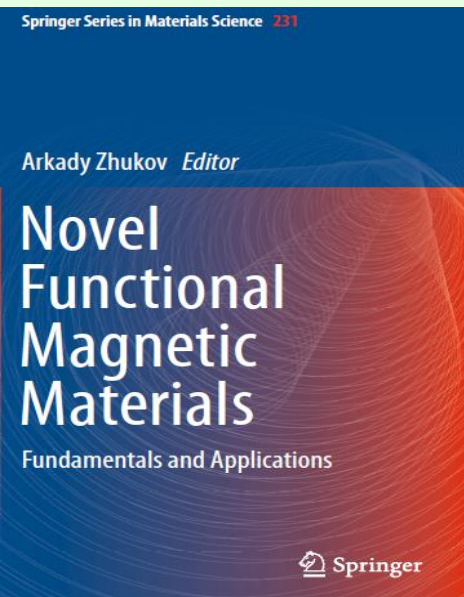
A. Zhukov, M. Ipatov, J.J. del Val, S. Taskaev, M. Churyukanova and V. Zhukova, "First-order martensitic transformation in Heusler-type glass-coated microwires", *Appl. Phys. Lett.* DOI: 10.1063/1.5004571

V. Zhukova, J. M. Blanco, J. Del Val, M. Ipatov, A. Martinez-Amesti, R. Varga, M. Churyukanova, A. Zhukov, "Magnetoresistance and Kondo-like behaviour in Co₅Cu₉₅ microwires", *J. Alloys Compound.* 674 (2016) 266-271

Conclusions

- Soft magnetic properties, GMI and fast DW propagation are observed in magnetic microwires.
- By appropriate selection of chemical composition and post-processing conditions we can considerably improve GMI effect and magnetic softness in Co-rich microwires and DW velocity in Fe-rich microwires
- Excellent magnetic properties are suitable for several sensor applications

Thank you for the attention!



“Advances in Giant Magnetoimpedance Materials” by A. Zhukov, M. Ipatov and V. Zhukov (issue October 2015)